EVALUATION OF PORTABLE NEAR-INFRARED SPECTROMETER FOR RAPID AND NON-DESTRUCTIVE DETERMINATION OF QUALITY AND AUTHENTICITY OF BAOBAB (*ADANSONIA DIGITATA* L.) FRUIT PULP IN KENYA

DENIS KIMUTAI YEGON

MASTER OF SCIENCE

(Food Science and Technology)

JOMO KENYATTA UNIVERSITY

OF

AGRICULTURE AND TECHNOLOGY

2023

Evaluation of Portable Near-Infrared Spectrometer for Rapid and Non-Destructive Determination of Quality and Authenticity of Baobab (*Adansonia Digitata* l.) Fruit Pulp in Kenya

Denis Kimutai Yegon

A Thesis Submitted in Partial Fulfillment of the Requirements for the Degree of Master of Science in Food Science and Technology of the Jomo Kenyatta University of Agriculture and Technology

2023

DECLARATION

This thesis is my original work and has not been presented for a degree in any other University

Signature…… ……Date……

Denis Kimutai Yegon

This thesis has been submitted for examination with our approval as University Supervisors

Signature…… ……Date……

Prof. Willis Owino, PhD

JKUAT, Kenya

Signature…… Date……

Prof. Ojijo, N.K.O, PhD

JKUAT, Kenya

DEDICATION

I would like to dedicate this thesis to my parents, Joseah Koske and Janet Koske. Your love, support and motivation have been invaluable to me throughout this process. Without your guidance and encouragement, I would never have been able to achieve my goals. Thank you for everything.

ACKNOWLEDGEMENT

I would like to give thanks to God for the support, good health, and guidance He has given me during my studies and research. His presence in my life has been an immense source of strength and comfort, and I am truly grateful for all that He has done for me.

I would like to express my deepest appreciation for my ever-supportive and loving supervisors Prof. Willis Owino and Prof. Ojijo N.K.O. Your guidance, patience, and mentorship have been invaluable to me throughout this process. Your willingness to help and your constant encouragement have been instrumental in helping me achieve my goals. Your kindness, understanding, and support have been a great source of strength, and I am truly grateful for everything you have done for me. Thank you so much for your unwavering dedication and for believing in me.

I would like to extend my deepest gratitude to Dr. Thorsten Tybusek and Dr. Elizabeth Wafula for their technical support throughout my research. Their thoughtful guidance and constructive comments have been instrumental in helping me reach my goals. I am truly thankful for the opportunity to work with such knowledgeable and experienced professionals. Their expertise and insight have been invaluable, and I am grateful for their support.

I would also like to thank the staff of Jomo Kenyatta University of Agriculture and Technology (JKUAT), especially from Food Science and Technology Department for the immense support they provided me during my studies and research and not forgetting my friends; Dr. Winne, Joyce, Maggy, Diana, Brenda, Wakaba, Collins, Lawrence, Caroline and others for their mentorship, moral support, constructive criticism, and helpful advice. Thank you all.

Finally, I am sincerely grateful for the financial support for my thesis research work from the Germany Federal Ministry of Food and Agriculture (BMEL) based on the decision of the parliament of the Federal Republic of Germany through the Federal Office of Agriculture and Food (BLE) as part of the “Quality improvement and more efficient utilization of products derived from the baobab tree (*Adansonia digitata* L.) to enhance

food security and nutrition in Sub-Saharan Africa (also known as the BAOQUALITY Project)", through Prof. W. Owino.

TABLE OF CONTENTS

DECLARATION ..... **ii**

DEDICATION ..... **iii**

ACKNOWLEDGEMENT ..... **iv**

LIST OF APPENDICES ..... **xvi**

ABSTRACT ..... **xx**

CHAPTER ONE **1**

INTRODUCTION **1**

1.1 Background Information 1

1.2 Problem Statement 3

1.3 Justification 5

1.4 Objectives of the Study 6

1.4.1 Main Objective 6

1.4.2 Specific Objectives 6

1.5 Scope of the Study 7

CHAPTER TWO **8**

LITERATURE REVIEW **8**

2.1 Description of Baobab Trees 8

2.2 Traditional and Modern Uses of Baobab Products 9

2.3 Proximate and Nutritional Composition of Baobab Fruit Pulp 11

2.4 Commercialization of Baobab Fruit Pulp 12

2.5 Quality Control of Baobab Fruit Pulp 13

2.6 Baobab Value Chain in Kenya 14

2.7 Baobab Fruit Processing 15

2.8 Postharvest Handling of Baobab Fruit Pulp 17

2.9 Baobab Fruit Pulp Adulteration 17

2.10 Near-infrared Spectrometer 18

2.11 Principles of Near-infrared Spectrometer 19

2.12 Instrumentation of NIR spectrometer 19

2.13 Interpretation of NIR Spectra 21

2.14 Chemometrics in NIR Spectrometer 23

2.14.1 Spectral Pre-processing 23

2.14.2 Multivariate Modelling 26

2.14.3 Validation of the Models 28

2.14.4 Application of NIR Spectrometer in Quality Assessment 30

2.15 Gaps in Knowledge 31

CHAPTER THREE 32

MATERIALS AND METHODS 32

3.1 Introduction 32

3.2 Sample Collection and Preparation 32

3.3 The application of a portable near-infrared (NIR) spectrometer in non-destructive testing of baobab quality attributes 33

3.3.1 Spectral Acquisition 33

3.3.2 Total Soluble Solids (TSS) and Titratable Acidity (TTA) 34

3.3.3 Vitamin C Content 35

3.3.4 Moisture Content 35

3.4 The use of a portable NIR spectrometer to monitor changes in baobab quality parameters during storage 36

3.4.1 Storage Experimental Design and Set-up 36

3.4.2 Microbial Load 37

3.4.2.1 Total Aerobic Count (TAC) and Total Yeasts and Moulds Count (TYMC) 37

3.5 The application of portable NIR spectrometer for rapid and non-destructive detection and quantification of BFP adulteration 38

3.5.1 Adulteration Experiment 38

3.5.2 Particle Size Determination 39

3.6 Data Preparation and Analyses 39

3.7 Data Preprocessing and Partitioning 40

3.8 Construction and Validation of Multivariate Models 41

3.8.1 Partial Least Square Regression (PLSR) 41

3.8.2 Partial Least Square Discriminant Analysis (PLS-DA) 42

CHAPTER FOUR 44

RESULTS AND DISCUSSION 44

4.1 The application of a portable near-infrared (NIR) spectrometer in non-destructive testing of baobab quality attributes 44

4.1.1 Quality Attributes of Baobab Fruit Pulp (BFP) 44

4.1.2 Total Titratable Acidity (TTA) 44

4.1.3 Total Soluble Solids (TSS) 45

4.1.4 Vitamin C Content 45

4.1.5 Moisture Content 46

4.2 Characterization of NIR Spectrum of BFP 47

4.3 Predictive Models 48

4.3.1 Total Titratable Acidity 48

4.3.2 Total Soluble Solids 51

4.3.3 Vitamin C Content 52

4.3.4 Moisture Content 53

4.4 The use of a portable NIR spectrometer to monitor changes in baobab quality parameters during storage 55

4.4.1 Effects of storage conditions and packaging on baobab quality parameters ... 56

4.4.2 Total Titratable Acidity 57

4.4.3 Total Soluble Solids (TSS) 59

4.4.4 Vitamin C Content 60

4.4.5 Moisture Content 62

4.5 Microbial Load 64

4.6 The application of a portable NIR spectrometer for rapid and non-destructive detection and quantification of BFP adulteration 67

4.6.1 Sample Particle Size Distribution 67

4.6.2 Characterization of NIR Spectra 68

4.6.3 Detection of adulterants using partial least square discriminant analysis models. 70

4.6.3.1 Two-class PLS-DA Models 70

4.6.3.2 Four-class PLS-DA Models 73

4.6.3.3 Quantification of adulterants using partial least square regression (PLSR) . 76

CHAPTER FIVE **80**

CONCLUSION AND RECOMMENDATION **80**

5.1 Conclusion 80

5.1.1 Applicability of NIR spectrometer in non-destructive testing of baobab quality 80

5.1.2 The use of a portable NIR spectrometer to monitor changes in baobab quality parameters during storage 80

5.1.3 Applicability of NIR spectrometer for rapid and non-destructive detection and quantification of BFP adulteration 81

5.2 Recommendation 82

5.2.1 Recommendation for Further Research 82

5.2.2 Recommendation for the Policy 82

5.2.3 Recommendation for Baobab Value Chain Actors 83

REFERENCES **84**

APPENDICES **107**

LIST OF TABLES

Table 4.1: Measured values for baobab quality attributes obtained through wet chemistry. 46

Table 4.2: Summary of calibration and prediction results for PLSR models for TTA, TSS, vitamin C, and moisture content. 55

Table 4.3: ANOVA P-values for main and interaction effects of storage duration, condition, and packaging on physicochemical and microbiological properties of stored baobab fruit pulp 57

Table 4.4: Statistical parameters for PLS-DA models for discrimination of pure and adulterated BFP using pre-processed spectra. 73

Table 4.5: PLS-DA classification parameters for discrimination of pure baobab and baobab samples individually adulterated with different types of adulterants, constructed using pre-processed spectra. 75

Table 4.6: PLSR results for the individual model for quantifying the concentration of the adulterants. 76

Table 4.7: PLSR results for the individual model for quantifying the concentration of the adulterants. 77

LIST OF FIGURES

Figure 2.1: Shows (a) baobab tree, (b) baobab fruit, (c) cracked baobab fruit and (d) baobab fruit pulp (World Economic Forum and Resita So Image 8

Figure 2.2: Portable/handheld NIR spectrometer (Model: NIR-S-G1, Tellspec, Toronto, Canada). 19

Figure 2.3: Main components of a portable NIR spectrometer 20

Figure 2.4: Major bands and their relative peak positions for prominent near-infrared absorptions 23

Figure 3.1. Spectral data acquisition using Tellspec NIR spectrometer. 34

Figure 3.2. Schematic representation of the storage experiment. 37

Figure 3.3: Experimental set-up for adulteration experiment. 39

Figure 4.1: Raw mean spectrum for BFP.....47

Figure 4.2: Partial Least Square Regression (PLSR) score plots for the quantification of titratable acidity in baobab fruit pulp. (A) Calibration model and (B) Prediction model. 50

Figure 4.3: Partial Least Square Regression (PLSR) score plots for the quantification of total soluble solids in baobab fruit pulp. (A) Calibration model and (B) Prediction model. 51

Figure 4.4: Partial Least Square Regression (PLSR) score plots for the quantification of vitamin C content in baobab fruit pulp. (A) Calibration model and (B) Prediction model. 53

Figure 4.5: Partial Least Square Regression (PLSR) score plots for the quantification of moisture content in baobab fruit pulp. (A) Calibration model and (B) Prediction model. 54

Figure 4.6: Changes in TTA over six months storage period in BFP samples packaged in UbKP and LDPE bags and kept at 25°C/75%RH and 35°C/83%RH storage conditions. 58

Figure 4.7: Changes in TSS over six months storage period in BFP samples packaged in UbKP and LDPE bags and kept at 25°C/75%RH and 35°C/83%RH storage conditions. 59

Figure 4.8: Changes in vitamin C over six months storage period in BFP samples packaged in UbKP and LDPE bags and kept at 25°C/75%RH and 35°C/83%RH storage conditions. 61

Figure 4.9: Changes in moisture content over six months storage period in BFP samples packaged in UbKP and LDPE bags and kept at 25°C/75%RH and 35°C/83%RH storage conditions. 63

Figure 4.10: Changes in TAC over six months storage period in BFP samples packaged in UbKP and LDPE bags and kept at 25°C/75%RH and 35°C/83%RH storage conditions 65

Figure 4.11: Changes in TYMC over six months storage period in BFP samples packaged in UbKP and LDPE bags and kept at 25°C/75%RH and 35°C/83%RH storage conditions 65

Figure 4.12: Particle size distribution curves for BFP, rice, wheat, and maize flours. 67

Figure 4.13: Average spectra (950-1650nm) for baobab fruit pulp powder, maize flour, rice flour, and wheat flour 69

Figure 4.14. Two-class PLSDA classification scatter plot for detection of rice flour adulterants in baobab fruit pulp powder. (A) Calibration model and (B) Prediction model 71

Figure 4.15: Two-class PLSDA classification scatter plot for detection of wheat flour adulterants in baobab fruit pulp powder. (A) Calibration model and (B) Prediction model. 72

Figure 4.16: Two-class PLSDA classification scatter plot for detection of wheat flour adulterants in baobab fruit pulp powder. (A) Calibration model and (B) Prediction model. 72

Figure 4.17: Four-class PLSDA classification scatter plot for detection of maize flour adulterants in baobab fruit pulp powder. (A) Calibration model and (B) Prediction model. 74

Figure 4.18: PLSR classification score plot for quantification of rice flour adulterants in baobab fruit pulp powder. (A) Calibration model (B) Prediction model.... 78

Figure 4.19: PLSR classification score plot for quantification of wheat flour adulterants in baobab fruit pulp powder. (A) Calibration model (B) Prediction model 78

Figure 4.20: PLSR classification score plot for quantification of maize flour adulterants in baobab fruit pulp powder. (A) Calibration model (B) Prediction model. 79

LIST OF APPENDICES

Appendix I: Set-up for the storage experiment.....107

Appendix II: NIR spectra pre-processed with (A) Raw (Unprocessed), (B) Smoothed with SG, (C) Multiplicative scatter correction and mean-centered (MSC+MC), (D)Standard Normal Variate (SNV). 108

Appendix III: Summary of statistical results for models predicting baobab quality attributes developed using different pre-processing methods.....109

Appendix IV: Summary of statistical results for models predicting the amounts of adulterants trained after pre-processing raw spectra using different methods.....111

Appendix V: X-loading weight plots of the optimal models for (a) TTA prediction, (b) TSS prediction, (c) Vitamin C prediction, and (d) moisture content prediction 113

Appendix VI: RMSECV against LVs plot for baobab fruit pulp adulterated with; (A) rice flour, (B) wheat flour, (C) maize flour, and (D) all adulterants.....114

ACRONYMS AND ABREVIATIONS

ANOVA	Analysis of Variance
AS	Autoscaling
B	Billion
BFP	Baobab Fruit Pulp
CAGR	Compound Annual Growth Rate
Cal	Calibration
CFU	Colony Forming Unit
CPFA	Cyclopropenoid Fatty Acid
DC&M	Data Collection and Management
DLP	Digital Light Processing
DMD	Digital Micromirror Display
FD	First Derivative
FDA	Food and Drug Administration
FN	False Negative
FP	False Positive
FTIR	Fourier Transform Infrared
GRAS	Generally Recognized as Safe
HPLC	High-Performance Liquid Chromatography
InGaAs	Indium Gallium Arsenide
IR	Infrared
KCl	Potassium Chloride

KEBS	Kenya Bureau of Standards
LDPE	Low-Density Polyethylene
LED	Light Emitting Diodes
LOD	Limit of Detection
LV	Latent Variable
MC	Mean Centering
MF	Maize Flour
MSC	Multiplicative Scatter Correction
NaCl-	Sodium Chloride
NIR	Near-infrared
NM	Nanometers
OH	Hydroxyl
PC	Principal Component
PCA	Principal Component Analysis
PCA	Plate Count Agar
PLS-DA	Partial Least Squares Discriminant Analysis
PLSR	Partial Least Squares Regression
Pred	Prediction
R^2	R-squared
RF	Rice Flour
RH	Relative Humidity
RMSE	Root Mean Square Error

RMSEC	Root Mean Square Error of Calibration
RMSECV	Root Mean Square Error of Cross-validation
RMSEP	Root Mean Square Error of Prediction
RPD	Residual Predictive Deviation
SG	Savitzky-Golay
SNV	Standard Normal Variate
SSC	Soluble Solid Content
TAC	Total Aerobic Counts
TN	True Negative
TP	True Positive
TPC	Total Plate Count
TSS	Total Soluble Solids
TTA	Total Titratable Acidity
TYMC	Total Yeast and Mold Counts
UbKP	Unbleached Kraft paper
US	United States
UV-Vis	Ultraviolet–Visible spectrometer
VRBGA	Violet Red Bile Glucose Agar
WF	Wheat Flour

ABSTRACT

The demand for baobab fruit pulp (BFP) is growing significantly due to increasing popularity of natural, organic, and nutritious ingredients. This demand has created the need for quality control to ensure quality and safety of the pulp. Conventional methods of assessing the quality of BFP are subject to human error, destructive and costly. Therefore, this study evaluated the ability of portable NIR spectrometer for rapid and non-destructive determination of key quality attributes of BFP. The study also evaluated the potential of the technique to monitor quality changes of stored BFP and to detect adulteration. A portable NIR spectrometer (Model: NIR-S-G1, Tellspec, Toronto, Canada) was used to acquire BFP spectra. Reference measurements on total titratable acidity (TTA), total soluble solids (TSS), vitamin C, and moisture content were immediately collected through specific wet-chemistry procedures. Chemometrics of partial least square regression (PLSR) was used to correlate between NIR spectra and reference measurements. Prediction model specific to each parameter was constructed and validated. This study proved that portable NIR spectrometer could be used for rapid, accurate, and non-destructive determination of BFP quality parameters with R^2 of above 0.63 and RPD of above 2.00. A 2^3 factorial design storage experiment establishing the effect of storage duration (six months), storage conditions (25°C/75%RH and 35°C/83%RH), and packaging materials (unbleached kraft paper, UbKP and low-density polyethylene, LDPE) on quality of BFP. Constructed models were used to monitor changes in stored BFP. Additionally, microbial safety of stored pulp (total aerobic counts, TAC and total yeast and mold counts, TYMC) was determined through specific wet-chemistry procedures. Results indicated that the nutrient composition of stored BFP deteriorated regardless of the effect of packaging material and the storage conditions used. The TTA declined insignificantly ($P>0.05$) while TSS and vitamin C significantly reduced ($P<0.05$) at the end of the storage period. The moisture content of stored samples also increased significantly regardless of the protection offered by the packaging material. There was a significant growth of TAC over time ($P>0.05$) in all samples regardless of packaging and storage conditions. Yeast and molds were not detected in samples kept in LDPE bags until the end of storage. However, the increase in moisture content and microbial load of stored pulp did not surpass the upper limits stipulated by KEBS. Finally, the potential of portable NIR spectrometer to detect and quantify the adulterants in BFP was evaluated. Partial Least Square Discriminant Analysis (PLS-DA) was adopted for classification purpose. The device was sensitive and precise in the discrimination of pure and adulterated BFP. It detected rice, wheat, and maize fours adulterants with sensitivity and specificity of above 0.982 and error of below 0.009 for all two-class PLS-DA models. Finally, the PLSR was also used to establish predictive modes for quantifying the amount of adulterants present in BFP. The models proved to be efficient with prediction R^2 and RMSE of above 0.88 and below 6.20% respectively. The models also resulted in reasonably low limits of detection (LODs) of 8.79%, 11.01%, 13.79% for rice, wheat and maize flours, respectively. Therefore, portable NIR spectrometer paired with chemometrics could be used for rapid, non-destructive, and cost-effective quality assessment of BFP. The adoption of portable NIR spectrometers by baobab value chain actors could help reduce

post-harvest losses by enabling rapid, non-destructive quality screening of fruits to identify and reject immature or poor-quality batches. Furthermore, this cost-effective technique could be utilized to monitor changes in stored BFP, and rapidly screen for adulteration, thereby maintaining product authenticity and quality.

CHAPTER ONE

INTRODUCTION

1.1 Background Information

Baobab (*Adansonia digitate* L.) fruit is part of a long-standing, iconic, and multipurpose tree belonging to the family Bombaceae and Malvales order that is widely distributed in the savannas and savanna woodlands in sub-Sahara Africa (Ismail et al., 2019). Baobab fruit is long and barrel-shaped with black seeds ingrained in a white and chalky pulp. Baobab fruit, also known as "monkey bread" or "cream of tartar," is traditionally consumed by local communities in various countries on the continent, including Senegal, Ghana, and Zimbabwe (Ibrahima *et al.*, 2013). Baobab pulp is rich in nutrients such as carbohydrates, proteins, lipids, fibers, and minerals such as potassium, magnesium, calcium, and sodium (Chadare et al., 2009). The fruit is high in vitamin C and has a tart, citrus-like flavor and it qualifies as homegrown vitamin C for Africans (Sidibe and Williams, 2002). Additionally, it contains many different phenolic compounds such as procyanidin, epicatechin, gallic acid, hydroxycinnamic acid, glycosides (Ibrahima *et al.*, 2013) tannins, phenols, and flavonoids (Kamatou *et al.*, 2011) which are linked to various biological properties such as anti-microbial, anti-oxidant and anti-inflammatory (Ismail et al., 2019). Due to its incredible nutrient density, baobab fruit as a source of food, holds promise of achieving Zero Hunger. The fruit can also empower local communities, increase incomes, improve food security, and build resilience.

Recently, baobab fruit pulp (BFP) has received a lot of attention from vendors and processors. This is due to its usefulness in several products such as juices, sweets, seed oil, and other valuable products (Ismail et al., 2019). It is also applied in various formulations such as sauces, yogurt, and appetizers (Rahul *et al.*, 2015). In 2008, European Union certified baobab pulp as a novel food ingredient and authorized it to be merchandised and applied in the food industry. This opened the door for the exportation of BFP from African countries (Christine *et al.*, 2010). In 2009, Food and Drug Administration (FDA) gave Generally Recognized as Safe (GRAS) status through

scientific procedures and approved it as a food ingredient for use in fruit drinks and fruit cereal bars in the United States. In the United Kingdom, baobab fruit imports have increased by over 1600% due to its application in chocolates, jams, cereals, bars, sauces, and alcoholic spirits (Wang et al., 2017). According to Baobab Research Report. (2020), the global market for baobab is expected to reach US$3.75 billion by 2024.

In Kenya, BFP is gaining recognition for health benefits, as food industries incorporate it into "healthy" products (Wegelin, 2021), while scientific publications demonstrate its nutritional and phytochemical value (Chadare et al., 2009; Coe et al., 2013). This has driven BFP demand and baobab powder exports from small community facilities, where rural workers manually harvest, deseed, and dry the pulp, as well as from medium processors that collaborate with local communities on packaging and distribution (Egbadzor et al., 2023). However, a key challenge facing this business is biopiracy and illegal export of whole baobab trees and warranting a potential ban would prevent smuggling across the borders.

In scientific literature, the edible dehydrated powder is typically referred to as baobab fruit pulp or simply baobab pulp. In commercial trade and among food vendors or processors, this same baobab fruit pulp powder is commonly labeled and marketed as baobab powder. While scientifically it is more precise to specify baobab fruit pulp powder, the term baobab powder has become widely used and understood in the food industry and marketplace to refer specifically to the dried, milled fruit pulp material. Therefore, food scientists studying baobab pulp chemistry and nutrition refer to it as "baobab fruit pulp" while commercial providers label essentially the same product as "baobab powder." Despite differing terminology, both terms refer to the edible nutritional powder from dried baobab fruit mesocarp (Munissi., et al. (2022).

The development in instrumentation has resulted in alternative, non-destructive, cheap, and rapid methods of determining the internal quality parameters of intact fruits and vegetables. Specifically, near-infrared (NIR) spectrometer has found its use in the food industry for qualitative and quantitative analysis. This is because NIR spectrometer is simple, rapid, non-destructive, requires minimal or no sample preparation. It enables

simultaneous determination of several parameters using single measurements. It is also fast, has non-contact operation procedures and low operating cost (Li et al., 2019). The NIR region of the electromagnetic spectrum lies between the visible and infrared regions with wavelengths ranging between 750-2500 nm (Beghi *et al.*, 2013). Recent advances in NIR spectrometer have led to the development of miniature, commercial handheld/portable scanners that have contributed to additional speed, simplicity, sensitivity, and convenience (Amuah *et al.*, 2019). These scanners are ideal for onsite quality determination of intact fruits either in the fields or in cold rooms during inspection. A handheld/ portable spectrometer coupled with chemometric techniques has been used to determine internal quality parameters such as total titratable acidity (TTA), total soluble solids (TSS), and sugar content of fruits (Chia *et al.*, 2012; Li et al., 2019). Additionally, a portable NIR spectrometer has been used to classify and quantify adulteration in palm oil (Basri *et al.*, 2017), authenticate paprika powder (Oliveira et al., 2020), and predict the eating quality of apples (Mart *et al.*, 2013). However, the ability of this technique for non-invasive quality assessment of BFP has not been explored. Therefore, this study aimed at evaluating the potential of a portable NIR spectrometer for rapid and non-destructive testing of quality and authenticity of BFP in Kenya. The use of this technique both by producers in the field and the baobab value chain actors will ensure the uniformity of batches of fruits not only in terms of external appearance but also in terms of pulp quality parameters such as texture, color, titratable acidity, sugar, and vitamin content.

1.2 Problem Statement

Baobab fruit has gained recognition as 'super fruit' due to its high nutrient content and associated health benefits. The fruit pulp is normally consumed raw or processed into different products such as beverages, food, dietary supplements, and even personal care products. Due to these multiple applications, quality control of BFP is paramount in ensuring the safety and attainment of certain quality standards. The quality of fruit is normally assessed through visual inspection, measurement of physical characteristics, wet-chemistry analyses, and sensory evaluation using taste panels (Shewfelt, 2014). These

procedures involved are laborious, destructive, require sample preparation, and often use expensive chemicals and equipment (Jiang *et al.*, 2016).

Lack of efficient quality testing techniques leads to postharvest losses and safety issues (Barbin et al., 2012). Massive quantities of food are lost due to spoilage and infestation on their way to consumers or processors (Blakeney, 2019). In Africa, food losses and waste goes up to 40-50% due to poor infrastructure and storage conditions (Spore, 2011). Extracted BFP often goes to waste due to improper post-harvest handling e.g. poor storage, yeast/mould infestation, unhygienic conditions, and poor processing (James *et al.*, 2022). Eldoom *et al.*(2014) reported significant nutrient loss especially vitamin C in poorly stored BFP. Microbial contamination and infestation during storage not only causes sensory defects but also introduce toxins, making BFP unsafe for consumption. Mycotoxins from mold growth pose a health risk if the contaminated pulp is consumed. Bacterial contaminants like Salmonella, E. coli, and Staphylococcus aureus have been isolated from baobab pulp samples stored in unhygienic conditions (James *et al.*, 2022).

Food commodities have always been vulnerable to fraudulent adulteration with cheaper and inferior materials. In sub-Sahara Africa, food safety has been a growing concern with rampant instances of adulteration and contamination of food products (Onyeaka *et al.*, 2021). It is estimated that more than 20% of foods are likely to be adulterated (Pal and Mahinder, 2020) with a cost implication of US$ 49 (McGrath *et al.*, 2018). The BFP is well known in Sub-Saharan Africa due to its incredible nutrient density, application in several consumer products, and rapidly growing demand worldwide. The potential adulterant for baobab is cereal flour with the main motive being high weight adjustment, increase sales and profits, or stretch the supply of the product (Chepngeno *et al.*, 2022a). Adulteration of BFP is a concern because it compromises the safety and quality of the product. It dilutes the nutrient composition and destroys the reputation of genuine baobab producers. It also mislead consumers about the true nature of the product and those who pay premium for quality BFP does not get value for their money (Muthai *et al.*, 2017).

1.3 Justification

Conventional methods of BFP quality assessment such as visual inspection, measurement of physical characteristics, and physico-chemical testing have several limitations. They are highly subjective in nature, relying on personal bias and interpretation. They require specialized equipment, skilled personnel, and are generally destructive to the samples being analyzed (Amuah *et al.*, 2019). Conventional quality testing also tends to be tedious, labor-intensive and time-consuming (Ncama *et al.*, 2017; Magwaza and Opara, 2015). For instance, assessing parameters like TSS and TTA involves extraction of juice from the BFP, making solutions, and running multiple tests (Munyebvu et al., 2022). This is time consuming and the cost implications of acquiring equipment and chemicals, and also training staff adds to the complexity of conventional testing. These deficiencies of traditional quality evaluation restrict the ability to carry out rapid, reliable, and routine assessment of BFP at critical points along the supply chain such as harvest, transport, storage, and processing sites.

NIR spectrometer has emerged as a viable alternative to subjective conventional methods for non-destructive quality testing of agricultural produce (Amuah *et al.*, 2019). NIR spectrometer is simple to use, rapid, and requires no or minimal sample preparation. It allows simultaneous measurement of multiple parameters using a single scan and has low operating costs compared to traditional wet-chemistry techniques (Ncama *et al.*, 2017). The development of miniaturized handheld NIR devices has enabled portability, speed, and ease-of-use for on-site quality analysis (Tugnolo *et al.*, 2021). The use of chemometrics makes it easier to retrieve chemical information from complicated spectrum data (Amuah *et al.*, 2019). Implementing portable NIR spectrometer could significantly improve efficiency, accuracy and objectivity in routine quality control practices for BFP. This would in turn help reduce post-harvest losses, ensure safety and standards compliance, and support income generation across the baobab value chain in sub-Saharan Africa.

Adoption of efficient quality testing techniques could help reduce postharvest losses by ensuring harvesting of fruits that meets the required quality standards. It would help

address safety issues and support the livelihoods and income generation of baobab producers and traders in sub-Saharan Africa. Quick, non-destructive quality checks using portable NIR spectrometer gives information about quality and also identify pulp that does not meet safety standards. This allows problematic batches to be sorted out early, reducing post-harvest losses that can severely impact incomes. Equipping producers and cooperatives with portable NIR units enables them to guarantee the quality of their pulp before transport to processing sites or export markets. This increases chances of acceptance and profitability. Traders and vendors also benefit from being able to rapidly authenticate the quality of purchased BFP. Avoiding losses helps baobab value chain actors maximize revenues and make their operations more financially sustainable. Increasing incomes for the predominantly rural baobab harvesters and processors contributes to poverty alleviation and greater food security, aligning with Sustainable Development Goals like Zero Hunger. Therefore, this study aimed at evaluating the ability of portable NIR spectrometer for non-destructive assessment of quality and authenticity BFP.

1.4 Objectives of the Study

1.4.1 Main Objective

To evaluate the potential of portable NIR spectrometer for rapid and non-invasive determination of quality and authenticity of BFP in Kenya.

1.4.2 Specific Objectives

1. To determine the ability of a portable NIR spectrometer for rapid, non-destructive, and simultaneous determination of BFP quality parameters (TTA, TSS, vitamin C and moisture content).
2. To evaluate changes in BFP quality during storage using portable NIR spectrometer.
3. To assess the potential of a portable NIR spectrometer for rapid and non-destructive detection and quantification of BFP adulteration.

1.5 Scope of the Study

The study was targeted to determine the ability of a portable NIR spectrometer as a rapid and non-destructive alternative method for checking the quality, nutrient deterioration during storage, and authenticity of BFP. The study used a portable NIR spectrometer (Model: NIR-S-G1, Tellspec, Toronto, Canada) to collect spectral data in the wavelength range of 900-1700 nm. Each sample scan recorded 256 data points across the NIR region. Wet chemistry (TTA, TSS, vitamin C, and moisture content) analyses were carried out immediately after spectral data acquisition using wet-chemistry methods. The study used chemometrics of partial least square regression (PLSR) to correlate spectra and reference quality parameters of BFP. Constructed PLSR models were validated both internally using cross-validation and externally using external set of samples. Constructed models were used to predict the degradation of quality parameters of BFP during storage. Additionally, microbial safety of stored BFP samples was assessed through standard wet-chemistry procedures. The study also involved evaluating the ability of a portable NIR spectrometer for the detection and quantification of rice, wheat, and maize flour adulterants in BFP. Adulteration level exceeding 10% was utilized as the delineation between accidental and deliberate adulteration (Chepngeno et al., 2022). The study utilized partial least square discriminant analysis (PLS-DA) and partial least square regression (PLSR) to classify adulterants and quantify the level of adulteration.

CHAPTER TWO

LITERATURE REVIEW

2.1 Description of Baobab Trees

Adansonia digitata L. (Malvaceae) commonly known as the 'Baobab tree' is a long-lived and multipurpose African native species commonly found in the African thorny woodlands. It belongs to the family of Bombaceae and Malvales order that is widely distributed in the savannas and savanna woodlands in sub-Sahara Africa (Sidibe and Williams, 2002). It is a massive tree characterized by a distinctive huge trunk and a height of up to 20 m and a diameter of between 10-12 m (Figure 2.1).

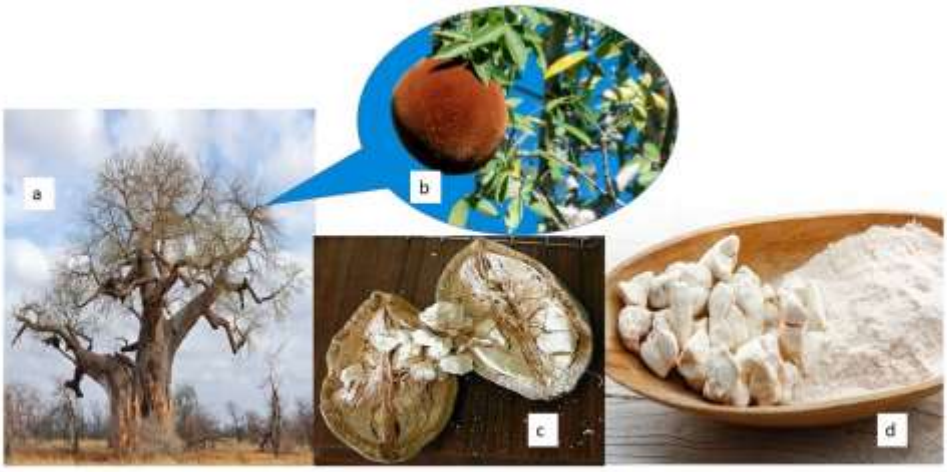

Figure 2.1: Shows (a) baobab tree, (b) baobab fruit, (c) cracked baobab fruit and (d) baobab fruit pulp (World Economic Forum and Resita So Image

https://t.ly/S6AW7).

Globally, there are eight species of baobab trees and six of them are native to Madagascar where it is believed that the name *Adansonia* originated (Sidibe and Williams, 2002). In Africa, baobab trees are plenty in several countries such as Mozambique, Zimbabwe,

Kenya, Malawi etc. (Kamatou *et al.,* 2011). Recently, another species of baobab called *Adansonia Kilima* has been discovered in Tanzania, Kenya, Zambia, Namibia, and South Africa (Douie *et al.,* 2015). Baobab trees do well in semi-arid areas with low annual rainfall. It also grows on a wide range of well-drained soils from clay to sand and a latitude of 16°N and 26°S in areas limited to frost annually (Gebauer *et al.*, 2002). They grow slowly probably due to an insufficient amount of water received annually and can have a lifespan of up to 1000 years (Rahul *et al.*, 2015).

Baobab trees growing in fields begin to bloom eight to twenty-three years while grafted ones takes less than five years to start flowering (Anjarwalla *et al.*, 2017). Peak flowering occurs at the same time usually in November each year and the flowering stops altogether in April (Wickens, 2007). Flowering is determined by the temperature and the conditions of the previous season (Munyebvu *et al.,* 2018). Seasonally, a matured baobab tree is estimated to produce about 200kg of fruits (Kabbashi *et al.,* 2017). The previous season of baobab and the ability of the tree to flower influence flowering and fruit production (Venter and Witkowski, 2019). Baobab fruit, also known as "monkey bread" or "cream of tartar fruit," is eaten by local communities in various countries on the continent, including Senegal, Ghana, and Zimbabwe. The fruit is high in vitamin C and other nutrients and has a tart, citrus-like flavor. It is often used to make juice, jam, and other food products.

2.2 Traditional and Modern Uses of Baobab Products

Rural communities in some African developing countries depend on products and services from baobab trees for their livelihoods. In northern Namibia, the rural communities consider all parts of the baobab tree to be useful and they obtain benefits such as food, medicine, fiber, fodder, materials for crafts, aesthetics, and spiritual services (Lisao *et al.*, 2017). All parts of the tree are used for traditional medicine although the medicinal purpose differ from country to country. Leaves, fruits, seeds, stems, and roots are used as a traditional remedy to treat conditions such as malaria, fever, diarrhea, dysentery, asthma, and inflammation among other illnesses (Rahul *et al.*, 2015). The leaves and pulp are used to stimulate the immune system (De Caluwé *et al.*, 2009). Indians use baobab pulp to treat diarrhea and young leaves as a remedy for swellings (Sidibe and Williams, 2002).

Leaves are also used to treat different conditions such as infections of the urinary tract and Guinea worms (Sidibe and Williams, 2002), and as an insect repellant in West Africa (Denloye, et al., 2006). The seed oil is utilized against loose bowels and hiccups (De Caluwé *et al.*, 2009). In Africa, the bark is used to treat malaria and paste made from the fruit pulp is used to treat swollen joints (Wickens, G.E., 2008). Baobab's medicinal properties include; anti-oxidant, pre-biotic-like activity, antipyretic, anti-inflammatory, anti-dysentery, and anti-diarrhea (Sidibe and Williams, 2002).

Baobab pulp is rich in carbohydrates (in form of sugars and pectin) and is currently used in a variety of formulations such as juices, sauces, yogurt, and as an appetizer in seasoning (Christine *et al.*, 2010). Also, the dry pulp is either eaten directly or dissolved in water or milk to make a beverage (Sidibe and Williams, 2002). The crude oil obtained from baobab seeds is used in cosmetics due to its high fatty acid composition (Kamatou *et al.*, 2011) and to treat skin diseases because it does not irritate or cause allergic reactions (Sidibe and Williams, 2002). Additionally, crude oil obtained from baobab seeds is suitable for cosmetics and pharmaceutical industries because it is excellent in restoring and re-moisturizing the skin. The oil is rich in vitamin A and vitamin F for the rejuvenation and cell integrity, and vitamin E for antioxidant and anti-aging (Muthai *et al.*, 2017). It also contain vitamin D_3 which helps in increasing calcium absorption and reducing blood pressure (Nyam *et al.*, 2009). Despite the nutritional components of baobab seed oil, it contains a high degree of cyclopropenoid fatty acid (CPFA) which is dangerous to human health and perceived to be carcinogenic (Msalilwa *et al.*, 2020). It contains CPFA at a range between 10-12.8% (Msalilwa *et al.*, 2020) which is above the 0.4% minimum allowable limits. In Kenya, extracted pulp powder is used in a wide range of consumer products such as juices, smoothies, ice creams, herbal teas, cereal bars, biscuits, and chocolates. Baobab seeds are also coated with a colored, fragrant sugar layer to make baobab candies which are locally known as *Mabuyu* or *Ubuyu* which are commonly made and marketed in coastal and other parts of Kenya (Lisa et al., 2019).

2.3 Proximate and Nutritional Composition of Baobab Fruit Pulp

Baobab pulp contains moisture content of between 8.81 and 10.4% (wet basis) with those from Kenya and Mali having the highest moisture content compared those from Zambia (Osman, 2004; Muthai et al., 2017; Stadlmayr et al., 2013). The low moisture content is due to low annual rainfall, high temperatures, sunlight, and wind exposure which has been reported to contribute to dryness (Abiona DL *et al.*, 2015). The baobab fruit pulp (BFP) is an excellent source of carbohydrates in form of pectin and sugars. Pectin ranges between 61 to 71% (Edogbanya, 2016; Coe et al., 2013; Chadare et al., 2009) while total sugars ranges between 16.9 to 25.3% (Asogwa *et al.*, 2021). Different studies have reported a low amount of crude protein between 1.86 to 8.2% that is contained by the pulp (Muthai et al., 2017; Edogbanya, 2016; Sidibe & Williams, 2002). The fat content of pulp is extremely low with levels reported by different studies to range from 0.3 to 13% (Osman, 2004; Muthai et al., 2017; Ibrahima et al., 2013) and fiber content ranging between 4.0 to 28.0% (Stadlmayr et al., 2013; Osman, 2004; Ibrahima et al., 2013).

The ash content of different varieties of BFP from different ecological zones is reported to range between 3.86 and 5.0% (Muthai et al., 2017; Abiona DL et al., 2015; Stadlmayr et al., 2013). The pulp is an excellent source of potassium, calcium, and magnesium but a poor source of zinc, iron, and copper. The high calcium content of the fruit makes it natural calcium supplementation for young and elderly as well as pregnant and lactating mothers (Assogbadjo *et al.*, 2012). Both seeds and pulps contain high amounts of amino acids (glutamic acids, aspartic acids, and arginine) and are low in sulphur-containing amino acids (Sidibe and Williams, 2002). Additionally, BFP contains several vitamins which include vitamins A, F, C, D_3, E, and B (Nyam *et al.*, 2009). Baobab fruit has been referred to as a 'super fruit' because of the high amount of vitamin C and fiber it contains. Chadare et al (2009) reported that consumption of 40g of BFP by a pregnant woman (19-30 years) provides 100% of the daily requirement of vitamin C. Various studies have revealed that the vitamin C content of BFP ranges between 60.0 to 467.08.1mg/100g (Dandago, 2016; Eldoom et al., 2014; Chadare et al., 2009; Ibrahima et al., 2013).

In addition to both macro and micronutrients, it contains many different phenolic compounds such as procyanidin, epicatechin, gallic acid, hydroxycinnamic acid, glycosides (Ibrahima *et al.*, 2013) tannins, phenols, and flavonoids (Kamatou *et al.*, 2011). These compounds are linked to various biological properties such as anti-microbial, anti-oxidant and anti-inflammatory activity (Ismail *et al.*, 2019). These polyphenols together with the high vitamin C content of the pulp make baobab fruit superior in preventing oxidation activity in the human body (Ibrahima *et al.*, 2013).

2.4 Commercialization of Baobab Fruit Pulp

Baobab fruits are collected either in small or large-scale quantities and sold to vendors or commercial companies for processing into powder, candies, fruit juice, seed oil, and other valuable products (Ismail et al., 2019). Some rural African communities bartered baobab fruits for other useful food items or sold them to generate income that supports the livelihoods of the people (De Caluwé *et al.*, 2009). In Zimbabwe, more than 5000 rural producers are engaged in exporting baobab pulp to European countries, with many involved in selling fruits on local markets (Wynberg *et al.*, 2015). The demand for baobab pulp has recently moved to global markets after being certified as a novel food ingredient by Food and Drug Administration (FDA) allowing it to be traded and applied in European food and cosmetic industries (Christine *et al.*, 2010). This gave an additional valuable ingredient to the food, cosmetic and pharmaceutical industries both locally and abroad. Luckert et al. (2014) reported that every household in South Africa is gaining between US$ 350 and US$ 1500 per year from the direct or indirect business of baobab pulp. Baobab pulp is expected to earn up to US$1 billion annually for producer countries (Wynberg *et al.*, 2015).

The sales of baobab pulp in the United Kingdom have increased significantly due to its uses in several commercial products (Wang *et al.*, 2017). According to the baobab research report of the year 2020, the global market is projected to reach US$ 3.75 billion by 2024 and grow at a significant Compound Annual Growth Rate (CAGR) of 9.4% during the period from 2019 to 2024. Also, according to Market Research Future. (2021), the global market for BFP is showing healthy growth and is expected to grow at a CAGR

of 8.5% between 2021 and 2027. The global market for baobab powder is expected to reach US$ 10 billion (€ 9.3 billion) by 2027 (Future Market Insights., 2021). This growth is driven by an increase in demand for nutrient-rich and antioxidant-rich organic products in the global health and wellness industry. In addition, the rising awareness of the health benefits of BFP is also driving market growth. Europe is the world's largest market for baobab powder, accounting for 25% of the global market in 2017. The market for baobab powder in Western Europe is anticipated to expand at an average annual rate of 6.3% and 2.6% in terms of value and volume from 2017 to 2027 (Future Market Insights., 2021). Innova Market Insights. (2019) reported that 52% of all food and beverage launches with baobab occurred in Europe.

2.5 Quality Control of Baobab Fruit Pulp

Quality control is considered as the activities involved in the food chain to avoid production, storage, distribution, marketing, traceability, and safety problems (Chen *et al.*, 2021). The baobab pulp business presents a lucrative business opportunity to rural communities, vendors, and processors especially due to its nutritious content and certification by Food and Drug Administration. The rising demand for baobab pulp worldwide has created the need to quality control in order to guarantee quality, safety and compliance to the set standards (Munissi et al., 2022). Conventional methods of BFP quality assessment are subjective and highly based on external attributes such as appearance, color, freshness, texture, presence of debris and insects, and freedom of decay (Munissi et al., 2022). Sensory parameters, which are frequently linked to the internal composition of fresh produce, have emerged as important factors that determine the consumers' perceptions of the quality (Magwaza and Opara, 2015). Consumers and even small-scale processors consider BFP with a smooth, creamy texture, pale yellow to off-white color, and unique citrus-like flavor, which is often described as tangy or sour, to be of high quality (Mpofu et al., 2014).

With the advancement in technology and improvement in income and living standards, objective methods employing modern technologies, which are quite accurate and reliable, are increasingly replacing the commonly used conventional methods of fruit quality

assessment (Nguyen et al., 2014). Commercially, the organoleptic quality of fruit is currently evaluated by measuring total soluble solids (TSS) and total titratable acidity (TTA) which contributes to sweetness and flavor (Chen and Opara, 2013). Currently, the most significant quality criteria to indicate sweetness used by the industry to establish marketing standards is the TSS content, which is typically determined from extracted juice using a refractometer (Kader, 2002). However, TSS is majorly composed of 75-85% sugar and the remaining components constitutes dissolved acids and minerals, and phenolic compounds (Magwaza and Opara, 2015). Another factor shaping consumers' perception of the flavor of the fruit is its TTA. This is often measured in the laboratory by extracting the juice from the fruit and titrating it against a known concentration of a base usually 0.1N sodium hydroxide (Kader, 2002). Apart from the appearance, texture, and flavor of fruits, other factors such as nutritional value (carbohydrates, proteins, lipids, vitamins, and minerals) and safety (naturally occurring toxicants, contaminants, mycotoxins, and microbial contamination) influence consumers' purchase decision and are considered during quality evaluation (Ncama *et al.*, 2017). Objective methods of fruit quality assessment are typically more reliable and accurate than subjective methods which are generally less reliable as they are influenced by personal bias or subjective interpretation (Lorente *et al.*, 2012).

2.6 Baobab Value Chain in Kenya

BFP is gaining popularity in Kenya and worldwide as a nutritious superfood due to its high nutrient content and interests from health-conscious consumers. Baobab fruit harvesting and processing provides income opportunities to rural communities in Kenya's arid and semi-arid lands where the baobab trees grow (Fischer et al., 2020). During the harvesting season, local women often pick the baobab fruits by hand (Meinhold & Darr, 2022). The work is labor-intensive, requiring the fruit to be cracked open and seeds separated from the chalky white pulp. But it provides jobs for female pickers, pulp producers, transporters, and processors in rural villages. These roles in the baobab value chain help generate incomes for women and their families (Meinhold & Darr, 2022). Once harvested, the BFP must undergo processing to produce the final product. The fresh pulp

is manually deseeded, then sun-dried or dehydrated to remove moisture (Muthai *et al.*, 2017). After drying, mills grind the pulp into a fine powder. This multi-step production process often occurs in small community facilities, often powered by manual labor instead of machines. However, it provides local employment opportunities for those involved in the production (Momanyi et al., 2019).

Some key companies in Kenya processing and exporting BFP include Vokenel Limited and Ecovibes Africa Investment Limited. These companies partner with fruit harvesters, then handle processing, packaging, and distribution of the baobab powder. They sell the packaged pulp in powdered form, under their brands, to Kenyan and export markets. Exporting processed Kenyan baobab powder to Europe, the US, and Asia is an important part of the value chain, with the supplement and nutrition industries as major markets (Egbadzor et al., 2023). The major challenges in the baobab value chain include lack of organization among producers, lack of processing equipment, need for consistent quality standards, and biopiracy of baobab trees. The unlawful harvesting and export of baobab trees deprives local communities in Kenya of natural resources while destroying vulnerable tree populations before their benefits are fully explored (Odhiambo., 2023). Implementation and enforcement of an outright ban on the export of whole baobab trees could help alleviate this challenge by making it illegal to transport these uprooted trees across borders.

2.7 Baobab Fruit Processing

After harvesting, the baobab fruits are transported to processing sites, where the fruits are thoroughly cleaned to remove the fur in the shells before dehusking. The hard outer shells of the fruits are cracked open, often by pounding with a mortar and pestle. This breaks open the hairy coating to reveal the white powdery pulp, fibers, and seeds inside. On a large commercial scale, baobab fruits are dehusked mechanically using specialized equipment such as roller crushers. This machine is consisting of two parallel rotating rollers with ridges that crush and shear off the hard shells as fruits pass through (Munyawiri et al., 2022). Direct steam treatment (90°C to 100°C) is at times applied to intact baobab fruits to loosen and soften the pulp inside, making it easier to extract and

separate fibers and seeds from the pulp (Galanakis, 2012). After dehusking, the content is sieved to separate the seeds and fibers before drying and milling of the pulp into a fine powder (De Caluwé et al., 2009).

Sun drying, solar drying, spray drying or oven drying are methods used to achieve the desired moisture specifications for the powder (Mpofu et al., 2014). Drying is aimed at reducing the high moisture content and water activity of the fresh pulp to make it shelf stable (Mpofu et al., 2014). Industrial pulp producers use thermal drying such as spray drying or heating using kilns (Mpofu et al., 2014). The dried pulp is ground into powder using mechanical mills like hammer mills or attrition mills. This produces the final baobab fruit pulp powder which is then packaged, sealed, and stored awaiting for sale and distribution (Mpofu et al., 2014). The coarsely ground powder is further micronized into finer powder to enable formulation into different matrices.

Sieving and straining separate the fibers from the pulp during baobab fruit processing (Mpofu et al., 2014). The fibers are dried along with the pulp, but not incorporated into the final powder. Traditionally, the fibers were discarded as waste or used as animal feed or cooking fuel (Chadare et al., 2009). But recently, fibers have been incorporated into compost as organic matter (Mwale et al., 2016). Additional treatments are also subjected to the fiber to extract remaining nutrients like pectins, cellulose and hemicellulose (Boukari et al., 2021). The fibers can also be used to reinforce composite materials like bioplastics (Manjang et al., 2022).

The seeds are cold-pressed to extract baobab seed oil for use in cosmetics (Chadare et al., 2009). The crude oil typically undergoes refining processes like degumming, neutralization, bleaching and deodorization to remove impurities and improve aroma, flavor, color and stability (Gebauer et al., 2002). This produces a refined baobab seed oil suitable for consumption and cosmetic use. The refined seed oil is then packaged into containers like glass bottles, plastic bottles, or metal cans (Silva et al., 2021). Packaged baobab seed oil is distributed to retailers, wholesalers, and industrial buyers. It can be branded and marketed based on origin, sustainably wild-harvested, cold-pressed, organic, etc (Jasinska et al., 2006).

2.8 Postharvest Handling of Baobab Fruit Pulp

BFP storability and shelf-life depend on several intrinsic and extrinsic factors. The intrinsic factors (e.g., maturity stage, moisture content, and nutrient composition) and extrinsic factors (e.g., temperature, humidity, pest and diseases, packaging, gases, and vapors) affect physical, chemical, and biochemical changes in stored fruits (Li *et al.*, 2017). Temperature and type of packaging materials are the most important factors affecting food deterioration and the shelf life can be extended by controlling these parameters (Li et al., 2017). The blackening of BFP is a result of enzymatic activity on phenolic compounds and ascorbic acids. The reaction is attributed to the initial enzymatic oxidation of phenols into slightly colored quinines following polymerization (Zhu *et al.*, 2010).

Extracted baobab pulp is liable to deterioration on exposure to environmental conditions. For instance, exposure to heat, oxygen, moisture, and light accelerate chemical reactions leading to nutrient loss (Chadare, 2010). Poor handling and storage of BFP often trigger a decline in nutritional quality and unfavorable color changes resulting in postharvest losses. Dandago. (2016) studied the effects of storage conditions on the ascorbic acid content of BFP and reported an overall decrease in vitamin C content during storage. The author also recommended storage of pulp inside a refrigerator, with unbroken pods, and wrapped in black polythene to preserve the ascorbic acid content. Packaging has significant effects on the nutritional value of BFP especially vitamin C, total titratable acidity (TTA), ash, moisture, pH, and total and reducing sugar content (Eldoom *et al.*, 2014).

2.9 Baobab Fruit Pulp Adulteration

Food fraud is any suspected deliberate action committed when a person intentionally decides to deceive customers about the quality and/or content of the food they are purchasing to gain an undue financial advantage (FAO, 2021). The main motivating factor for food adulteration is economic since the adulterants used are cheaper or they are added to cover the low quality of the original product and consequently increase the price of the product (Galvin-King *et al.*, 2018). It is estimated that around 22% of foods are

adulterated yearly (Pal and Mahinder, 2020) with an estimated cost implication of US $49 billion (McGrath *et al.,* 2018). This high economic loss related to food adulteration is attributed to a lack of detection techniques and a rampant increase in malicious fraudsters (Bouzembrak and Marvin, 2016). Other factors contributing to food adulteration opportunities are; the increase in the complexity of supply networks, advancement in technology, and modernization (Meerza and Gustafson, 2018). Much interest has been directed to adulterations that have serious health implications and less directed to adulteration on economic aspects (Oliveira *et al.*, 2019). Some of the cases of food adulteration that have been reported include; the adulteration of paprika powder with lead oxides (Everstine., 2013), the adulteration of cumin with almond peel in the UK (Everstine et al., 2013), and the adulteration of spices with Sudan dye (Kearney., 2010). Adulteration of baobab powder with cereal flours has been reported with the main motivation being weight increase for economic gains (Chepngeno *et al.*, 2022).

2.10 Near-infrared Spectrometer

For the past 40 years, near-infrared (NIR) spectrometer (wavelength range of 800-2,500 nm or 12,500 to 4,000cm^{-1}) has emerged as one of the most popular and widely used techniques for food analysis and quality control (Liu *et al.*, 2015). It is a non-destructive analytical tool that enables quick and simultaneous means for qualitative and quantitative assessment of various samples concerning their chemical and physical composition (Ozaki *et al.,* 2006). The NIR spectrometer serves as the best alternative for the determination of parameters characterizing the quality of fruits since it non-invasive and provide real-time analysis of samples. It is also quick, simple, cost effective and require minimal or no sample preparation (Hao *et al.*, 2022). Miniaturization of NIR spectrometer has led to the development of portable NIR devices that has led to the additional speed, accuracy, simplicity, cost-effectiveness, and convenience (Amuah *et al.*, 2019; Wang *et al.*, 2020). Figure 2.2 shows a portable NIR spectrometer in the wavelength range of 900-1700 nm

Figure 2.2: Portable/handheld NIR spectrometer (Model: NIR-S-G1, Tellspec, Toronto, Canada).

2.11 Principles of Near-infrared Spectrometer

NIR spectrometer is a technique based on the absorption of electromagnetic radiation in the near-infrared region of the electromagnetic spectrum (Shaw et al., 2022; Mishra et al., 2022). It relies on the molecular overtone and combination vibrations involving C-H, O-H, and N-H functional groups (Roger et al., 2020). The fundamental principle behind NIR spectrometer involves illuminating a sample with NIR light and measuring how much light is absorbed at each wavelength (Workman, 2020). The energies associated with NIR photons are low enough that they allow overtones and combinations of fundamental molecular vibrations to be excited. As a result, the positions and intensities of the absorption peaks in an NIR spectrum provide a unique molecular 'fingerprint' corresponding to the sample composition (Rinnan., 2021). During NIR analysis, a broadband NIR light source illuminates the sample, and the transmitted or reflected light is measured by a detector. The obtained spectrum depicts the absorbance intensities across the NIR region, governed by the Beer-Lambert law. Chemometric techniques are then utilized to correlate the absorption patterns to the chemical information of interest, which allows qualitative and quantitative analysis of sample properties (Rinnan., 2021).

2.12 Instrumentation of NIR spectrometer

The main components of the Tellspec enterprise scanner are a light source, wavelength selection, and a detector (Figure 2.3). This commercial spectrometer uses two integrated

tungsten halogen lamps. These lamps are thermal emitters where tungsten filament is resistively heated to high temperatures to emit broadband NIR light (Beć *et al.*, 2021). These lamps are reliable and inexpensive therefore providing stable output once thermally equilibrated. However, thermal stability can be a concern in handheld spectrometers which experience fluctuating external temperatures and have limited thermal mass (Beć *et al.*, 2021).

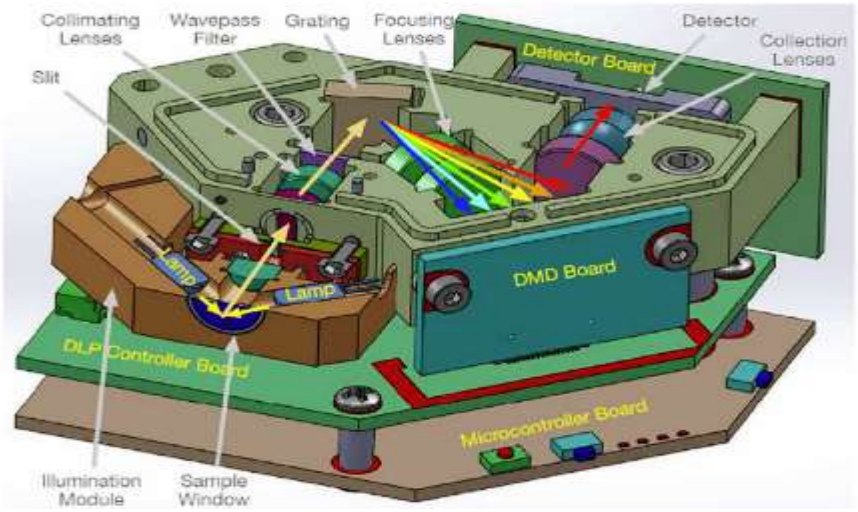

Figure 2.3: Main components of a portable NIR spectrometer

Source: (Chen et al., 2020).

Other commercial portable scanners use light-emitting diodes (LEDs). LEDs operate via electronic recombination in semiconductors, emitting photons (Lu et al., 2019). They offer compact size, low power consumption, durability, and low cost (Huang *et al.*, 2018). LEDs covering the visible/short-wave NIR are used in some miniaturized spectrometers emphasizing compactness over bandwidth (Masawat et al., 2020).

Wavelength selection is a critical component of spectrometer design, and digital light processing (DLP) offers an effective approach for a miniaturized NIR spectrometer. By utilizing a digital micromirror device (DMD), the DLP modulate incident light intensity and filter specific wavelengths by tilting the micromirrors to direct light either to the detector or away from it (Huang *et al.*, 2020). Careful selection of the wavelengths

sampled by selectively tilting micromirrors arrays allows the spectrometer to isolate and measure light intensity at targeted wavelengths across the NIR spectrum (Ou *et al.*, 2022). DLP thus provides a pathway to create a highly compact spectrometer with versatile wavelength tuning capabilities ideal for ultraportable device (Jakubíková *et al.*, 2016). The programmable nature of the DMD enables flexible spectral filtering tailored to the analytes of interest.

The indium gallium arsenide (InGaAs) photodetector is a critical component providing high sensitivity and low noise detection across the near-infrared spectral range of the compact spectrometer (Ou *et al.*, 2022). InGaAs has a wider bandgap compared to silicon detectors, allowing detection of photons from ~0.8 to 1.7 μm wavelength (Beć *et al.*, 2022). This covers the 900-1700 nm span of the NIR spectrum targeted by the spectrometer. The InGaAs detector also exhibits high quantum efficiency of over 80% across much of the NIR band (Huang *et al.*, 2018). This enables efficient conversion of the filtered NIR light into electrical charge carriers and a strong electrical signal. InGaAs can operate at high speeds required for scanning the programmable micromirror filters across the NIR spectrum (Beć *et al.*, 2022). Along with having a small footprint amenable to miniaturization, these attributes make InGaAs an ideal photodetector choice. It provides the sensitivity, resolution, and rapid response needed for the spectrometer to acquire high-quality NIR spectra for mobile analytical applications (Zhou *et al.*, 2016).

2.13 Interpretation of NIR Spectra

The near-infrared region of an electromagnetic spectrum ranges from the end of the visible region to the beginning of the infrared (IR) spectral region i.e. between 700-2500 nm. This region is characterized by absorption bands that are related to overtones and combination bands for the C-H, O-H, and N-H functional groups (Liu et al., 2015). An overtone is a higher-frequency signal that is produced when an object vibrates or stretches. When two or more vibrational modes of a molecule overlap or interact with each other, they produce a combination band in the spectrum.

Figure 2.4 shows absorption bands for different functional groups at a specific wavelength within the NIR region of an electromagnetic spectrum.First, second, and third overtone C-H absorption bands occur at around 1500-2000 nm, 1000-1600 nm, and 700-1100 nm, respectively (Workman and Weyer, 2007). The combination bands occur at around 1300-1500 nm and 2100-2500 nm (Ismail et al., 2005). The hydroxyl group (OH) representing water molecule in the matrix has absorption at around 1950 nm, 1450 nm, 1000 nm, and 750 nm for the combination band, first, second, and third overtones respectively (Rongtong *et al.*, 2018).

The N-H absorption bands are located around 2200 nm, 1950 nm, 1500 nm, 1050 nm, and 850 nm for combination band, first, second, and third overtones respectively (Liu et al., 2015). The C-H, O-H, and N-H functional groups represent H_2O, ROH, and NH_2 functional groups i.e. water molecules, carbohydrates, and proteins (Cen and He, 2007). Most chemical molecules exhibit NIR absorptions at specific wavelengths and therefore can be used for quantitative and qualitative assessment of an organic matter. NIR absorption bands are 10-100 times weaker compared to those of mid-IR spectrometer and this is advantageous to the analysis of strongly absorbing and high light scattering matrices like powders and pastes. NIR absorption bands are very broad and highly overlapping and it contains both chemical and physical information of samples being analyzed.

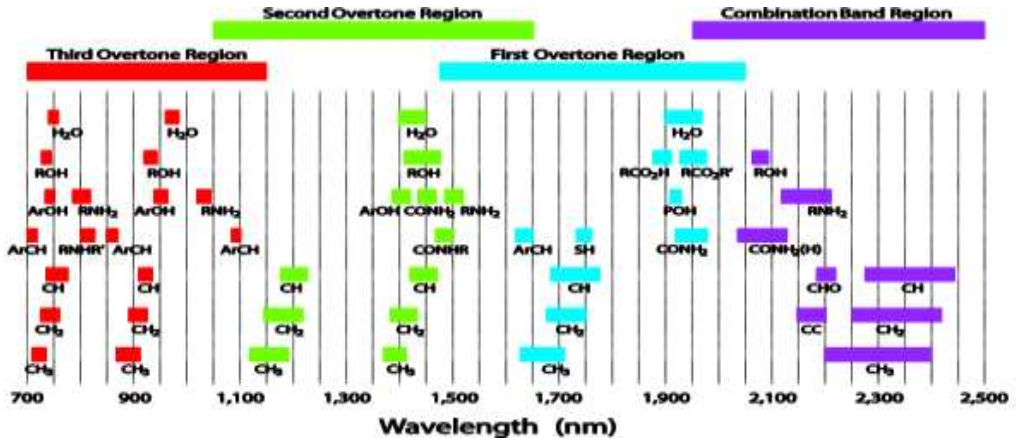

Figure 2.4: Major bands and their relative peak positions for prominent near-infrared absorptions

Source: (Liu et al., 2015).

2.14 Chemometrics in NIR Spectrometer

2.14.1 Spectral Pre-processing

Chemometrics is the scientific field that deals with the mathematical and statistical analysis of chemical data. It combines the principles of chemistry and mathematics to extract meaningful information from complex chemical data sets with the main motive of developing algorithms and models that can be used to process and interpret chemical data more efficiently and accurately. Interest in NIR spectrometer has risen due to the improvement in the instrumentation and software, and the development of chemometrics making the interpretation of NIR spectra easy (Roggo *et al.*, 2007). The main chemometric techniques comprise spectral pre-treatments, classification, and regression methods.

Spectral pre-processing involves a set of techniques that are used to remove artifacts, noise, and interferences in the spectra and the process improves the quality and usefulness of spectral data before analysis. The NIR spectra can be negatively affected by the sample particle sizes, variations of the optical path length, and crystalline forms. To avoid these interferences, spectral pretreatments are applied to the spectra. The most commonly used pretreatment methods include multiplicative scatter correction (MSC), standard normal

variate (SNV), Savitzky Golay (SG) derivatives, mean centering (MC), and autoscaling (AS) (Roggo *et al.*, 2007). Multiplicative scatter correction (MSC) is applied to the spectra to correct additive effects caused by light scattering. It is a row-oriented transformation that removes physical effects like particle size and surface blaze from the spectra. By MSC, it is presumed that each spectrum is determined by both actual sample characteristics and particle size, and using standard spectrum, the particle size can be represented by a baseline effect and the trend. This method then corrects the differences between the baseline and the trend in the spectrum (Maleki *et al.*, 2007). The MSC transformation is executed through the equation below;

$$x_{ik(new)} = \frac{[x_{ik(old)} - a_i]}{b_i}, \qquad \text{Equation 2.1}$$

where; xik(old) and xik(new) are the optical values before and after MSC transformation in k wavelengths; ai is the estimated effect of specular reflection in the sample; i and (1/bi) are the estimated scatter interferences in sample i.

Standard normal variate (SNV) is the second most used pre-processing method after MSC. The SNV transformation is often used to correct for variations in the intensity of different wavelengths caused by changes in the measurement conditions, such as the sample size or the instrument used to measure the spectra. The SNV spectral preprocessing involves transforming the original spectra by subtracting the mean and dividing by the standard deviation at each wavelength (Olmos *et al.*, 2018). This is done according the following formula;

$$Z = \frac{X - mu}{Sigma\ Z'} \qquad \text{Equation 2.2}$$

where X is the original spectra, mu is the mean of the spectra at each wavelength, and sigma Z is the standard deviation of the spectra at each wavelength. This transformation results in a new set of spectra that follows a standard normal distribution with a mean of 0 and a standard deviation of 1 at each wavelength.

The SG derivatives is a digital filter that is used for resolving overlapped band characteristics to NIR spectra thus bringing out spectral information hidden in raw spectra (Yao and Lewis, 2010). It increases the precision of data without distorting the chemical

information contained in the data. It does this through a process known as convolution where adjacent spectral data points are fitted by a low degree of polynomial through linear least squares. This is achieved mathematically through the following equation;

$$Y^{*}\,\mathrm{j} = \frac{\sum_{i=-m}^{m} C_i Y_{j+i}}{N}, \qquad \text{Equation 2.3}$$

where Y is the raw spectra, Y^{*} is the transformed spectra, C_i is the convolution coefficient for the i^{th} spectral value of the filter within the filter window and N is the number of convolution integers, m is the half-width of the filter window and index j is the running index of the original ordinate data table.

Mean centering (MC) is a preferred spectral pre-processing technique that is used for resolution enhancement. It ensures that mean-centered spectra are interpreted in terms of variation around the mean (Iacobucci *et al.*, 2016). Mean centering is mathematically done as per equation 8;

$$MC\ spectra = X_1 - \bar{X}_1, \qquad \text{Equation 2.4}$$

where X_1 is the absorbance value and $\bar{X}_1$ represent the mean absorbance.

Autoscaling (AS) implies mean centering and dividing the spectra values by their standard deviation. This means that auto-scaled spectra have means equal to zero and standard deviation equal to one (Olmos *et al.*, 2018). Autoscaling is executed according to equation 9;

$$AS\ Spectra = \frac{X_1 - \bar{X}_1}{SD}, \qquad \text{Equation 2.5}$$

where SD is the standard deviation.

Therefore, pre-processing NIR spectra before multivariate analysis is important in improving the quality of the spectral data, reducing background noise and variations not related to samples, and identifying the most important variables for modeling, leading to more accurate and reliable models.

2.14.2 Multivariate Modelling

Multivariate modelling refers to statistical techniques that are used analyze complex data that contains multiple variables. The principal component analysis (PCA) is a dimensionality reduction method that is used for unsupervised classification purposes. It does this by finding the directions in which the data varies the most, and projecting them onto a new set of axes that are related to each other. The resulting axes are called principal components, and the number of principal components is usually less than the original number of variables in the data. The PCA is often used to pre-process data before performing other statistical analyses, such as regression or clustering. It can be used to reduce the complexity of the data, visualize the data in two or three dimensions, and identify patterns or trends in the data (Lavine *et al.*, 2006). The maximum of the total variance is accounted for by the first principal component (PC1), the maximum of the residual variance is accounted for by the second principal component (PC2), and so on, until the maximum of the total variance is accounted for (Berrueta *et al.*, 2007). It is paramount to retain those principal components that account for the highest percentage of the total variance explained. The correlation coefficients between variables and the principal components are called loadings. The values that represent the samples in the space defined by the principal components are called scores (Tewari and Irudayaraj, 2005).

Partial least square discriminant analysis (PLS-DA) is an all-round algorithm that is used for supervised classification purposes (Barker and Rayens, 2003). The PLS-DA is used to classify different groups of samples. It does this by linking X (spectral data) and Y (groups or class membership) and can handle multiple dependent categorical variables (Barker and Rayens, 2003). It is useful for modeling high-dimensional data since it integrates dimensionality reduction and discriminant analysis into one approach. The PLS-DA modelling has been applied in diverse fields such as forensic science, banking, medical diagnosis, food analysis, metabolomics, and soil science (Lee *et al.*, 2018). By locating a linear subspace of the explanatory variables, this method aims to maximize the covariance between the independent variables (spectral data) and the corresponding dependent

variable Y (reference data) of highly multidimensional data. This new subspace enables the estimation of the Y variable based on fewer factors. Factors also referred to as latent variables or PLS components.

The PLS-DA method is able to handle highly colinear and noisy spectroscopic data (Millington and Stevens, 2011). In addition, PLS-DA provides information on wavelengths or variables that took the major role in modelling process (Mehmood et al., 2011; Krishnan et al., 2011). The PLS-DA generates low-dimensional and easily interpretable score plots that provide a visual interpretation of complex datasets. These score plots illustrate the discrimination between different groups and assign a class entry of either 0 or 1 depending on the class to which the samples are assigned (Worley *et al.*, 2013). Combination of score and loading plots facilitates the investigations of important variables that are relevant to the specific groups of interest (Hasegawa and Funatsu, 2012).

Partial least square (PLS) regression is a data reduction and modelling method for spectroscopic data. It is similar to PCA in extracting components or factors but differs in that both spectral and reference data are used together to construct a prediction model (Passos *et al.*, 2019). The reference data, also known as chemical data collected from wet chemistry analysis are used to find patterns in spectral data and correlate with them. The goal of PLS is to determine components in the spectral data that have the greatest correlation with the desired value in chemical data while also describing as much as possible the relevant variations in the input variables (Berrueta *et al.*, 2007). To be specific, PLS models both spectral and reference data simultaneously and identifies latent variables in spectral data that will predict the latent variables in the reference data.

A latent variable is a group of underlying variables that influences the relationship between the larger sets of data matrices i.e. spectral and reference data. The PLS components are like principal components but are referred to as factors. An optimal number of factors or latent variables can be obtained by using cross-validation or external test sets. These factors are critical in constructing a robust model. A higher or lower number of factors will result in over-fitting and under-fitting the models, respectively.

When developing models, too many factors will result in more worthless information and dimensions, while too few components will result in a lack of key features in the spectrum data (Sisouane *et al.*, 2017).

2.14.3 Validation of the Models

Validating a model means checking how well the model will perform on new data of the same kind that was used in developing the model. It estimates the uncertainty of future predictions that may be made with the model and if the uncertainty is reasonably low, the model can be considered valid and robust. After the successful construction of models, it is important to determine its ability to predict the unknown concentration of response (y values). An ideal parameter for estimating calibration errors is the root means square error of calibration (RMSEC). It calculates the average difference between the predicted and reference values and provides a general assessment of how well the model fits the data (how well the model predicts the same samples that were used to calculate the model). The main disadvantage of RMSEC is that it is an estimation of the model error and not of the prediction error (Ziegel, 2004). Prediction testing is based on partitioning data into two sets, the calibration set (normally 75%) and the prediction set (25%). Prediction testing estimates the prediction error called room means square error of prediction (RMSEP). It is the simplest validation method since RMSEP estimates the prediction ability of the model to be used with all coefficient estimates already calculated. A drawback to this method is that a lot of samples are put aside for this purpose only which could have been used for the construction of more accurate and robust calibration models (Ziegel, 2004).

Cross-validation (RMSECV) is another method that is similar to RMSEP only that a portion of samples used in the construction of the models is set aside for validating the model. Then the values for samples that were not used for modelling are predicted and the prediction errors are computed. It does this by comparing the mean values of the predicted response versus the actual response during the construction of the model (Ziegel, 2004). The same procedure is repeated several times until every sample has been left out once. The two major versions of cross-validation, are full cross-validation and segmented cross-

validation. Full cross-validation is one that leaves only one sample at a time while segmented cross-validation leaves out a whole group of samples at a time.

R-squared (R^2) is a metric that measures the proportion of the total variation in the reference data that is explained by the model. The R^2 value ranges between 0 and 1, where a value of 1 indicates that the model explains all of the variation in the data, and a value of 0 suggests that the model explains none of the variations. In PLS regression, a high R^2 value of close to 1 indicates that the model can explain a large proportion of the variation in the actual data collected from the wet chemistry (Palermo *et al.*, 2009).

The correlation coefficient (R) is another statistical metric for assessing the performance and validity of a PLS model. It assesses the relationship between the predicted values from a PLS model and the actual observed values in the validation data set. In the context of PLS modeling, a high R between the predicted values and the actual observed values indicates that the PLS model is accurately predicting the behavior of the data. A low R may indicate that the PLS model is not accurately capturing the underlying relationships in the data, and may require further refinement or improvement (Alexopoulos, 2010). Residual prediction deviation (RPD) is also another measure of PLS model validity that is defined as the standard deviation of actual (reference values) divided by the RMSEP. The RPD provides a measure of model validity that is more objective than the RMSEP. A PLS model with an RPD of above 2 is considered robust and excellent (Davey et al., 2009; Bellon-Maurel et al., 2010).

PLS-DA models are normally assessed in terms of sensitivity, specificity, and discrimination error (Yegon et al., 2023). Sensitivity also called recall refers to the proportion of true positives (TP) that are correctly identified by the model i.e. it measures the percentage of test samples that actually belong to a particular class and are correctly classified by the model as belonging to that class. It is calculated by dividing the number of true positives (TP) by the sum of true positives (TP) and false negatives (FN). A high sensitivity indicates that the model is effective at identifying positive classes of samples (Oliveira et al., 2020). Specificity refers to the proportion of true negatives (TN) that are properly detected by the model. It is determined by dividing the number of true negatives

(TN) by the sum of true negatives (TN) and false positives (FP). A high specificity suggests that the model is robust at identifying the negative class of samples (Oliveira et al., 2020).

Discrimination error refers to the proportion of incorrect classifications made by the model. More specifically, it measures the percentage of test samples that are misclassified by the model, based on a threshold that is used to assign a sample to a particular class. It is calculated by dividing the number of misclassified samples by the total number of samples. A lower discrimination error indicates better performance of the model in accurately classifying new samples (Oliveira et al., 2020). Limits of detection (LOD) is another measure of validating PLS-DA models. The LOD is a measure of the smallest concentration of analyte that can be reliably detected by the model. It is calculated by analyzing a set of spiked samples with known concentrations of the compound of interest. The spiked samples are then analyzed using the PLS-DA model, and the LOD is defined as the lowest concentration that can be correctly classified with a certain level of confidence (Armbruster and Pry, 2008). Low LOD suggests that the PLS-DA model is robust and reliable.

2.14.4 Application of NIR Spectrometer in Quality Assessment

Near-infrared (NIR) spectrometer has emerged as an essential technology integrated into modern food quality monitoring and authentication systems (Cozzolino, 2022). It provides a potent and non-invasive analytical method for validating and quantifying the chemical constituents of biological materials (Amuah et al., 2019). The technique is based on detecting molecular vibrations stemming primarily from C-H, O-H, and N-H functional groups (Tao et al., 2021). A key advantage of NIR is its ability to penetrate deeper into samples relative to mid-infrared radiation, enabling analysis of bulk material with minimal sample preparation (Bellon-Maurel et al., 2010). This has enabled accurate quantification of complex components including proteins and carbohydrates in diverse foodstuffs via NIR spectrometer (Barbin et al., 2015). For example, prediction models based on NIR spectral data have been developed for determining strawberry soluble solids content with high accuracy ($R2 = 0.939$) (Guo et al., 2013). Mango internal quality parameters were

also assessed using visible and NIR spectrometer of intact fruit combined with multivariate partial least squares analysis (Cortés et al., 2016). Portable NIR devices coupled with chemometric analysis have been applied for on-site measurement of olive oil properties and for differentiating pineapple maturity stages (Fernández-Espinosa, 2016; Amuah et al., 2019). Moreover, NIR spectrometer has proven capable of reliable quantification of sugars, acids, anthocyanins, and other quality markers in apple crops (Beghi et al., 2013).

2.15 Gaps in Knowledge

NIR spectrometer is a non-invasive analytical tool that is used for quantitative and qualitative assessment of organic matrix. Chemometrics of data pre-processing, classifications, and regression is necessary for making sense of the vast amount of NIR data and the construction of robust models that could be used to make predictions about the composition, structure and properties of samples with high confidence. NIR spectrometer together with chemometrics techniques has been used to determine the quality indices of several different samples with high efficiency and reliability. However, to the best of my knowledge, there is no published study on the application of NIR spectrometer in the quality assessment of baobab fruits or related products.

CHAPTER THREE

MATERIALS AND METHODS

3.1 Introduction

This study aimed at evaluating the potential of a portable near-infrared (NIR) spectrometer for rapid, non-destructive and accurate determination of quality and authenticity of baobab fruit pulp (BFP). Portable NIR spectrometer (Model: NIR-S-G1, Tellspec, Toronto, Canada) with spectral range 900-1700 nm was used to scan BFP samples. Immediately after spectral data acquisition, BFP samples were subjected to wet-chemistry analyses for the determination of quality attributes. Chemometrics were adopted to remove unwanted sample variation, train and validate predictive models. Constructed models were then used to monitor the deterioration in quality attributes of stored BFP samples. Finally, the spectrometer's capacity for screening adulterated BFP was also examined.

3.2 Sample Collection and Preparation

A random experimental design, evaluating the potential of a portable NIR spectrometer for rapid and non-invasive determination of quality and authenticity of BFP was adopted. Samples were collected from Kilifi County located in the coastal part of Kenya. Kilifi County is characterized by a high prevalence of baobab trees which are well adapted to the semi-arid conditions prevailing in the region (Momanyi *et al.,* 2019). Ten fully mature baobab trees located at least 2 km apart were randomly selected. The selected trees were georeferenced for repeated sampling. The trees selected were mature and bearing fruits. At each tree, 30-40 intact and mature fruits were randomly selected and hand-picked from different spots around the tree to obtain good representation.

The freshly harvested fruits were immediately transported to the postharvest laboratory at JKUAT for sample preparation and analysis. The fruits were then thoroughly cleaned by removing the fur on the exterior part of the shell using a washing brush and manually cracked using a machete. Edible portions of the baobab (pulp) were collected after removal of the inedible portion (bark, fiber, and seeds), hand-pounded using a wooden

pestle and motor to powder, and then sifted through a 0.09-micron sieve. The resulting powder was packed in ziplock bags and stored in a deep freezer at a temperature of -20 to -25°C awaiting experiments.

Adulterants (rice, wheat, and maize flours) were purchased from a reputable miller (Kirinyaga Millers) located in Nairobi City. Packaging materials (unbleached kraft paper (UbKP) bags, and low-density polyethylene (LDPE) bags) were purchased from known dealers of packaging materials in Nairobi City.

3.3 The application of a portable near-infrared (NIR) spectrometer in non-destructive testing of baobab quality attributes

3.3.1 Spectral Acquisition

Near-infrared (NIR) spectral data were collected from 240 different pulp samples. The pulp samples were extracted from 240 individual fruits and scanned over the wavelength range of 900-1700 nm to acquire NIR absorption spectra containing 256 data points per sample. The spectrometer (Model: NIR-S-G1, Tellspec, Toronto, Canada) fitted with tungsten halogen lamps was used to scan the samples. The scanner was connected to a smartphone (Redmi 10C, Android version 12) with a pre-installed application (DC&M2) for spectral data management as shown in Figure 3.1. A microscope glass slide placed on top of the scanning window was used to hold samples for scanning. About 1.5 grams of baobab pulp was placed onto a clean glass slide before putting it at the top of a scanning window. Collected data were transferred to analytical software for processing and analysis.

Figure 3.1. Spectral data acquisition using Tellspec NIR spectrometer.

3.3.2 Total Soluble Solids (TSS) and Titratable Acidity (TTA)

Immediately after the spectral data acquisition, the TSS and TTA values of scanned samples were determined through the wet-chemistry procedures. The TSS was determined according to the method described by Jafari *et al.* (2017). Three replicates (of about 1 gram) of pulp were dissolved in 50 ml distilled water, shaken well, and filtered using a Whatman number 4 filter paper. A hand refractometer (Model PAL-S, ATAGO Co., Ltd., Japan) was used to determine the TSS by placing two to three drops of the filtrate on the refractometer prism. Between each measurement, the refractometer prism was cleaned with distilled water and then dried with tissue paper before being used again. Before the experiment, the refractometer was calibrated with distilled water containing 0 °Brix and adjusted to room temperature.

The TTA was determined using the method by Ncama *et al.* (2017), where 10 ml of the filtrate was measured and 2 to 3 drops of phenolphthalein indicator were added. The solution was titrated against 0.1N sodium hydroxide until a permanent pink solution was observed. The titer volume was recorded and the TTA (expressed as % citric acid) was calculated based on the equation below.

TTA (% Citric acid) =

$$\frac{0.0064 \times Titre\ (Volume\ of\ NaOH\ used) in\ ml \times Dilution\ Factor}{weight\ of\ the\ sample} \times 100 \qquad \text{Equation 3.1}$$

3.3.3 Vitamin C Content

The concentration of vitamin C contained in BFP samples was determined according to Vikram et al. (2005), where about 2 g of samples was weighed and extracted using 25 ml of 0.8% metaphosphoric acid. The solution was centrifuged for 10 minutes at 10,000 RPM (Revolutions per minute). Using 0.45µ microfilters, the supernatant was filtered and about 20µL injected into the high-performance liquid chromatography (HPLC) system (Model; 20A, Shimadzu Corp., Tokyo, Japan). The HPLC system comprised an autosampler, UV-VIS detector (SPD 20A) at a wavelength of 266 nm, and a C-18 ODS column. The mobile phase was 0.8% metaphosphoric acid at a 1.2 mL/min flow rate. Vitamin C standards were prepared with different concentrations ranging from 0, 10, 20, 40, 60, 80, and 100 ppm. These concentrations of vitamin C standard were used to generate a standard curve for the quantification of vitamin C content in the samples.

3.3.4 Moisture Content

The moisture content was determined using the oven drying method described by Reeb et al. (1999) where about 2 g of BFP samples was weighed into an aluminum dish and oven-dried at 105 $\pm$3°C for 3 hours. The percentage moisture content was calculated through the following equation.

$$\%\ \text{Moisture Content} = \frac{Initial\ weight - Final\ weight}{Initial\ weight} \times 100 \qquad \text{Equation 3.2}$$

3.4 The use of a portable NIR spectrometer to monitor changes in baobab quality parameters during storage

3.4.1 Storage Experimental Design and Set-up

A 2^3 factorial design experiment establishing the effect of the storage duration, storage condition and the packaging material on the quality parameters of BFP during storage was laid out. There were two levels of storage duration (before storage (M0) and after storage (M5), two levels of storage conditions (25°C/75% RH and 35°C/83% RH), and two levels of packaging ((unbleached kraft paper (UbKP), and low-density polyethylene (LDPE)). Four BFP samples of about 300 g each were weighed and packaged in UbKP and LDPE bags. UbKP bag is permeable to oxygen and moisture, while LDPE offers a moderate barrier to moisture content and oxygen. The aforementioned bags are used on daily basis at homes and retail markets for packaging, distribution and selling of BFP.

Packed BFP samples were stored for six months in incubators with pre-set temperatures and relative humidity (25°C/75% RH and 35°C/83% RH) as described by Hemery et al. (2020). The percentage relative humidity (%RH) conditions were maintained constant using saturated salt solutions, namely; sodium chloride (NaCl) for maintaining a relative humidity of 75% at 25°C and potassium chloride (KCl) for 83% at 35°C. These storage conditions were meant to imitate the climatic conditions experienced in the coastal and inland parts of Kenya. Figure 3.2 shows a schematic illustration of how the storage experiment was conducted. Spectral measurements were taken monthly starting from month zero (M0) until the end of the storage period (M5).

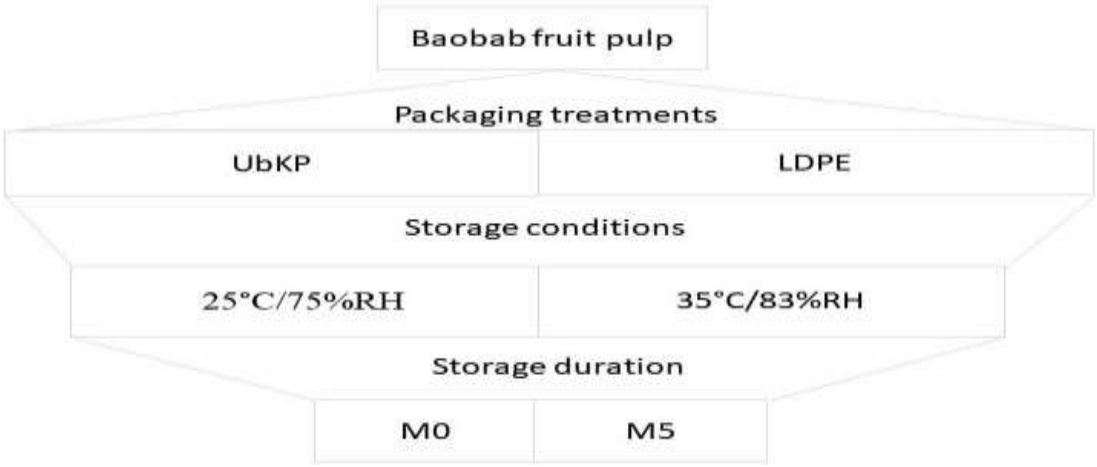

Figure 3.2. Schematic representation of the storage experiment.

NIR spectral measurements were collected monthly over the 6-month storage duration for all BFP samples under different experimental conditions. For each storage time point, approximately 1.5 g of pulp was scooped from the sample bags and placed onto a clean glass slide. The glass slide was positioned on the scanning window of a portable NIR spectrometer connected to a smartphone for spectral data collection. To obtain representative spectral measurements for each sample, triplicate scans were performed at each time point by completely replacing the pulp on the slide between replicate scans.

3.4.2 Microbial Load

3.4.2.1 Total Aerobic Count (TAC) and Total Yeasts and Moulds Count (TYMC)

The microbial load of the stored BFP samples was monitored monthly over the 6-month storage duration using standard microbial enumeration techniques. Specifically, the total aerobic counts (TAC) and total yeast and mould counts (TYMC) were determined using the total plate count method (TPC) (Arifan *et al.*, 2019). This method provides an estimate of the total number of viable bacteria and fungi in the sample. One gram from each sample (under storage experiment) was weighed into 9 ml of 0.1% (w/v) peptone water in a test tube and allowed to stand for 2 minutes while stirring using a sterile glass rod. On pre-prepared nutrient media, aliquots (0.1ml) of the sample were aseptically inoculated and spread onto the ready-to-use plate count agar (PCA agar) plates, followed by an incubation

period of 24 hours at 37°C. The colony counting method was used to count the number of colonies formed after incubation. The counts were expressed as logarithms of colony-forming units per gram (Log_{10}CFU/g) of BFP.

For the determination and enumeration of yeasts and moulds, 0.1ml of the samples was inoculated and spread onto ready-to-use violet red bile glucose (VRBGA) agar plates followed by incubation for a period of 24hrs at 37°C. Colonies were enumerated and expressed as the logarithm of colonies forming units per gram (Log_{10}cfu/g) of BFP.

3.5 The application of portable NIR spectrometer for rapid and non-destructive detection and quantification of BFP adulteration

3.5.1 Adulteration Experiment

Adulteration of BFP was done according to Oliveira *et al.* (2020) with little adjustment. Maize flour (MF), rice flour (RF) and wheat flour (WF) were deliberately and separately added to BFP at 12 different adulteration levels; 0%, 1%, 3%, 5%, 10%, 15%, 20%, 25%, 30%, 40%, 50%, and 60%. For every adulteration level, 15 replicates were prepared, making a total of 180 samples for each adulterant used. The BFP is reported to be adulterated with cereal flours by malicious fraudsters in order to add weight, extend supply and gain undeserved profits (Chepngeno *et al.*, 2022). The 12 levels of adulteration and 15 replicates each were systematically chosen to rigorously evaluate the NIR spectrometer technique over a broad contamination scope while capturing natural sample diversity through sufficient replication (Oliveira *et al.*, 2020). Afterward, the mixtures were vortexed for two minutes to obtain homogenous samples and minimize possible particle dispersion. The NIR spectral measurements were then taken for the homogenized samples. Figure 3.3 shows the experimental setup on how adulteration experiment was done.

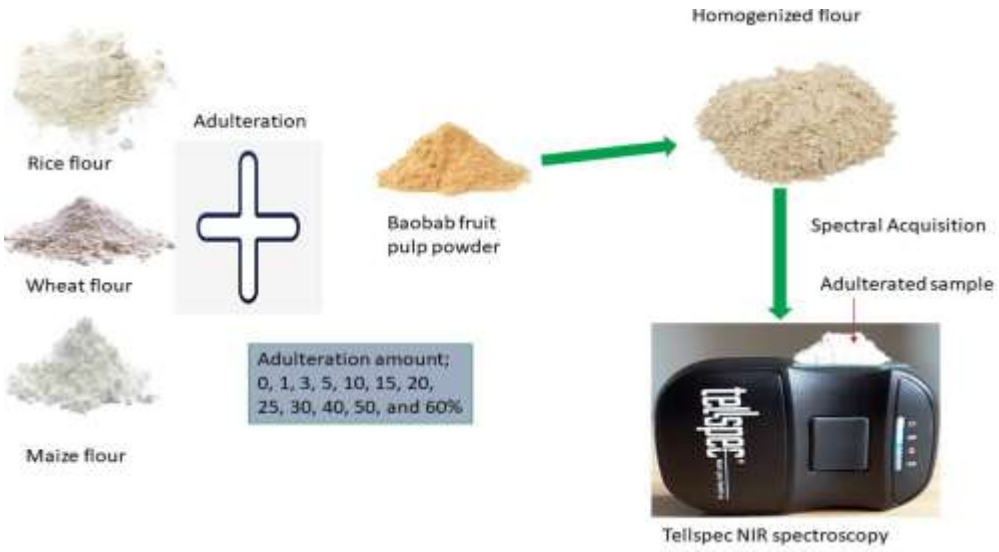

Figure 3.3: Experimental set-up for adulteration experiment.

3.5.2 Particle Size Determination

The particle size distribution for BFP and all adulterants was determined according to Buzera *et al.*(2022). A laser diffraction particle size analyzer (SALD-2300; Shimadzu Corporation, Kyoto, Japan) was used to measure the particle size distribution of samples and adulterants. This machine was equipped with a cyclone injection unit (SALD-2300 Cyclone Injection Type Dry Measurement Unit SALD-DS5) and capable of measuring particle sizes ranging from 17 nm to 2500 μm. About 5 grams of samples placed into a hopper was sucked across the laser beam by tapping the injector. The diffraction patterns formed by particles scattering light were used to determine the particle size distribution of the samples and the results were interpreted using Wing SALD II software (version 3.1.0, Shimadzu, Kyoto, Japan).

3.6 Data Preparation and Analyses

The raw spectral data were transferred to an Excel sheet (Microsoft Office Professional Plus, 2019) where they were converted into absorbances (log 1/R) before the construction of models. The mean, range, and standard deviation for the reference data were also calculated using an Excel sheet.

For the storage experiment, the data were subjected to a three-way analysis of variance using STATA MP (Version 17.0). Specifically, a three-way ANOVA (involving the main factors i.e. storage duration (A), storage conditions (B), and the packaging (C)), three-two-way interactions (AB, BC, and AC), and three-way interactions (ABC) was run to establish their effects on the quality of BFP during storage. The P value of less than 0.05 ($P<0.05$) was considered significant. Data organization and curve charts were done using MS Excel (Microsoft Office Professional Plus, 2019).

Multivariate analysis; spectral visualization, pre-processing, construction, and validation of models were done using the Unscrambler X software (CAMO Software, 0349 Oslo Norway version 10.4) and Eigenvector PLS toolbox (Solo stand-alone software, version 7.0). These software were designed for multivariate spectral data analysis and are used for the construction of calibration and predictive models.

3.7 Data Preprocessing and Partitioning

Raw spectra contain both chemical information related to the sample composition and noise signals. These unwanted noise signals interfere with the calibration models and the prediction of unknown sample composition (Rinnan *et al.*, 2009). Hence, spectral pre-processing is an essential part of chemometrics before modeling to reduce unwanted signals in the spectra (Cortés *et al.*, 2016). For this present study, raw spectra were pre-processed using multiplicative scatter correction (MSC), Savitzky Golay's first derivative (SG FD, Savitkzy Golay smoothing (SGS), and standard normal variate (SNV), mean centering (MC), and autoscaling (AS) techniques. The dataset (both spectral and reference measurements) after pre-processing with suitable techniques was randomly divided into two sets, the calibration set (75%) for the construction of models and the prediction set (25%) for validating the performance of constructed models.

3.8 Construction and Validation of Multivariate Models

3.8.1 Partial Least Square Regression (PLSR)

The spectrum contains information relating to sample molecular structure and chemical elements. This information cannot be obtained directly by visualization of the spectrum. Therefore, a bridge has to be created between spectral information and chemical attributes through multivariate modeling (Ncama *et al.*, 2017; Amuah *et al.*, 2019). The PLSR algorithm was used to build linear regression models to predict BFP quality parameters from a set of spectral data (Coury and Dillner, 2008). The NIR spectral readings were used as independent variables and the standard values as dependent variables to construct the PLSR models. To calibrate, validate (internal validation), and predict (external validation), the dataset (both spectral and wet chemistry/reference values) was randomly divided into two subsets; calibration and validation (75%) and prediction (25%).

Random cross-validation with 20 segments was used for the construction and validation of the calibration models. Specifically, the dataset used for training the model was divided into 20 groups in which all of them except one group were used for training the model. The remaining group was set aside for validating the model (internal validation). The same procedure of training the model leaving out one group of samples was repeated until all groups had been left once. The values for the samples that were not used for modeling were predicted and the prediction errors were computed. Later, an external set (prediction set) of samples was used to evaluate the performance of the constructed models. The performance of calibration models was evaluated based on the root mean square error of calibration (RMSEC) (equation 3.3) and R squared/correlation coefficient (R^2) (equation 3.4) (Amuah et al., 2019). The prediction models were validated by root mean square error of prediction (RMSEP) (equation 3.5) bias (equation 3.6), R squared (R^2) (equation 3.7), residual predictive deviation (RPD)(equation 3.8) (Liu *et al.*, 2010) and limits of detection (LODs) (equation 3.9) (Allegrini and Olivieri, 2014).

$$RMSEC = \sqrt{\sum (y_{cal} - y_{act})^2 / n,} \qquad \text{Equation 3.3}$$

$$R^2 = 1 - \frac{\sum(y_{cal} - y_{act})^2}{\sum(y_{cal} - y_{mean})^2}, \quad \text{Equation 3.4}$$

$$RMSEP = \frac{\sqrt{\sum(y_{pred} - y_{cal})^2}}{n}, \quad \text{Equation 3.5}$$

$$Bias = \frac{1}{n}\sqrt{\sum(y_{pred} - y_{act})^2}, \quad \text{Equation 3.6}$$

$$RPD = \frac{SD}{RMSEP}, \quad \text{Equation 3.7}$$

$$LOD = \frac{3 \times \sigma\sigma}{S}, \quad \text{Equation 3.8}$$

Where n is the total number of samples, y_{cal} is the predicted values, y_{act} is the reference value from wet chemistry, y_{mean} is the mean of predicted values, and y_{pred} is the predicted value of the fruit parameter, *SD* is the standard deviation of the reference data, $\sigma\sigma$ is the standard deviation of the Y-residuals and S is the slope of the calibration curve.

3.8.2 Partial Least Square Discriminant Analysis (PLS-DA)

The PLS-DA is a multivariate technique that is used for the identification of patterns and grouping of the multi-dimensional dataset into different classes or groups. In this study, the discrimination of pure and impure BFP samples as well as the classification of different types of adulterants was done using PLS-DA. Models were constructed using transformed spectra and evaluated based on sensitivity (equation 3.9), specificity (equation 3.10), and error (equation 3.11) (Oliveira et al., 2020).

$$Sensitivity = \frac{TP}{TP + FN}, \quad \text{Equation 3.9}$$

$$Specificity = \frac{TN}{TN + FP}, \quad \text{Equation 3.10}$$

$$Error = \frac{FP + FN}{TP + TN + FP + FN}, \quad \text{Equation 3.11}$$

where TP is the true positive (i.e., the number of samples that belongs to class X that are classified as truly belonging to class X), FN is the false negative (i.e., the number of samples that belongs to class X, but not classified as belonging to class X), TN is the true negative (i.e., the number of samples not belonging to class X and truly classified as not belonging to class X), and FP is the false positive (i.e., the number of samples that do not belong to class X and are classified as not belonging to class X).

CHAPTER FOUR

RESULTS AND DISCUSSION

4.1 The application of a portable near-infrared (NIR) spectrometer in non-destructive testing of baobab quality attributes

4.1.1 Quality Attributes of Baobab Fruit Pulp (BFP)

To create predictive models for BFP quality attributes, reference measurements were obtained through standard wet-chemistry analyses. Quality parameters of BFP including total titratable acidity (TTA), total soluble solids (TSS), vitamin C, and moisture content were determined. These reference measurements from wet-chemistry analyses enabled the development of multivariate calibration models correlating spectral data from the portable near-infrared (NIR) spectrometer to the laboratory-based quality parameters. The reference measurements served as the known dependent variables that were predicted by the spectral data (independent variables) using chemometrics techniques like partial least squares regression (PLSR). This allowed predictive models to be constructed that could estimate BFP quality parameters rapidly and non-destructively using only NIR spectral data as input. The reference wet-chemistry analyses provided the target values necessary to train and validate predictive models for quality analysis of BFP using a portable NIR spectrometer.

4.1.2 Total Titratable Acidity (TTA)

The TTA is a measure of the concentration of acid and is typically expressed as a percentage of the weight of the sample. The acidity of BFP is largely due to the presence of organic acids such as citric acid, malic acid, tartaric acid (Tembo et al., 2017), succinic acid, and vitamin C (Chepngeno, 2018). The predominant organic acid contained in baobab fruits is citric acid (Ahmed, 2020; Chepngeno, 2018). The mean TTA of 240 BFP samples expressed as a percentage citric acid was 11.8±1.6% with a minimum of 7.3% and a maximum of 18.8% (Table 4.1). The variation in TTA was due to tree-to-tree variability, geographical location, and maturity stage of the fruit (Assogbadjo *et al.*, 2012;

Tembo *et al.*, 2017). The results of this study were close to 9.85-13.92% citric acid reported by Chepngeno. (2018) and 6.7-14.9% citric acid obtained by Stadlmayr *et al.* (2020). Also, the average TTA obtained by this study (11.8±1.6%) was not far from the 14.05% citric acid reported by Dandago. (2016). However, the TTA content of BFP was high compared to 0.175 to 0.427% reported by Ahmed. (2020) and 0.62% citric acid reported by Adedokun et al. (2021). This variation was due to geographical location, the maturity stage of the fruit, and the tree variety (Muthai *et al.*, 2017).

4.1.3 Total Soluble Solids (TSS)

The TSS content is currently the most important quality parameter that indicates the sweetness of fruits and is used by the industry to determine marketing standards (Nordey et al., 2019). The TSS is a measure of dissolved sugars (hexoses and sucrose), organic acids, vitamins, and trace elements in a food matrix. This current study reported an average TSS of 1.6 ±0.3 °Brix with the lowest and highest values of 0.7 and 2.4 °Brix, respectively (Table 4.1). These results were consistent with 1.8-2.0 °Brix reported by Chepngeno *et al.* (2018) and varied from 79.3% reported by Nour *et al.* (1980), 4.83 °Brix by Adedokun et al. (2021), and 13-15 °Brix by Ahmed. (2020). The differences in TSS reported by these authors may be due to variations in geographical location, maturity stage of fruits during harvesting, soil composition, genetic variation, and method of analysis (Chadare et al., 2010).

4.1.4 Vitamin C Content

Vitamin C is a very crucial nutrient and is considered a major selling point for BFP. Vitamin C of BFP was highly fluctuating with an average of 160.2±19.3 mg/100g. The lowest vitamin C content was 100.0 mg/100g and the highest was 205.9 mg/100g (Table 4.1). Chepngeno. (2018) reported an average vitamin C content of 113.1 mg/100g and 181.6 mg/100g for baobab fruit from Kitui and Kilifi counties in Kenya, respectively. Several published articles have reported a wide range of vitamin C content between 60.0 to 567.0±8.1 mg/100g of BFP (Dandago, 2016; Eldoom *et al.*, 2014; Chadare *et al.*, 2009; Ibrahima *et al.*, 2013). As an example, Chadare et al. (2009) reported a range of 150 – 500

mg/100 g pulp and attributed this to tree variability. Several factors such as species, climatic conditions, the stage of ripeness at harvest, postharvest management, storage conditions, and analytical techniques used are responsible for the variations in the composition of plant foods (Aron and Kennedy, 2008; Chadare, 2010; Tembo *et al.*, 2017; Chepngeno, 2018).

4.1.5 Moisture Content

Moisture content is a vital component of BFP as it influences the texture and storability. For the purpose of training the model for moisture content prediction, samples were spiked to create variation within the samples. Spiking is the deliberate addition of analyte (moisture for this study) to increase the range of moisture content within the set of samples used for modeling. This was done because the natural moisture content of dried BFP powders does not vary substantially on its own. By artificially adding differing amounts of water to individual BFP samples, a wider moisture range could be achieved. This would improve the accuracy and precision of the model because the NIR spectrometer capitalizes on sample variation (Guy et al., 2015). The average moisture content of BFP in this study was 19.5%. The moisture content ranged from a minimum of 9.8% to a maximum of 34.6%, as shown in Table 4.1. Sufficiently dried BFP contains a very low moisture content of between 6.5-13.7% (Eldoom et al., 2014; Osman, 2004; Tembo et al., 2017).

Table 4.1: Measured values for baobab quality attributes obtained through wet chemistry.

Parameter	No. of samples	Average	Range	Std
TTA (%citric acid)	240	11.8	7.3-18.8	1.6
TSS (°Brix)	240	1.6	0.7-2.4	0.3
Vitamin C (mg/100g)	240	160.2	100.0-205.9	19.3
% Moisture	130	19.5	9.8-34.6	5.8

TTA; total titratable acidity, TSS; total soluble solids, std; standard deviation.

4.2 Characterization of NIR Spectrum of BFP

Figure 4.1 shows the raw mean (unprocessed) NIR spectrum in the wavelength range of 950-1650 nm. Moreover, Appendix 2 shows various pre-processed spectra: (A) raw spectra, (B) pre-processed with Savitzky Golay (SG) smoothing, (C) transformed with multiplicative scatter correction (MSC) and mean-centered (MC) (D) treated with standard normal variate (SNV).

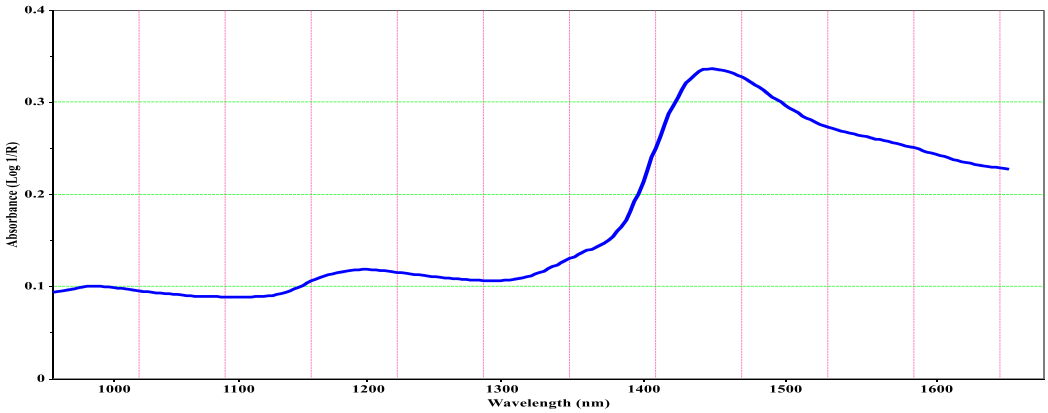

Figure 4.1: Raw mean spectrum for BFP

In all the spectra, the characteristic NIR peaks were observed at wavelengths around 950 nm, 1200 nm, and 1500 nm. The major peak at around 1300-1400 nm is a combination band. These wavelengths were due to the vibrational modes of O-H, N-H, and C-H chemical bonds (Nicolaï et al., 2022). These functional groups represented water, carbohydrates, and proteins in BFP (Cen and He, 2007; Stadlmayr et al., 2020). The predominant band of the NIR fingerprint was at 1450 nm which was dominated by water absorption bands due to the first overtone O-H stretch (Barbin et al., 2014). In this study, it was possible to observe the two characteristic water absorption bands at 950 nm and 1450 nm related to the second and first overtone O-H stretch respectively.

The absorption band centralized at 1200 nm corresponded to the second overtone C-H group and was associated with the presence of carbohydrates (Guthrie et al., 2005). The

absorption bands of starch and sugars are normally located near strong water absorption regions, therefore, hindering their visualization (Delwiche et al., 2008). Organic acids normally show bands corresponding to the O-H group at about 1445 nm and 1000 nm for the first and second overtone, respectively (Workman and Weyer, 2007). These bands also overlapped with the main water bands. Signals at around 1000 nm, 1210 nm, 1360 nm, and 1580 nm have been reported to correlate with the concentration of vitamin C (Yang and Irudayaraj, 2010). Moisture, TSS, TTA, and vitamin C are organic compounds that contain C-H and O-H that produce signals at different wavelengths and NIR could be used for rapid and non-destructive prediction of these compounds.

It is difficult to estimate the concentration of the analyte by visual inspection of the spectra due to associated spectral interferences, overtones, and combination of absorption bands. Therefore, pre-processing raw spectra before modeling was carried out to get rid of unwanted variation and technical artifacts. Pre-processing of the spectra is an integral part of multivariate modeling to get rid of background information and noise from the spectra and retain useful signals that reflect the chemical properties of the samples. It brought out slight spectral variations not evident in raw spectra and made the data more linear. It also allowed models to focus on the most relevant information contained in the data, thus improving prediction performance. As a common practice in NIR spectrometers, different pre-treatment techniques, both singly and in combination, were evaluated before the construction of the models, to determine the method(s) that could lead to better calibration and prediction models. The choice of the pre-treatment method(s) was based on the results of RMSECV, R^2, and RMSEP. The best pre-treatment method (s) that resulted in the lowest RMSECV and RMSEP and the highest R^2 were picked.

4.3 Predictive Models

4.3.1 Total Titratable Acidity

The best model achieved for TTA had the optimum number of seven factors (latent variables), R -squared (R^2) of 0.81, and a calibration error (RMSE) of 0.77% citric acid (Table 4.2). Upon validation with the prediction set of samples, the model returned an R^2

value of 0.82, a prediction error (RMSE) of 0.70% citric acid, a bias of 0.085, and an RPD of 2.29 (Table 4.2). Appendix 3 shows results for different pre-processing methods. This model was achieved after pre-processing near-infrared spectra with standard normal variate (SNV) to remove spectral scattering. The number of factors in a model was used to determine if the model was underfitted or overfitted. Too many factors result in an overfitted model because the model is closely fitted to the training data, captured noisy and irrelevant information, and therefore cannot accurately predict new samples. Underfitting happens when a model is overly straightforward and fails to recognize significant patterns and relationships in the data, therefore resulting in poor performance on both calibration and prediction sets (Sisouane *et al.*, 2017). During the training of the models, the software (The Unscrambler X version 10.4) was able to suggest a model with an optimum number of factors.

The calibration and prediction errors (0.77 and 0.70% citric acid respectively) were low considering a wide range of TTA reported through the wet chemistry (7.3-18.8%). The model also presented a low bias of 0.085 and RPD of 2.29 indicating that this model could be reliable in predicting the total acidity of BFP in terms of % citric acid. The data points for predicted and measured TTA (Figure 4.2) were distributed so close to and along the regression line, meaning NIR could be used for non-destructive and rapid quantification of TTA in the form of percentage citric acid contained by baobab fruits.

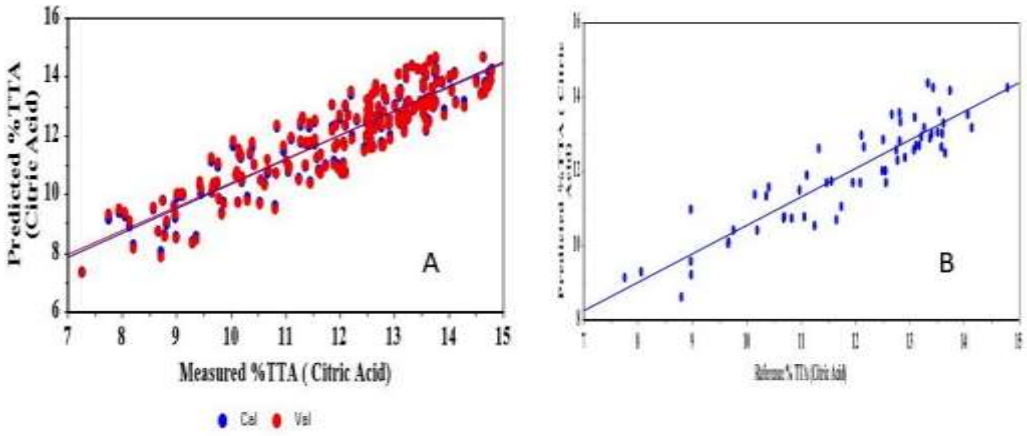

Figure 4.2: Partial Least Square Regression (PLSR) score plots for the quantification of titratable acidity in baobab fruit pulp. (A) Calibration model and (B) Prediction model.

A similar observation was also reported by Borba *et al.* (2021a) and Ncama *et al.* (2017). In addition, the results of this model were close to those obtained by Liu *et al.* (2010), Xie *et al.* (2011), and Arruda de Brito *et al.* (2022) using portable near-infrared spectrometer for non-destructive determination of TTA in different samples. Munawar *et al.* (2021) used a portable near-infrared spectrometer and constructed a four-factor PLSR model for the estimation of TTA in mangoes and reported R^2 of 0.92, RMSEC of 35.73, and RPD of 4.28.

The main absorption bands responsible for the construction of the PLSR model, obtained through spectral loading weight, were 1150-1170 nm, 1350-1360 nm, 1440 nm, 1450 nm, and 1600 nm (Appendix 5). These wavelengths are associated with O-H and C-H stretch as indicated by Workman and Weyer. (2007). Citric acid is an organic carboxylic compound containing C-H and O-H in its chemical structure suggesting that a portable NIR scanner coupled with chemometrics of PLSR could potentially be used to predict the concentration of citric acid contained by BFP.

4.3.2 Total Soluble Solids

The PLSR model for TSS was developed after pre-processing the raw spectra (950-1650 nm) with SG smoothing to remove background noise and other unwanted variations from the spectra, and to improve the accuracy and precision of the data. The model resulted in an optimum of four factors with R^2 and RMSE of 0.62 and 0.15°Brix respectively. The model was also evaluated with an external prediction set and it resulted in R^2, RMSEP, bias, and RPD of 0.63, 0.15°Brix, 0.086, and 2.00 respectively (Table 4.2). A linear trend was observed between predicted and measured TSS (Figure 4.3).

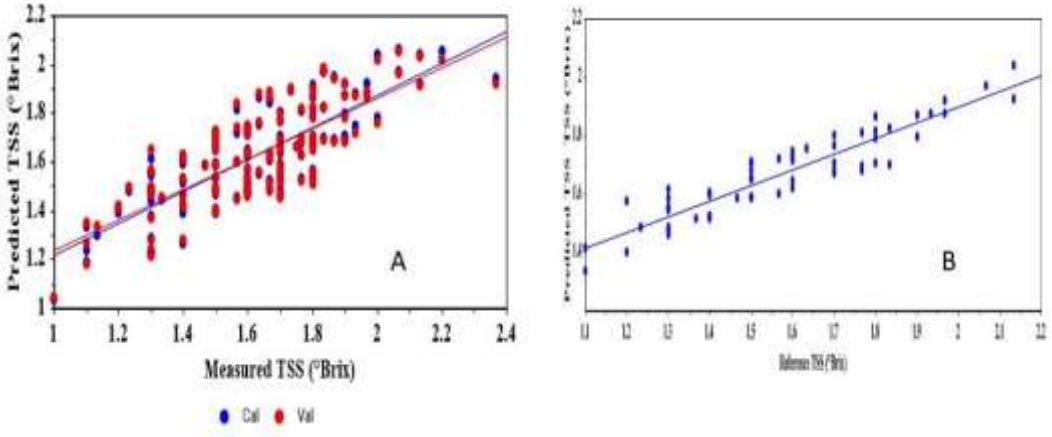

Figure 4.3: Partial Least Square Regression (PLSR) score plots for the quantification of total soluble solids in baobab fruit pulp. (A) Calibration model and (B) Prediction model.

Appendix 3 shows results for different pre-processing methods. A low RMSE of 0.15°Brix from both internal and external validation was ideal in respect of the 0.7-2.4°Brix range contained by samples used for the training and validation of the models. Despite low R-squared (R^2) for both calibration and prediction set, the model demonstrated high accuracy and reliability in the prediction of TSS in BFP with an RPD of 2.00. A model with residual predictive deviation (RPD) of above 2.00 is considered robust and excellent and therefore could be relied on (Davey et al., 2009; Bellon-Maurel et al., 2010).

The statistical results of this model were comparable to the report by Liu *et al.* (2010) even though the RPD of this study was much better (2.00) than the 1.43 reported by the authors. Ferrara *et al.* (2022) used a SCiO^{TM} scanner (wavelength 740-1070 nm) to predict TSS in different cultivars of grapes and reported RMSE of below 0.83°Brix and RPD of 7.13. Agulheiro-Santos *et al.* (2022) used the first derivative (FD) to pre-process NIR signals and constructed a seven-factor PLSR model for predicting TSS in strawberries. The model gave R^2 of 0.67 and RMSECV of 0.6°Brix. The characteristic wavelengths responsible for TSS prediction were 950 nm, 1440 nm, 1450-1550 nm, and 1650 nm (Appendix 5). These wavelengths are related to the second overtone O-H stretch, first overtone O-H stretch, and first overtone C-H stretch (Liu *et al.*, 2015). TSS is an organic compound that contains C-H and O-H chemical groups (Amuah et al., 2019), and could be possible to predict TSS using a portable NIR spectrometer.

4.3.3 Vitamin C Content

The PLSR model was trained for the prediction of vitamin C content in BFP. Raw spectra were transformed using multiplicative scatter correction (MSC) to correct variations in the intensity of the spectra due to scattering or absorption of light, and then mean centered for resolution enhancement. The resulting model had an optimum of six factors, R^2 of 0.72, and RMSE of 9.29 mg/100g for the calibration set (Table 4.2). Appendix XXX shows results for different pre-processing methods. Upon evaluation with an external set of data, the model resulted in an R^2 of 0.74 and RMSE of 9.67 mg/100g (Table 4.2). It also presented a bias of 2.115 and an RPD of 2.00 (Table 4.2). These results were not far from R^2, RMSEC, and RPD of 0.80, 0.63, and 2.68, respectively reported by Munawar *et al.*(2021) for the determination of vitamin C of intact mangoes using a portable NIR spectrometer. Despite a high bias of 2.115, the model managed to accurately predict vitamin C with an error of less than 10% and an excellent RPD of 2.00. This shows that the model could be used reliably to quantify the vitamin C content of baobab fruit pulp.

The scatter plots for predicted and conventionally measured vitamin C content of BFP are shown in Figure 4.4. Most of the data points were distributed along the regression line

indicating the possibility of using the technique for rapid and non-invasive analysis of vitamin C content in BFP.

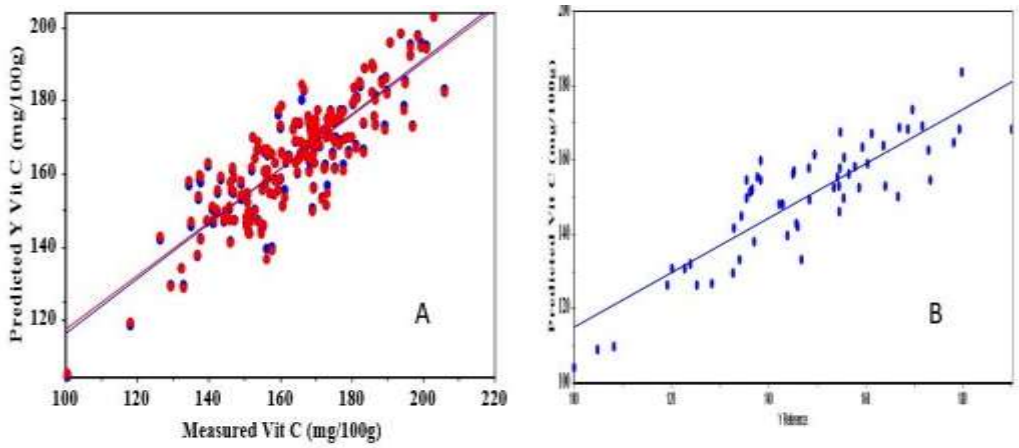

Figure 4.4: Partial Least Square Regression (PLSR) score plots for the quantification of vitamin C content in baobab fruit pulp. (A) Calibration model and (B) Prediction model.

The absorption signals that contributed the most to the construction of the model were 1000 nm,1100-1222 nm, 1300-1400 nm, 1450-1490 nm, and 1600 nm (Appendix 5). These wavelengths represented C-H and O-H stretch (Liu *et al.*, 2015). The C-H and O-H are the major bonds in the structure of vitamin C. Since the NIR spectrum provides a lot of information concerning the hydroxyl (O–H), and C–H absorption, the NIR technique could be a very powerful tool for the study of ascorbic acid (Liu *et al.*, 2006). Pissard *et al.* (2013) constructed a PLSR model for the prediction of vitamin C content in apples and obtained very good calibration models with a prediction error of less than 5% (3.4 mg/100 g) and an RPD of more than 3.0. An RPD value of above 2.0 indicates that the model is excellent and could be predicted with high accuracy (Davey *et al.*, 2009; Bellon-Maurel *et al.*, 2010).

4.3.4 Moisture Content

The PLSR model for moisture content estimation was also constructed using near-infrared spectra pre-processed with multiplicative scatter correction (MSC) and Mean centering

(MC). The best model had an optimum of four factors with R^2 and RMSE of 0.94 and 1.40%, respectively for the calibration set and R^2, RMSE, bias, and RPD of, 0.95, 1.31%, 0.383, and 4.43, respectively for the prediction set (Table 4.2). Appendix XXX shows results for different pre-processing methods. The model had an excellent performance in the prediction of the moisture content in BFP with a prediction error of less than 1.5% moisture content and an RPD of more than 4.0. These results indicated that this technique could be used for accurate and rapid screening of moisture content contained in BFP. As seen in scatter plots (Figure 4.5), the data points for predicted moisture content were close to conventional measurements. This also indicated the potential of the device to predict the moisture content in BFP.

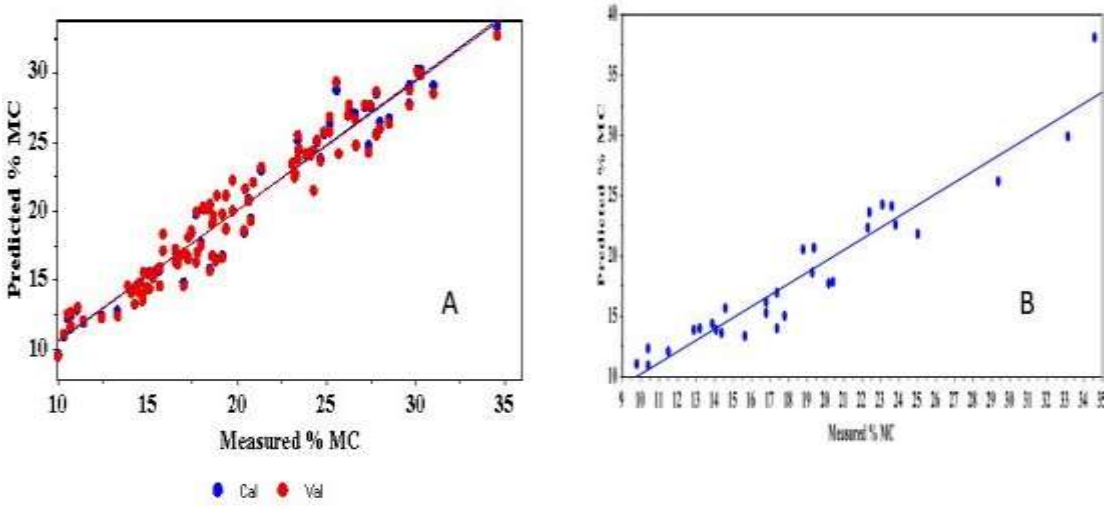

Figure 4.5: Partial Least Square Regression (PLSR) score plots for the quantification of moisture content in baobab fruit pulp. (A) Calibration model and (B) Prediction model.

The absorption bands responsible for moisture content determination were 1100-1250 nm, 1450 nm, and 1570-1600 nm (Appendix 5). All these wavelengths represent the O-H absorption bands that relate to the water molecule in the sample (Liu *et al.*, 2015). The near-infrared spectrometer has been extensively evaluated for its potential in non-destructive prediction of moisture content in different samples. Most of these studies have

reported promising results on the applicability of this technology for quick, reliable, and accurate measurement of water content in different samples with low prediction errors. The authors (Z. Liu et al., 202 2; Maduro Dias et al., 2021; Tugnolo et al., 2021; and Pan et al., 2015) used a portable near-infrared spectrometer to predict the moisture content of different samples and reported prediction errors of 0.049%, 2.18%, 0.15%, and 0.85%, respectively. Results from this current study were close to those obtained by the aforementioned authors, especially the associated prediction errors.

Table 4.2: Summary of calibration and prediction results for PLSR models for TTA, TSS, vitamin C, and moisture content.

Calibration model					Prediction model			
Parameter	**Pre-processing**	**Factors**	**R^2**	**RMSE**	**R^2**	**RMSE**	**RPD**	**Bias**
%TTA (Citric Acid)	SNV	7	0.81	0.77	0.82	0.70	2.29	0.085
TSS (°Brix)	Smoothing	4	0.62	0.15	0.63	0.15	2.00	0.086
Vitamin C (mg/100g)	MSC+MC	6	0.72	9.29	0.74	9.67	2.00	2.115
%Moisture	MSC+MC	4	0.94	1.40	0.95	1.31	4.43	0.383

R2; Correlation coefficient, RMSE; Root mean square error, RPD; Residual predictive deviation, TTA; Total titratable acidity, TSS; Total soluble solids, SNV; Standard normal variate, MSC; Multiplicative scatter correction, MC; Mean centering.

4.4 The use of a portable NIR spectrometer to monitor changes in baobab quality parameters during storage

To accurately monitor changes in quality attributes of stored BFP samples, acquired spectral data were pre-processed using the optimal techniques determined during initial model development. Specifically, spectra were transformed with standard normal variate (SNV) for TTA prediction, Savitzky-Golay (SG) smoothing for TSS, multiplicative scatter correction, and mean centering (MSC+MC) for vitamin C and moisture content prediction. The pre-treated spectral data were then loaded into the previously constructed and validated partial least squares regression (PLSR) models to predict TTA, TSS, vitamin C, and moisture content levels of the stored BFP samples in a non-destructive manner.

The microbial load (total aerobic counts and total yeast and mould counts) of stored samples was determined separately using standard laboratory procedures.

4.4.1 Effects of storage conditions and packaging on baobab quality parameters

The ANOVA results (Table 4.3) indicated that baobab quality parameters (TSS, vitamin C, moisture content, and TAC) were significantly affected by the storage duration. The TSS, vitamin C, and moisture content were greatly influenced by the storage conditions. The packaging material affected only the moisture content. However, changes in TTA and TYMC with storage time were not statistically significant. Additionally, TTA and TYMC were not affected by both main factors and their interactions. All quality parameters of BFP, except TSS, were not significantly affected by the interaction between the storage duration and condition used. The TSS and moisture content of the stored baobab samples were greatly affected by both interactions between storage duration and packaging. The TSS, vitamin C, and moisture content of the pulp were significantly affected by the interaction between the storage condition and the packaging material used. However, the interaction between the storage duration, storage condition, and packaging did not significantly affect the quality attributes of BFP except for TSS only.

Table 4.3: ANOVA P-values for main and interaction effects of storage duration, condition, and packaging on physicochemical and microbiological properties of stored baobab fruit pulp

Term	TTA	TSS	Vit. C	Moisture Content	TAC	TYMC
A	0.2268	0.0000	0.0000	0.0000	0.0000	0.0628
B	0.1777	0.0009	0.0106	0.0002	0.7189	0.0628
C	0.7846	0.4262	0.2062	0.0237	0.4998	0.0628
A*B	0.8992	0.0000	0.8998	0.1692	0.7189	0.0628
A*C	0.9879	0.0002	0.9190	0.0231	0.4998	0.0628
B*C	0.7500	0.0000	0.0367	0.0039	0.1475	0.0628
A*B*C	0.8713	0.0000	0.3427	0.2950	0.2132	0.0628

P<0.05 was considered a significant difference. A- storage duration, B-storage conditions, and C- Packaging material, *, Interaction, TTA-total titratable acidity, TSS-total soluble solids, Vit. C- vitamin C, TAC-total aerobic content, TYMC-total yeast, and mould counts

4.4.2 Total Titratable Acidity

The TTA values of stored BFP are presented in Figure 4.6. The TTA for all samples decreased slightly over time (P>0.05). For UbKP-packaged samples, the TTA decreased from the initial 15.39 to 14.48% citric acid (P=0.3239) and 15.02 to 14.14% citric acid (P=0.2675) for those stored at 25°C/75%RH and 35°C/83%RH, respectively. For those samples packaged in LDPE bags, the TTA also reduced insignificantly from the initial 15.53 to 14.72% citric acid (P=0.1438) for those samples stored at 25°C/75%RH and from 15.06 to 14.06% citric acid (P=0.1721) for those kept at 35°C/83%RH. In addition, the differences in TTA contents for all samples regardless of packaging and storage conditions used were minimal.

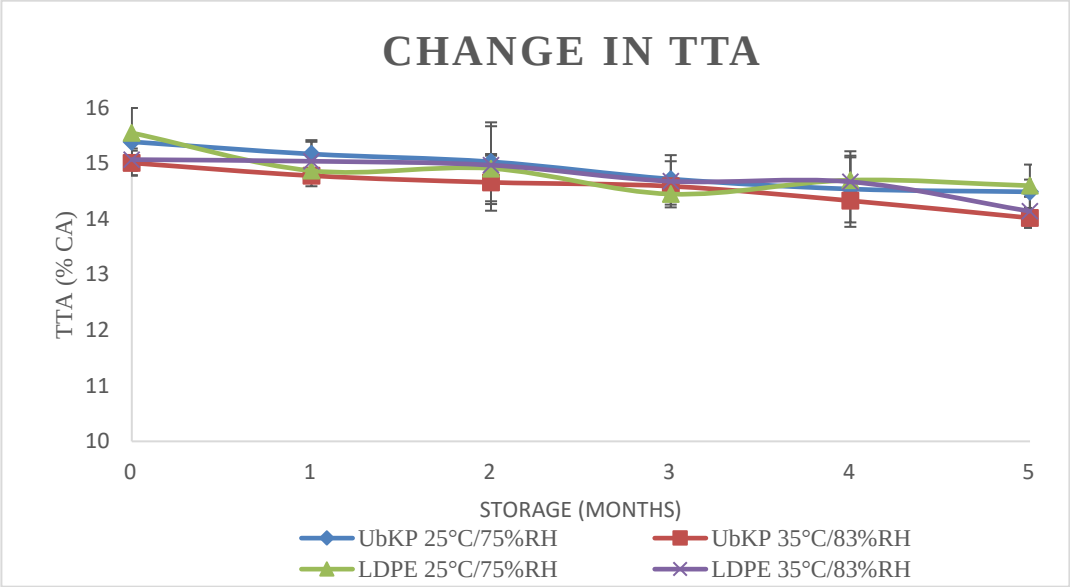

Figure 4.6: Changes in TTA over six months storage period in BFP samples packaged in UbKP and LDPE bags and kept at 25°C/75%RH and 35°C/83%RH storage conditions.

The progressive decrease in the amounts of TTA could be due to the decomposition process through both hydrolysis and oxidation. These processes led to a metabolic conversion of organic acids into other by-products such as carbon dioxide and water (Ferreira *et al.*, 2015). This finding was consistent with what was reported by Ferreira *et al.* (2015) who reported that fruit and vegetable residue flour subjected to storage experiment exhibited a significant decrease in TTA. Those authors also attributed the decline in TTA to the metabolic breakdown of organic acids during storage.

The results of this current study were also similar to what was reported by Dandago. (2016) study which evaluated the effects of different storage temperatures and packaging on the proximate and ascorbic acid content of BFP. The author reported a progressive decrease in TTA during storage. Eldoom et al. (2014) also reported a similar trend with a significant decrease in TTA of BFP regardless of the storage conditions and the packaging material used. Those authors attributed the decline in TTA to the esterification of organic acid by degradative enzymes and microorganisms such as bacteria and yeasts. Baobab samples in LDPE bags stored at 35°C/83% RH exhibited slightly more loss of TTA

(6.64%) at the end of storage compared to the rest of the samples. This was due to accelerated oxidation reactions due to slightly elevated temperatures and an increase in metabolisms through enzymatic and microbial activities.

4.4.3 Total Soluble Solids (TSS)

As shown in Figure 4.7, the TSS of stored BFP samples decreased significantly ($P<0.05$) with storage time. The UbKP-packaged samples had a decline in TSS from the initial 2.0 to 0.9 °Brix ($P=0.0001$) and 2.0 to 1.4 °Brix ($P=0.0001$) for those kept at 25°C/75%RH and 35°C/83%RH, respectively. For LDPE-packaged samples, TSS dropped from 1.9 to 1.3 °Brix ($P=0.0000$) and 1.8 to 1.3 °Brix ($P=0.0000$) for those stored at 25°C/75%RH and 35°C/83%RH, respectively. The highest loss in TSS (55.0%) was observed in UbKP-packaged samples that were stored at 25°C/75%RH.

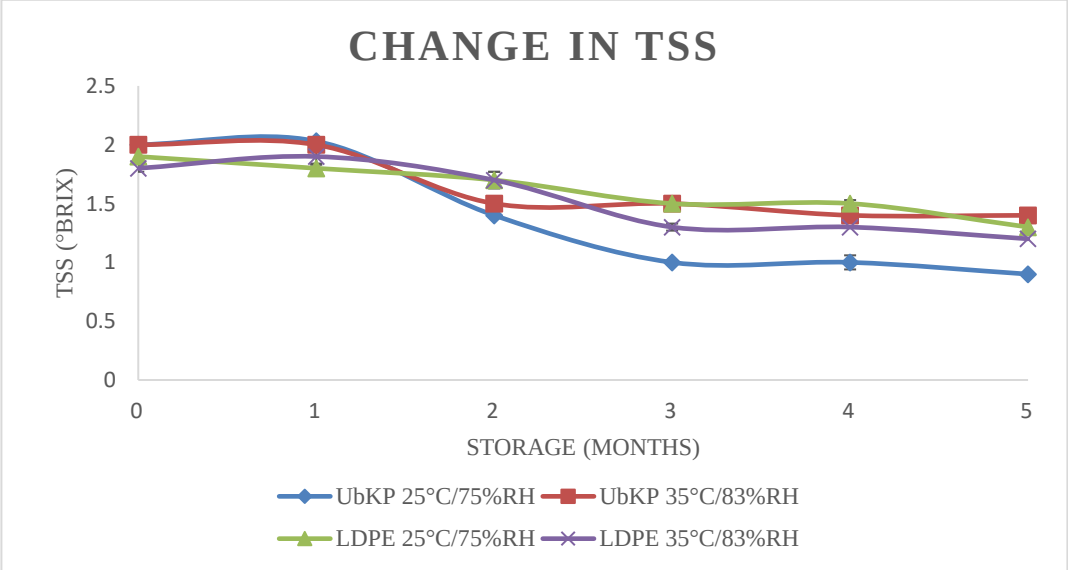

Figure 4.7: Changes in TSS over six months storage period in BFP samples packaged in UbKP and LDPE bags and kept at 25°C/75%RH and 35°C/83%RH storage conditions.

All samples exhibited a massive drop in TSS content despite the effect of packaging material and storage conditions. The decrease in TSS was due to the utilization of carbohydrates by microorganisms, particularly bacteria and fungi, oxidation of organic

acids and dissolved vitamins, and isomerization of phenolic compounds (Eldoom *et al.*, 2014; Mgaya-Kilima *et al.*, 2014; Tembo *et al.*, 2017). The decrease in TSS of stored baobab samples reported by this current study was consistent with what Eldoom *et al.* (2014) reported. The mentioned authors studied the effect of wrapping and packaging type on the quality of BFP during storage. Those authors reported a significant decrease in TSS after storing the pulp for twelve months. However, Eldoom *et al.* (2014) reported the highest loss of TSS by BFP samples packaged in polythene bags (28.6%) compared to those in jute (0.00%), basket (9.09%) and in the market (8.62%) in twelve months. This was contrary to the highest loss (55.0%) in UbKP-packed baobab samples stored at 25°C/75%RH reported by this study. The porous nature of the UbKP packaging allowed greater permeation of environmental oxygen and absorption of moisture compared to LDPE packaging. This created favorable conditions for oxidative degradation and hydrolytic breakdown of soluble components like vitamins and phenolic compounds in BFP (Tembo et al. 2017). Additionally, the excess moisture enabled proliferation of microorganisms which further utilized available carbohydrates as substrates for growth (Tembo et al., 2017).

4.4.4 Vitamin C Content

This study revealed that the vitamin C content of BFP samples dropped significantly ($P<0.05$) as the storage period advanced. The degradation of ascorbic acid occurred regardless of the influence of packaging material and storage conditions utilized in this study. The reduction in ascorbic acid concentration commenced promptly following the introduction of the samples into storage conditions. For UbKP-packaged samples, vitamin C declined from 183.18 to 115.53 mg/100g ($P=0.0002$) and 176.18 to 117.55 mg/100g ($P=0.0078$) for those kept at 25°C/75%RH and 35°C/83%RH, respectively (Figure 4.8). For LDPE-packaged baobab samples, vitamin C content reduced from 183.53 to 123.02 mg/100g ($P= 0.001$) and 165.94 to 98.50 mg/100g ($P=0.0007$) for samples kept at 25°C/75%RH and 35°C/83%RH, respectively (Figure 4.8).

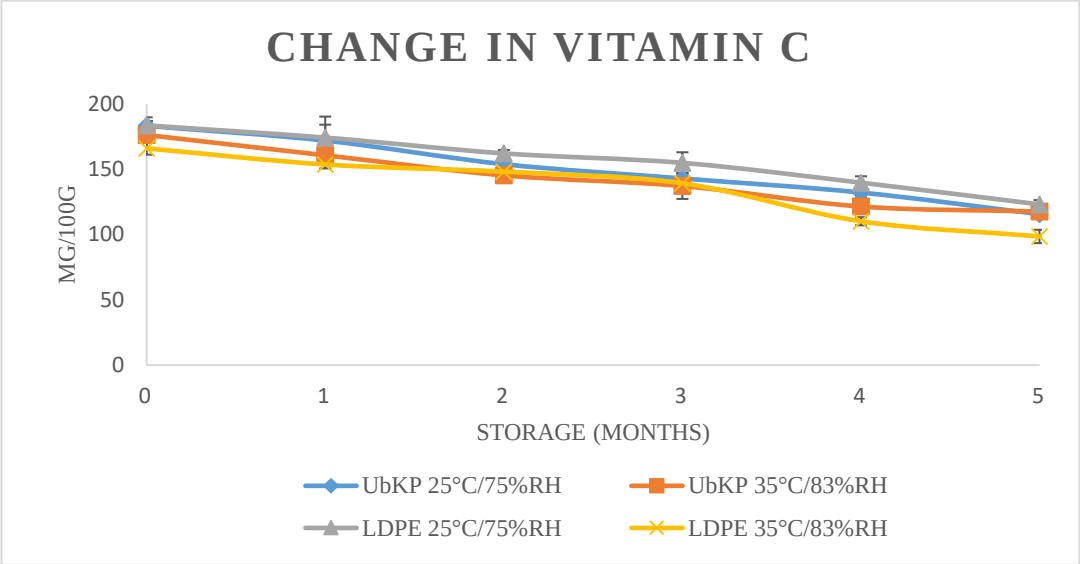

Figure 4.8: Changes in vitamin C over six months storage period in BFP samples packaged in UbKP and LDPE bags and kept at 25°C/75%RH and 35°C/83%RH storage conditions.

The reason for the drastic decrease in vitamin C content during storage was the interaction between the samples and the atmospheric oxygen. That resulted in the oxidation process that led to the degradation of vitamin C content (Odriozola et al., 2009; Sandhya, 2010; Tembo *et al.*, 2017). This was contributed by the packaging materials which permitted the interaction of the samples with the external environmental factors (Eldoom *et al.*, 2014). Those results were also consistent with what was reported by Dandago. (2016) study which assessed the effect of storage conditions on the proximate and ascorbic acid content of baobab pulp stored for 8 weeks. That author attributed the gradual decline in vitamin C content to the oxidation of vitamin C contained in the samples.

LDPE-packaged samples stored under 35°C/83%RH storage conditions had the highest loss of vitamin C of 40.64%. The changes in vitamin C and TTA levels both displayed similar downward trajectories across the storage intervals measured. The parallel decreasing trends observed for these two quality parameters suggested a possible correlation between loss of acidity and degradation of vitamin C in the stored BFP samples (Rop et al., 2012; Mgaya-Kilima et al., 2014). The highest loss of vitamin C content

(40.64%) was reported in LDPE-packed baobab samples stored at 35°C/83%RH. This was attributed to the high moisture content in the atmosphere, elevated temperatures, and the lights permitted by the LDPE bag. High temperature raises the mobility of water inside the powder particle favoring oxidative reactions (Rodríguez *et al.*, 2014). This was contrary to what was reported by Eldoom *et al.* (2014) who studied the effect of packaging on the quality of stored baobab fruit. Those authors reported the least change in ascorbic content of baobab fruits stored in black polythene bags.

4.4.5 Moisture Content

Regardless of the packaging material and storage conditions, the moisture content of all samples exhibited a significant increase after the storage period (Figure 4.9). The initial moisture content of UbKP-packaged samples increased from 6.55 to 10.18% (P=0.0058) and 8.23 to 13.37% (P=0.0009) for those kept at 25°C/75%RH and 35°C/83%RH, respectively. For LDPE-packaged samples, moisture content increased from 7.24 to 10.02% (P=0.0148) and 7.55 to 10.55% (P=0.0019) for those stored at 25°C/75%RH and 35°C/83%RH, respectively.

Moisture levels can impact the product's quality and shelf life (Li et al., 2017). The increase in moisture content of the pulp was majorly due to the water penetration through the packaging materials, high relative humidity, and the hygroscopic nature of the samples (Muthai *et al.*, 2017; Tembo *et al.*, 2017). Kraft paper bag is permeable to moisture content and oxygen since it is made up of adsorptive and porous material (SOBRAL, 2000). LDPE bag on the other hand is not entirely water resistant (Bastarrachea *et al.*, 2011). The samples packaged in paper bags and maintained at 35°C/83% RH demonstrated the maximum moisture content (13.37%) at the end of storage duration compared to the rest of the samples. That outcome was attributed to the inferior moisture barrier properties of paper packaging materials.

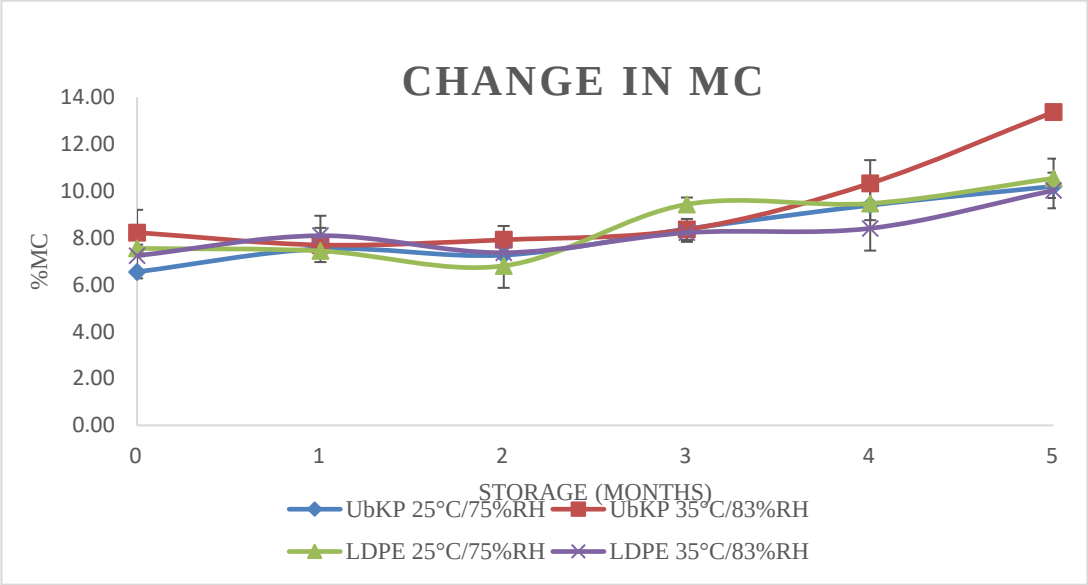

Figure 4.9: Changes in moisture content over six months storage period in BFP samples packaged in UbKP and LDPE bags and kept at 25°C/75%RH and 35°C/83%RH storage conditions.

Unlike LDPE bags, which resisted and retarded moisture content transmission, paper bags permitted the relatively unimpeded passage of moisture content (Ferreira *et al.*, 2015).The high temperature and humidity environmental conditions further promoted moisture migration into the paper packaging (Yan *et al.*, 2022). Consequently, the combination of the permeable paper bags and the warm, humid storage setting enabled absorption of appreciable moisture by the samples, culminating in the pronounced elevation in moisture content observed for this experimental treatment (Rahman, 2009). The inferior moisture content barrier functionality of the paper packaging, coupled with the high relative humidity storage ambience, collectively account for the substantial moisture content increase detected in these samples (Vartiainen *et al.*, 2014).

Despite an increase in moisture content, the moisture levels of all samples remained below the upper limit of 14% for edible pulp powders stipulated in the Kenya Bureau of Standards (KEBS) (KEBS., 2018).

4.5 Microbial Load

In addition to the non-destructive monitoring of quality attributes in stored baobab samples, microbial safety was also assessed through standard laboratory protocols. This was meant to provide additional information concerning the microbial safety of stored samples. Specifically, total aerobic counts (TAC) and total yeasts and mould counts (TYMC) were determined. Figure 4.10 and 4.11 shows the changes in TAC and TYMC, respectively, during storage. This study found that there was a significant increase in TAC with storage duration ($P<0.0002$). For UbKP-packaged samples, TAC rose to Log_{10} 2.63 and Log_{10} 2.86 cfu/g for baobab samples kept at 25°C/75%RH and 35°C/83%RH, respectively. For LDPE-packaged samples, TAC multiplied to Log_{10} 2.36 and Log_{10} 2.48 cfu/g for samples kept at 25°C/75%RH and 35°C/83%RH, respectively. In addition, yeast and moulds remained undetected throughout the storage experiment for LDPE-packaged samples. For UbKP-packaged samples, yeast and moulds were detected starting from the third month of storage.

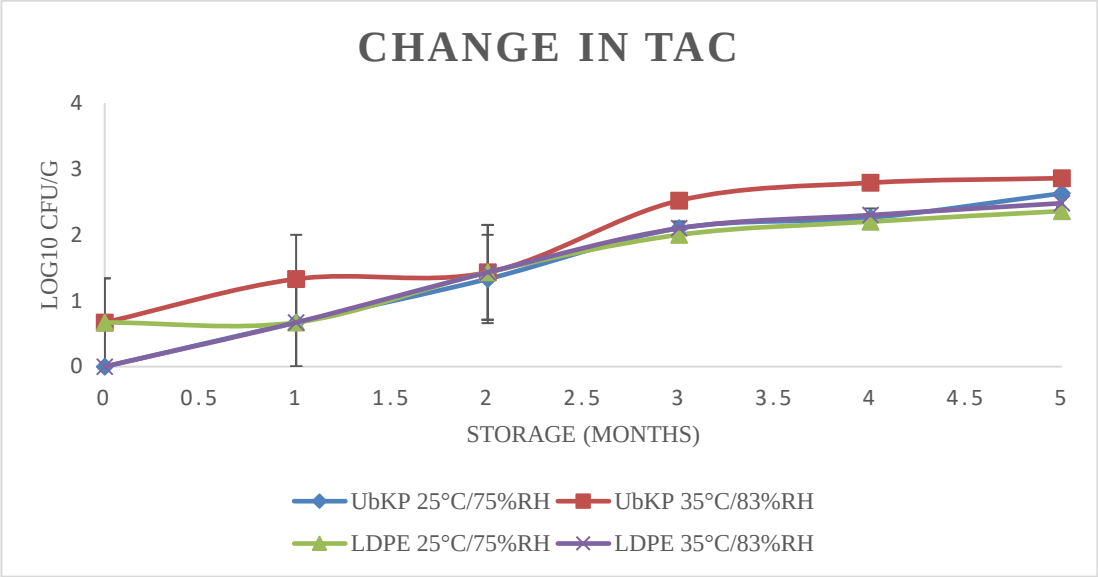

Figure 4.10: Changes in TAC over six months storage period in BFP samples packaged in UbKP and LDPE bags and kept at 25°C/75%RH and 35°C/83%RH storage conditions

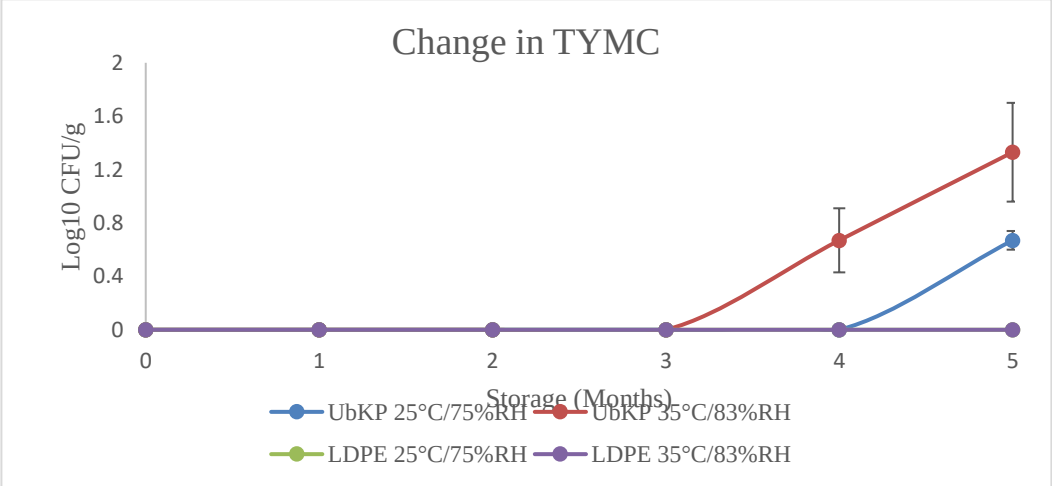

Figure 4.11: Changes in TYMC over six months storage period in BFP samples packaged in UbKP and LDPE bags and kept at 25°C/75%RH and 35°C/83%RH storage conditions

The growth of microorganisms could be linked to the relative permeability of the packaging materials to atmospheric factors such as oxygen, carbon dioxide, and moisture content (Ferreira *et al.*, 2015). Also, this was probably due to available nutrients and storage conditions employed in this study that were favourable for microbial growth (Akhtar et al., 2008; Hemery et al., 2020). Microorganisms require oxygen, carbon dioxide, source of carbon, and moisture to carry out their metabolic processes (Jay et al., 2005). The low moisture content of BFP likely inhibited the reproduction and growth of many microorganisms. However, some mesophilic bacteria are still capable of multiplying despite low moisture environments (Jeon and Kim, 2016). The increase in TAC among stored samples was consistent with what was reported by Adebowale et al.(2017) who subjected yam flour to different storage conditions. Catunescu et al. (2014) and Yim et al. (2019) also reported a significant increase in TAC in different samples as the storage period advanced.

Yeasts and moulds were not detected in samples kept in LDPE bags until the end of storage. However, yeast and moulds were detected from the third and fourth months of storage for UbKP-packaged samples stored at 35°C/83%RH and 25°C/75%RH, respectively. The LDPE packages provided superior protection against the absorption of moisture and oxygen compared to UbKP packaging. Moisture and oxygen availability have been shown to promote the growth of yeasts and moulds in stored food products (Petriccione *et al.*, 2015). Therefore, the LDPE packaging likely restricted moisture and oxygen levels, creating a less favorable environment for yeast and mold growth in the stored BFP compared to UbKP packaging.

Despite an increase in the microbial load during storage, the levels remained within acceptable limits of $\log_{10}$ 4 cfu/g for both TAC and TYMC (KEBS, 2018).

4.6 The application of a portable NIR spectrometer for rapid and non-destructive detection and quantification of BFP adulteration

4.6.1 Sample Particle Size Distribution

The particle size distribution of BFP samples and potential adulterants including maize, wheat, and rice flours was characterized before using a portable NIR spectrometer for adulteration detection. Determining particle size distributions served to provide insights regarding sample homogeneity and the potential impacts on spectral absorption intensities. Figure 4.12 also shows curves for both particle size distribution and cumulative particle sizes for all samples. For each sample, there are two curves, the one ending at the bottom right corner is for particle size distribution and the one touching the top right corner is for cumulative particle sizes. Unimodal particle size distribution was observed in maize flour. The rest of the samples displayed bimodal curves.

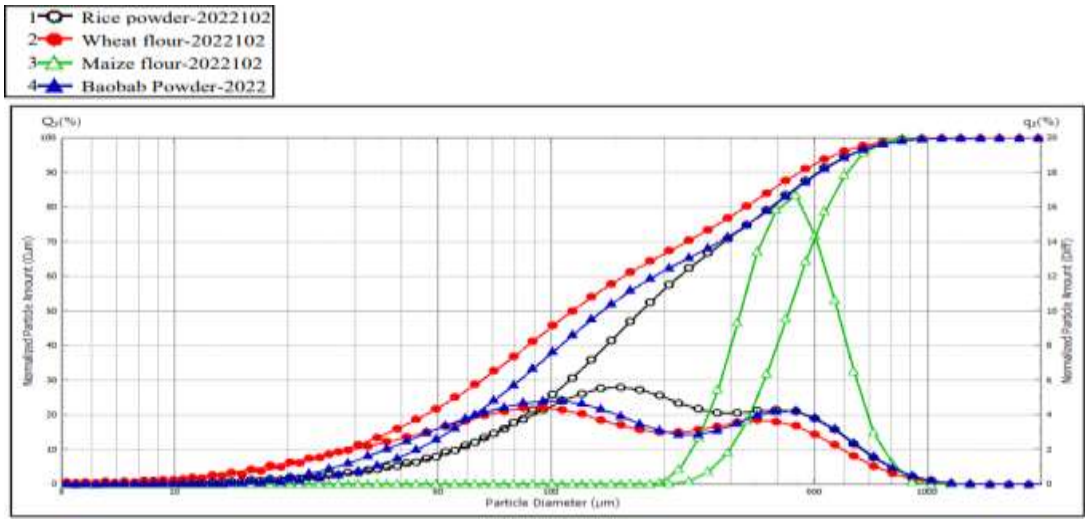

Figure 4.12: Particle size distribution curves for BFP, rice, wheat, and maize flours.

Maize flour (MF) had an extremely large particle size (425.68±0.12μm) compared to other samples (168.45±0.39, 113.79±0.47 and 145.59±0.41μm, for RF, WF and BFP, respectively). Despite (MF) having the highest particle size, it presented an unimodal particle size distribution curve, suggesting sample size homogeneity (Cristiano *et al.*, 2019). On the other hand, bimodal distribution curves were seen in BFP, RF, and WF

samples. This meant that there were two clusters of samples, a cluster of small samples and a cluster of large samples. This information on sample particle sizes was critical in the characterization of NIR spectra. Samples with high particle sizes are known to result in spectra with high absorption intensities while those with small particle size produces spectra with low absorption intensities (Ramalho *et al.*, 2019). This is because large particle sizes have a greater surface area and free electrons, which leads to a stronger interaction with incident radiation and therefore results in higher absorption intensity. On the other hand, the positioning and trends of absorption bands in the NIR spectrum remain consistent despite the effects of sample particle size. This is because the absorption bands are typically determined by the molecular structure (chemical bonds and functional groups) of a sample (Ramalho *et al.*, 2019).

4.6.2 Characterization of NIR Spectra

Absorption peaks characteristic of NIR spectra were seen around 1000 nm, 1200 nm, and 1450 nm in all the samples (Figure 4.13). Spectral variations were similar in the wavelength around 900 nm to 1140 nm and significant differences were seen from 1140 nm onwards (in all the samples). The similarity in the trend of all spectra for the entire wavelength could be due to the resembling composition of the samples since they are mostly composed of C-H, O-H, and N-H-containing compounds that produce peaks at certain specific wavelengths. The spectrum for BFP was different from the adulterants in terms of absorption intensities. The differences were brought by low intensities of C-H, N-H, and O-H absorption bands. On the other hand, the mean spectrum of maize flour had the highest absorption intensities followed by rice flour and then wheat flour. The differences in particle sizes for all the samples might have played a critical role in the variation of absorption intensities seen in the sample spectrum. Maize flour had the highest particle size of 425.68±0.12µm followed by rice flour with 168.45±0.39µm. On the other, BFP and wheat flour had the least particle sizes of 145.59±0.41µm and 113.79±0.47µm, respectively.

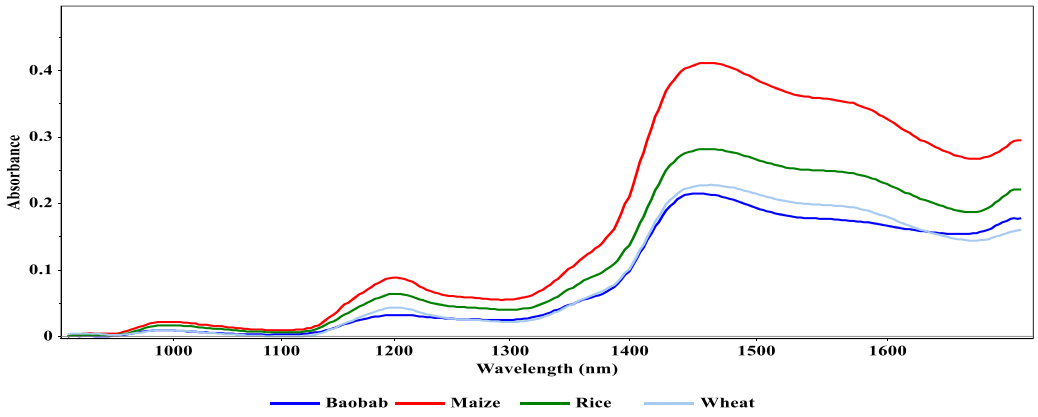

Figure 4.13: Average spectra (950-1650nm) for baobab fruit pulp powder, maize flour, rice flour, and wheat flour.

These differences in mean spectra also reflected important chemical properties of BFP and adulterants. The C-H, N-H, and O-H chemical bonds are major components of carbohydrates, proteins, and water molecules contained in organic materials. Among the adulterants used in this study, maize flour and rice flour were reported to contain the highest amount of total carbohydrates (approximately 78.74% and 82.45%, respectively) followed by BFP and wheat flour (approximately 74.74% and 72.72%, respectively) (Qamar et al., 2017; Vunain et al., 2020; Muthai et al., 2017; Ocheme et al., 2018). Absorption bands at around 1000 nm and 1200 nm were induced by the third and second overtone C-H stretch, respectively, while a broad band at 1450 nm was brought by the first overtone C-H and O-H stretch (Liu *et al.*, 2015). These are major components related to total carbohydrates.

The percentage moisture and protein content of the adulterants and BFP also vary. Maize flour, rice flour, and wheat flour were reported to have moisture and protein content of approximately 9.0-15.0% and 7.82-12.02%, 9.35-10.42% and 5.43-7.03%, and 5.46-7.08% and 8.13-9.50%, respectively (Qamar et al., 2017; Vunain et al., 2020; Jamal et al., 2016). BFP was reported to have moisture and protein content of 8.82-9.94% and 1.58-2.65%, respectively (Muthai *et al.*, 2017). The major peaks at around 1450 nm are combination bands attributed to the first overtone of the O-H, C-H, and N-H groups

(Workman and Weyer, 2007). The differences in the mean spectrum for BFP, maize flour, rice flour, and wheat flour were also possibly due to the varying amounts of carbohydrates, proteins, and moisture.

The spectral fingerprint for BFP significantly deviated from the rest of the adulterants at 1200 nm and it resembled that of wheat flour at about 1250 nm to 1450 nm. The two spectra had a similar shape and were highly overlapping. This wavelength range was possibly responsible for masking the chemical differences between BFP and wheat flour. However, it was quite difficult to classify the different adulterants by mere visualization of the spectra. This was due to the overlapping absorption bands and hidden information contained by the spectra (Ozaki *et al.*, 2006). Therefore, spectral transformation techniques were necessary to extract features from the spectra for pattern recognition and to make the detection of adulterants possible.

4.6.3 Detection of adulterants using partial least square discriminant analysis models.

4.6.3.1 Two-class PLS-DA Models

Partial least square discriminant analysis (PLDA) was adopted to distinguish between pure and adulterated BFPP samples. Individual PLS-DA models of two classes were constructed using pre-processed NIR spectra of adulterated samples. The two-class models were trained using different levels of adulteration ranging from 0-60%. Several pre-treatment techniques were applied to minimize background noise associated with the acquired spectra. These methods were used both singly and in combination and the best pre-processing techniques were adopted based on the improvement in model statistics, i.e., the sensitivity, specificity, and error rate. In principle, two-class PLS-DA models were constructed for each adulteration to discriminate between pure and impure BFPP samples.

Raw spectra (950-1650 nm) were transformed with mean centering (MC) for model A, multiplicative scatter correction (MSC) and mean centering (MC) for model B, and mean centering (MC) for model C. Figures 4.14, 4.15, and 4.16 show scatter plots for the

constructed two-class models for the discrimination of pure and BFP samples adulterated with rice, wheat, and maize flours, respectively. The first 4 latent variables (LVs) explained 99.82%, 99.52%, and 99.86% of the total explained variance in Model A, Model B, and Model C, respectively. All models were able to discriminate between pure baobab and those that were adulterated with RF, WF, and MF. Since all samples were correctly assigned, model A and B resulted in sensitivity, specificity, and classification error of 1.000, 1.000, and 0.000, respectively (Table 4.4). This indicated that all pure and adulterated samples were correctly classified by the models, with no false positives or false negatives. Model C on the other hand resulted in a sensitivity and specificity of above 0.982 and an error of 0.009 for both calibration and prediction models (Table 4.5). This also represents a very low misclassification rate.

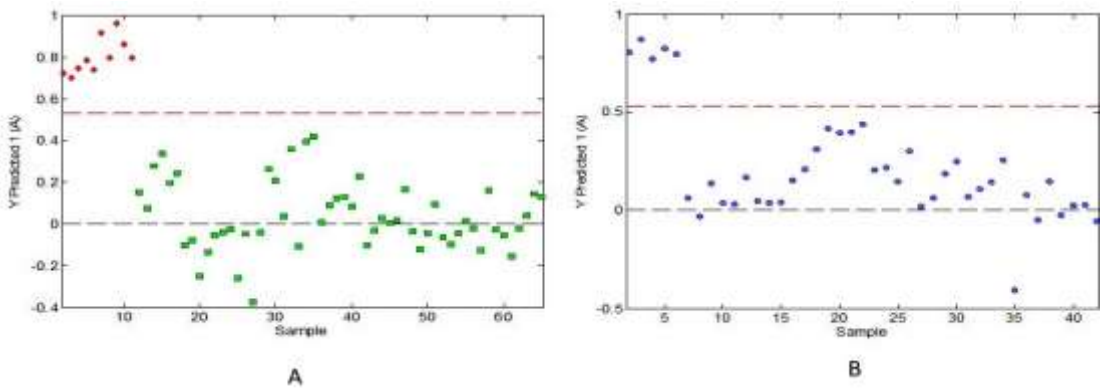

Figure 4.14. Two-class PLSDA classification scatter plot for detection of rice flour adulterants in baobab fruit pulp powder. (A) Calibration model and (B) Prediction model

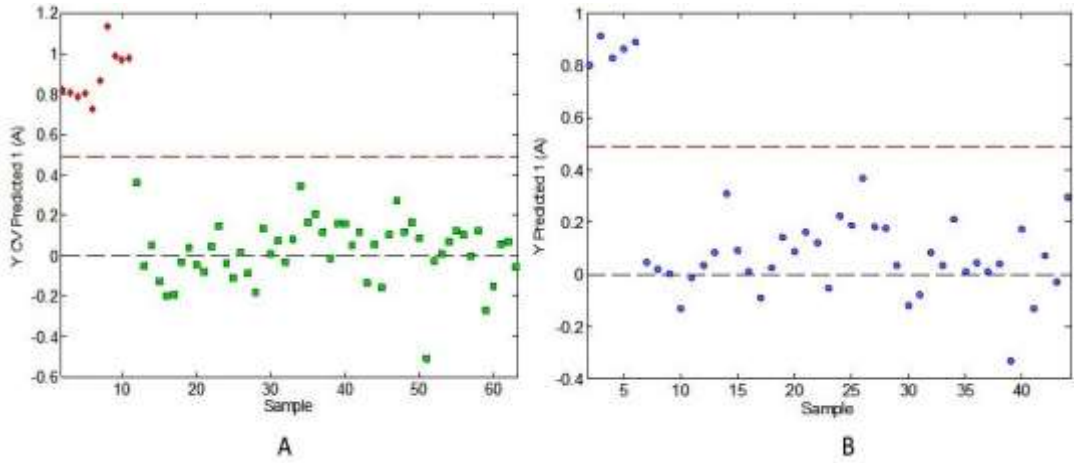

Figure 4.15: Two-class PLSDA classification scatter plot for detection of wheat flour adulterants in baobab fruit pulp powder. (A) Calibration model and (B) Prediction model.

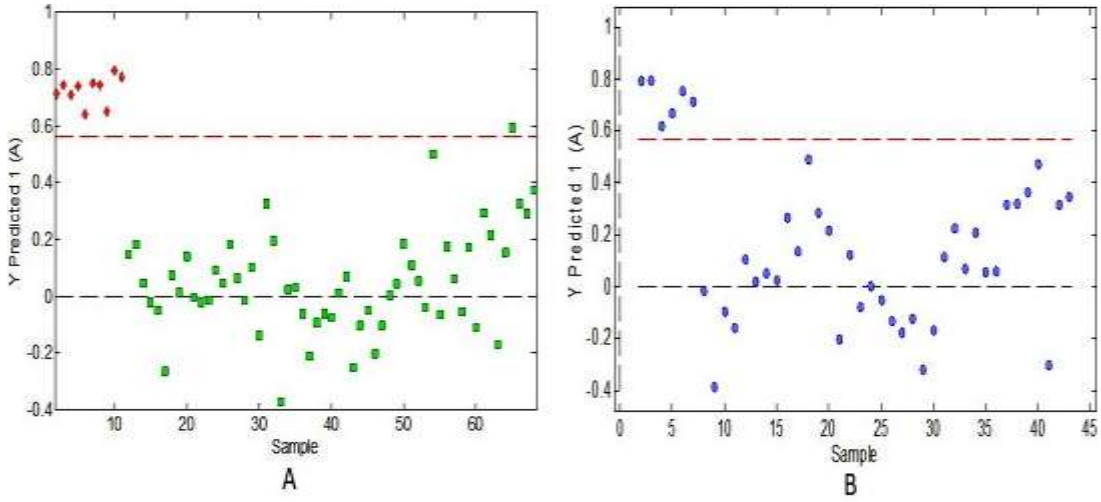

Figure 4.16: Two-class PLSDA classification scatter plot for detection of wheat flour adulterants in baobab fruit pulp powder. (A) Calibration model and (B) Prediction model.

According to Jakubíková *et al.* (2016), sensitivity and specificity above 0.900 indicate excellent discrimination performance for classification models. These results indicated that two-class PLS-DA models had exemplary performance in the identification of pure and adulterated samples and could effectively and accurately classify baobab adulteration.

These results were consistent with other studies that have applied portable NIR spectrometers and chemometrics for adulterant detection. For example, Orequent et al. (2022) achieved 100% sensitivity and specificity in discriminating between pure honey and honey adulterated with sugar syrups using PLS-DA modeling of NIR spectra acquired with a portable spectrometer.

Table 4.4: Statistical parameters for PLS-DA models for discrimination of pure and adulterated BFP using pre-processed spectra.

Model	**Model A (Rice flour)**		**Model B (Wheat flour)**		**Model C (Maize flour)**	
Pre-processing	**MC**		**MSC + MC**		**MC**	
LVs	4		4		4	
Class	Class 1	Class 2	Class 1	Class 2	Class 1	Class 2
Sensitivity (Cal)	1.000	1.000	1.000	1.000	1.000	0.982
Sensitivity (Pred)	1.000	1.000	1.000	1.000	1.000	0.982
Specificity (Cal)	1.000	1.000	1.000	1.000	0.982	1.000
Specificity (Pred)	1.000	1.000	1.000	1.000	0.982	1.000
Error (Cal)	0.000	0.000	0.000	0.000	0.009	0.009
Error (Pred)	0.000	0.000	0.000	0.000	0.009	0.009

LVs: Number of latent variables, Cal: Calibration set, Pred: Prediction set. Model A: Pure baobab (class 1) and baobab plus rice flour (class 2). Model B: pure baobab (class 1) and baobab plus wheat flour (class 2). Model C: pure baobab (class 1) and baobab plus maize flour (class 2).

4.6.3.2 Four-class PLS-DA Models

PLS-DA was also extensively used to identify the type of adulterant present in baobab fruit pulp samples. A four-class PLSDA model was constructed using 0-60% adulteration levels to discriminate and identify the type of adulterant present in BFP. Before modeling, raw spectra (950-1650 nm) were treated with multiplicative scatter correction (MSC). This corrected light scattering due to varying sample particle sizes. The spectra were then mean-centered (MC) to improve the resolution of the data. The model had an optimum of 3 latent variables (LVs) which explained 98.89% of the total spectral variance. The score

plots (Figure 4.17) revealed substantial class overlap, with several samples from different adulterant types clustering together.

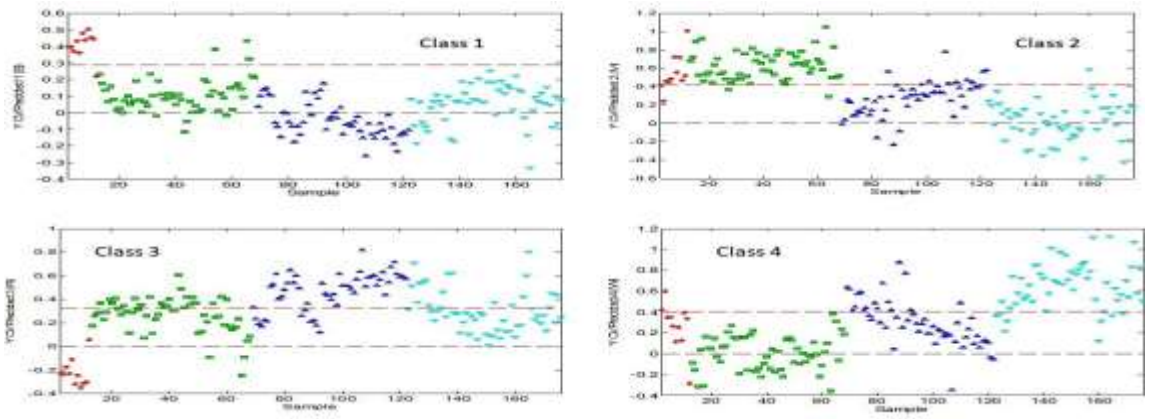

Figure 4.17: Four-class PLSDA classification scatter plot for detection of maize flour adulterants in baobab fruit pulp powder. (A) Calibration model and (B) Prediction model.

This indicated that the four-class model struggled to discriminate between adulterants, likely contributing to the moderate sensitivity (0.778-0.909), specificity (0.678-0.982), and higher error rates (0.055-0.272) for the prediction set (Table 4.5). The inability to reliably separate the adulterant classes supported the poor performance of the four-class model.

Table 4.5: PLS-DA classification parameters for discrimination of pure baobab and baobab samples individually adulterated with different types of adulterants, constructed using pre-processed spectra.

	Model D (All Adulterants)			
Pre-processing	**MSC+MC**			**LVs 3**
Class	**Class 1**	**Class 2**	**Class 3**	**Class 4**
Sensitivity (Cal)	1.000	0.964	0.778	0.852
Sensitivity (Pred)	0.909	0.964	0.778	0.833
Specificity (Cal)	0.982	0.824	0.669	0.851
Specificity (Pred)	0.982	0.832	0.678	0.843
Error (Cal)	0.009	0.106	0.276	0.148
Error (Pred)	0.055	0.102	0.272	0.162

LVs; Number of latent variables, Cal; Calibration set, Pred: Prediction set, Model D; Pure baobab (class 1), baobab plus rice flour (class 2), baobab plus wheat flour (class 3), and baobab plus maize flour (class 4).

Chemical similarities between the adulterants made it difficult for the model to differentiate the adulterants based on the NIR spectra. The chemical composition of BFP and the cereal flours used as adulterants have some similarities that lead to overlapping signals in their NIR spectra. All these samples contained varying proportions of carbohydrates, proteins, lipids, moisture, etc., which have C-H, O-H, and N-H bonds. That leads to overlapping NIR absorption bands making discrimination difficult (Liu *et al.*, 2015; Wilcock and Boys, 2014). For example, baobab and wheat flour have similar carbohydrate content of around 74% and 73% respectively (Muthai *et al.*, 2017; Ocheme *et al.*, 2018). This could lead to similar C-H absorption intensities.

Some of the wavelengths that contributed to the discrimination achieved in both two and four-class models were; 907-932 nm, 1106-1212 nm, 1350, 1440-1506 nm, 1630-1678 nm, 1630-1680 nm. Wavelengths 907-932 nm are related to the third overtone C-H stretch (Liu *et al.*, 2015) while 1106-1212 nm corresponded to the second overtone C-H stretch (Pedro and Ferreira, 2007). Combined C-H stretching was represented by absorption at 1350 nm while the first overtone O-H and N-H stretching were due to absorption signals at 1440-1506 nm (Liu *et al.*, 2015). Absorption bands at 1630-1678 nm resulted from the first overtone C-H stretch (Workman and Weyer, 2007). The C-H, O-H, and N-H chemical

bonds are major components of starch, water molecules, and proteins contained by BFP and adulterants. This indicated that the differences in the levels of these components between BFP and adulterants facilitated the discrimination achieved by the models.

4.6.3.3 Quantification of adulterants using partial least square regression (PLSR)

PLSR with cross-validation was adopted for the construction of multivariate calibration models for the quantification of adulterants present in BFP. Individual PLSR model for each adulteration was constructed using pre-processed spectra. Raw spectra were transformed with first derivative (FD) and mean centering (MC) for model 1, first derivative (FD), autoscaling (AS) for model 2, and first derivative (FD) and mean centering (MC) for model 3. The first four factors in model 1 explained 95.4%; the first 3 in model 2 explained 63.8%; and the first five factors explained 95.9% of the total spectral variance explained. The R^2 and RMSECV achieved by Model 1, Model 2, and Model 3 were 0.94 and 4.57%, 0.93 and 5.07%, 0.85 and 6, and 0.95%, respectively (Table 4.6). Constructed models performed better with the prediction set and resulted in the R^2 and RMSE of 0.98 and 2.74%, 0.94 and 4.86%, and 0.88 and 6.20% for model 1, model 2, and model 3, respectively (Table 4.6). This suggested that the prediction models were likely more reliable for estimating the level of RF, WF, and RF adulterants in new samples.

Table 4.6: PLSR results for the individual model for quantifying the concentration of the adulterants.

		Calibration set N=136				Prediction set N=44		
Model	**Adulterants**	**Pre-processing**	**Factors**	**R^2**	**RMSE**	**R^2**	**RMSE**	**LOD (%)**
Model 1	Rice	1D+MC	4	0.94	4.57	0.98	2.74	8.79
Model 2	Wheat	1D+AS	3	0.93	5.07	0.94	4.86	11.01
Model 3	Maize	1D+MC	5	0.85	6.95	0.88	6.20	13.79

N; Number of samples, R^2; Correlation coefficient, RMSE: Root mean square error, LOD; Limit of detection, 1D; First derivative, MC; Mean Centering, AS; Autoscaling.

Figures 4.18, 4.19, and 4.20 show scatter plots for PLSR models. The correlations between the measured spectra and the level of adulteration for rice flour, wheat flour, and maize flour were good with many points distributed along the regression lines. This indicated that a portable NIR spectrometer could be used to accurately measure the quantities of rice flour, wheat flour, and maize flour adulterants in BFP. Limits of detection (LODs) for each PLSR model were also computed to assess the sensitivity and ability of the models to detect the lowest level of adulterants present in BFP. Models 1, 2, and 3 resulted in 8.79%, 11.01%, and 13.79% LODs (Table 4.7).

Table 4.7: PLSR results for the individual model for quantifying the concentration of the adulterants.

		Calibration set N=136				Prediction set N=44		
Model	**Adulterants (Flour)**	**Pre-processing**	**Factors**	**R^2**	**RMSE**	**R^2**	**RMSE**	**LOD (%)**
Model 1	Rice	1D+MC	4	0.94	4.57	0.98	2.74	8.79
Model 2	Wheat	1D+AS	3	0.93	5.07	0.94	4.86	11.01
Model 3	Maize	1D+MC	5	0.85	6.95	0.88	6.20	13.79

N; Number of samples, R^2; Correlation coefficient, RMSE: Root mean square error, LOD; Limit of detection, 1D; First derivative, MC; Mean Centering, AS; Autoscaling

Those results suggested that a portable NIR spectrometer could estimate the level of MF, RF, and WF adulterants in BFP from as low as 8.79%. In general, the PLSR models for RF, WF, and MF indicated the high potential of a portable NIR spectrometer in predicting the level of RF, WF, and MF in BFP adulteration. The results of this study correlated well with those found by studies contacted by Ndlovu et al. (2021), Oliveira et al. (2020), Wang et al. (2022), and Da Costa Filho et al. (2022) involving the quantification of adulterants present in different samples using a spectrometer.

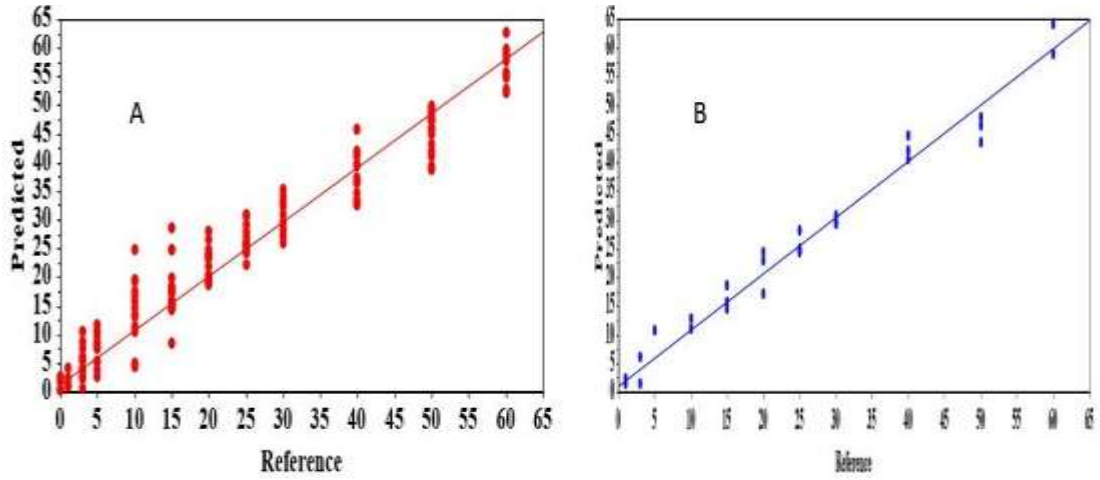

Figure 4.18: PLSR classification score plot for quantification of rice flour adulterants in baobab fruit pulp powder. (A) Calibration model (B) Prediction model

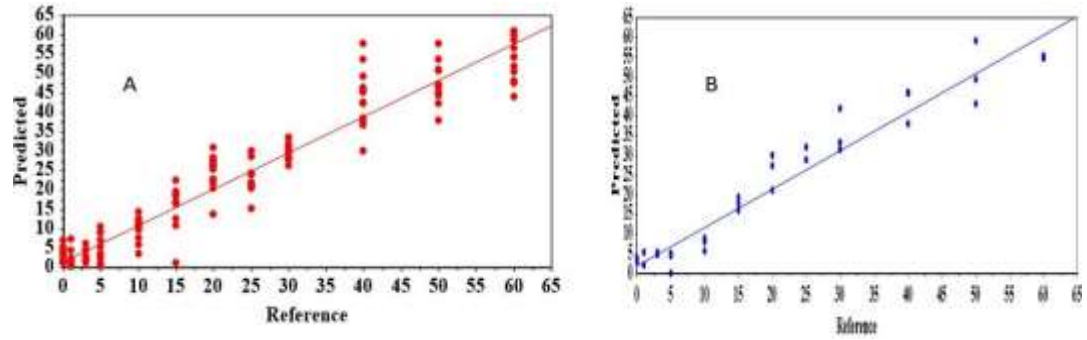

Figure 4.19: PLSR classification score plot for quantification of wheat flour adulterants in baobab fruit pulp powder. (A) Calibration model (B) Prediction model

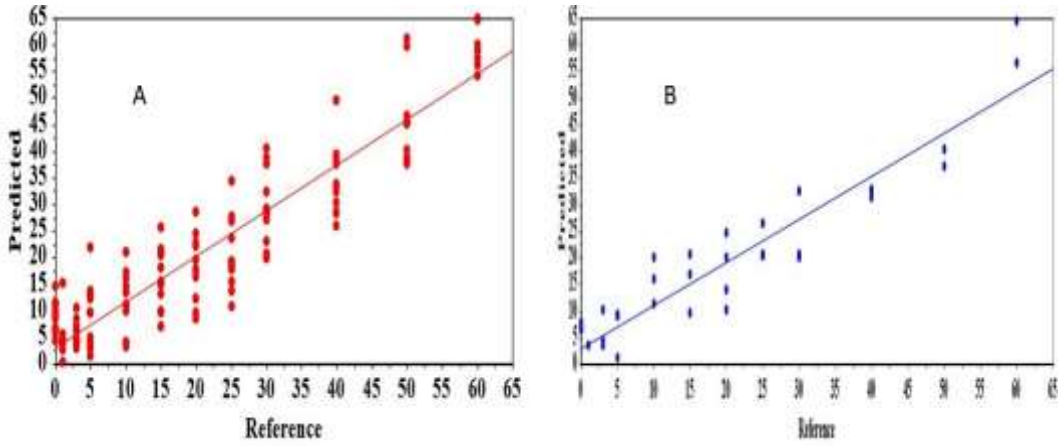

Figure 4.20: PLSR classification score plot for quantification of maize flour adulterants in baobab fruit pulp powder. (A) Calibration model (B) Prediction model.

CHAPTER FIVE

CONCLUSION AND RECOMMENDATION

5.1 Conclusion

In this study, the ability of a portable near-infrared (NIR) spectrometer to determine the quality of baobab fruit pulp (BFP) was evaluated. To realize this, a portable NIR spectrometer was evaluated for its ability to rapidly and non-destructively determine quality attributes, monitor the deterioration of quality parameters during storage, and detect and quantify adulterants present in BFP.

5.1.1 Applicability of NIR spectrometer in non-destructive testing of baobab quality

This study proved that a portable NIR spectrometer coupled with chemometrics of partial least square regression (PLSR) was capable of rapid, non-invasive, and accurate prediction of total titratable acidity (TTA), total soluble solids (TSS), vitamin C, and moisture content of BFP. Trained models performed exemplary in the prediction of TTA, TSS, vitamin C, and moisture content with prediction R^2 of above 0.63 and RPD of above 2.00.

5.1.2 The use of a portable NIR spectrometer to monitor changes in baobab quality parameters during storage

A portable NIR spectrometer was used to monitor changes in baobab quality parameters during storage. This study revealed that baobab quality attributes were affected during storage. The TTA, TSS, and vitamin C content deteriorated over time during storage. However, the intensity of deterioration varied depending on the parameters. The TTA declined during storage, but the changes were not significant. However, TSS and vitamin C greatly deteriorated during storage.

Moisture content on the other hand increased considerably over time despite the protection offered by the packaging materials. An unbleached kraft paper (UbKP) bag was not ideal for sample protection against the entrance of moisture content. The UbKP packaging

material permitted moisture content into the samples which promoted the growth of aerobic bacteria and yeast and moulds. Low-density polyethylene (LDPE) bags had better protection against the entry of moisture content. However, despite the absorption of moisture content by samples, the moisture levels remained below safe limits.

This study also revealed that the counts of aerobic bacteria and fungi rose during storage. In addition, samples packaged in LDPE bags had lower microbial load compared to those packaged in UbKP bags. However, despite the rise in microbial load, the levels of both aerobic bacteria and fungi were still below the acceptable limits.

5.1.3 Applicability of NIR spectrometer for rapid and non-destructive detection and quantification of BFP adulteration

The ability of a portable NIR spectrometer to detect and quantify adulteration of BFP was also investigated. Trained partial least square discriminant analysis (PLSDA) models proved to be efficient in the detection of pure and BFP adulterated with rice, wheat, and maize flours. Specifically, two-class models were the best in discriminating between pure and adulterated samples with specificity and sensitivity of above 0.982, and an error of below 0.009.

Finally, PLSR models were also constructed to predict the amount of adulterants present in BFP. The models performed exemplary with prediction R^2 of above 0.88 and error (RMSEP) of below 6.20%. A portable NIR spectrometer could accurately detect and quantify rice, wheat, and maize flours adulterants from as low as 8.79%.

In summary, a portable NIR spectrometer (wavelength 900-1700 nm) coupled with chemometrics of partial least square regression analysis and partial least square discriminant analysis could be a tool of choice for rapid, non-invasive, and precise prediction of baobab quality attributes, monitoring the degradation of baobab fruit pulp, and assessment of baobab authenticity.

5.2 Recommendation

5.2.1 Recommendation for Further Research

Similar research was recommended to compare the accuracy of Tellspec NIR (wavelength 900-1700 nm) and SCIO^{TM} (wavelength 700-1100 nm) spectrometers. Both of them are ultraportable NIR scanners but have different wavelength ranges, which dictates the penetration depth of the NIR radiation. Tellspec is ideal for probing bulk material which requires deeper penetration while SCIO^{TM} is suited for assessing materials that require shallow penetration. This study will provide information on the most accurate scanner for rapid assessment of BFP quality.

A research on the potential of portable NIR spectrometer to quantify other baobab quality parameters (e.g. dry matter, fiber, color, phenolic content, and aflatoxin level), the geographical origin, and the tree variety. In addition to the main attributes characterizing the quality of BFP, knowledge of the dry matter, fiber, color, phenolic content, and aflatoxin level is also very crucial for baobab quality. Traceability in terms of place of origin and tree variety is a key aspect of quality control of BFP. Therefore, this study recommends the use of an NIR spectrometer to determine other quality attributes as well as identify the origin and the variety of BFP.

5.2.2 Recommendation for the Policy

Due to a rising demand for BFP, farmers tend to harvest their fruits immaturely. This compromises the quality, leads to spoilage, and ruins the reputation of the baobab dealers. This study recommends the use of portable NIR spectrometers (Tellspec NIR scanner 900-1700 nm) by government agencies i.e. KEBS while carrying out the inspection, control, and standardization services on BFP products. This will enhance the use of new technologies that are more accurate, and faster and reduce the incidence of recall due to bad quality products.

5.2.3 Recommendation for Baobab Value Chain Actors

The demand for BFP is expanding massively both locally and abroad. Quality control is crucial for ensuring safety, customer satisfaction, and compliance with the set standards. Therefore, quality checks should be imposed at every stage along baobab value chains to guarantee the quality of BFP. For this purpose, this study recommends the use of a portable NIR spectrometer (Tellspec NIR scanner 900-1700 nm) for a non-invasive, rapid, onsite, reliable, and cheap method of analysing the quality of BFP.

REFERENCES

Abiona DL, Adedapo Z & Suleiman MK. (2015). Proximate Analysis, Phytochemical Screening and Antimicrobial Activity of Baobab (Adansonia digitata) Leaves. *IOSR Journal of Applied Chemistry Ver. I*, **8**, 60–65.

Adedokun, T.O., Matemu, A., Höglinger, O., Mlyuka, E. & Adedeji, A.A. (2021). Evaluation of Functional Attributes and Storage Stability of Novel Juice Blends from Baobab, Pineapple, and Black-Plum Fruits. *SSRN Electronic Journal*.

Agulheiro-Santos, A.C., Ricardo-Rodrigues, S., Laranjo, M., Melgão, C. & Velázquez, R. (2022). Non-destructive prediction of total soluble solids in strawberry using near infrared spectrometer. *Journal of the Science of Food and Agriculture*, **102**.

Ahmed, I. (2020). Uses, Constraints and Quality Characteristics of Juice Developed from a Wild Fruit-Baobab. *41.59.86.228*, **1**.

Alexopoulos, E.C. (2010). Introduction to multivariate regression analysis. *Hippokratia*, **14**.

Allegrini, F. & Olivieri, A.C. (2014). IUPAC-consistent approach to the limit of detection in partial least-squares calibration. *Analytical Chemistry*, **86**.

Amuah, C.L.Y., Teye, E., Lamptey, F.P., Nyandey, K., Opoku-ansah, J. & Adueming, P.O. (2019a). Feasibility Study of the Use of Handheld NIR Spectrometer for Simultaneous Authentication and Quantification of Quality Parameters in Intact Pineapple Fruits, **2019**.

Amuah, C.L.Y., Teye, E., Lamptey, F.P., Nyandey, K., Opoku-Ansah, J. & Adueming, P.O.W. (2019b). Feasibility Study of the Use of Handheld NIR Spectrometer for Simultaneous Authentication and Quantification of Quality Parameters in

Intact Pineapple Fruits. *Journal of Spectrometer*, **2019**.

Anjarwalla, P., Ofori, D., Owino, A., Matuku, D., Adika, W., Njogu, K. & Kehlenbeck, K. (2017). Testing different grafting methods for vegetative propagation of baobab (Adansonia digitata L.) in Kenya to assist its domestication and promote cultivation. *Forests Trees and Livelihoods*, **26**, 85–95.

Arifan, F., Winarni, S., Wahyuningsih, W., Pudjihastuti, I. & Broto, R.W. (2019). Total Plate Count (TPC) Analysis of Processed Ginger on Tlogowungu Village.

Armbruster, D.A. & Pry, T. (2008). Limit of blank, limit of detection and limit of quantitation. *The Clinical biochemist. Reviews*, **29 Suppl 1**.

Aron, P.M. & Kennedy, J.A. (2008). Flavan-3-ols: Nature, occurrence and biological activity. *Molecular Nutrition and Food Research*.

Arruda de Brito, A., Campos, F., Reis Nascimento, A. dos, Damiani, C., Alves da Silva, F., Almeida Teixeira, G.H. de & Cunha Júnior, L.C. (2022). Non-destructive determination of color, titratable acidity, and dry matter in intact tomatoes using a portable Vis-NIR spectrometer. *Journal of Food Composition and Analysis*, **107**, 104288.

Asogwa, I.S., Ibrahim, A.N. & Agbaka, J.I. (2021). African baobab: Its role in enhancing nutrition, health, and the environment. *Trees, Forests and People*.

Assogbadjo, A.E., Chadare, F.J., Kakaï, R.G., Fandohan, B. & Baidu-Forson, J.J. (2012). Variation in biochemical composition of baobab (Adansonia digitata) pulp, leaves and seeds in relation to soil types and tree provenances. *Agriculture, Ecosystems & Environment*, **157**, 94–99.

Barker, M. & Rayens, W. (2003). Partial least squares for discrimination. *Journal of Chemometrics*, **17**.

Barbin, D.F. et al (2012). Application of NIR spectrometer for online monitoring of fruit quality - a review. Postharvest Biology and Technology, Vol 71, pp 1-10. https://shorturl.at/xBNU3

Basri, K.N., Hussain, M.N., Bakar, J., Sharif, Z., Khir, M.F.A. & Zoolfakar, A.S. (2017). Classification and quantification of palm oil adulteration via portable NIR spectrometer. *Spectrochimica Acta - Part A: Molecular and Biomolecular Spectrometer*, **173**, 335–342.

Bastarrachea, L., Dhawan, S. & Sablani, S.S. (2011). Engineering Properties of Polymeric-Based Antimicrobial Films for Food Packaging. *Food Engineering Reviews*.

Beć, K.B., Grabska, J. & Huck, C.W. (2021). Principles and Applications of Miniaturized Near-Infrared (NIR) Spectrometers. *Chemistry - A European Journal*.

Beć, K.B., Grabska, J. & Huck, C.W. (2022). Miniaturized NIR Spectrometer in Food Analysis and Quality Control: Promises, Challenges, andfile:///C:/Users/hp/Downloads/Documents/foods-10-02377.pdf Perspectives. *Foods*, **11**.

Beghi, R., Spinardi, A., Bodria, L., Mignani, I. & Guidetti, R. (2013). Apples Nutraceutic Properties Evaluation Through a Visible and Near-Infrared Portable System. *Food and Bioprocess Technology*, **6**, 2547–2554.

Bellon-Maurel, V., Fernandez-Ahumada, E., Palagos, B., Roger, J.M. & McBratney, A. (2010). Critical review of chemometric indicators commonly used for assessing the quality of the prediction of soil attributes by NIR spectrometer. *TrAC - Trends in Analytical Chemistry*.

Berrueta, L.A., Alonso-Salces, R.M. & Héberger, K. (2007). Supervised pattern recognition in food analysis. *Journal of Chromatography A*.

Blakeney, M. (2019). *Food loss and food waste: Causes and solutions*. *Food Loss and Food Waste: Causes and Solutions*.

Borba, K.R., Aykas, D.P., Milani, M.I., Colnago, L.A., Ferreira, M.D. & Rodriguez-Saona, L.E. (2021). Portable near infrared spectrometer as a tool for fresh tomato quality control analysis in the field. *Applied Sciences (Switzerland)*, **11**.

Boukari, H., Jourdes, M., Le Floch, F., Riverain, F., Meudec, E., Lebail, A., & Davrieux, F. (2021). Baobab fruit shells and fibers: Promising sources of polysaccharides. Foods, 10(4), 717.

Bouzembrak, Y. & Marvin, H.J.P. (2016). Prediction of food fraud type using data from Rapid Alert System for Food and Feed (RASFF) and Bayesian network modelling. *Food Control*, **61**, 180–187.

Buzera, A., Gikundi, E., Orina, I. & Sila, D. (2022). Effect of Pretreatments and Drying Methods on Physical and Microstructural Properties of Potato Flour. *Foods*, **11**.

Caluwé, E. De, Halamová, K. & Damme, P. Van. (2009). Baobab (Adansonia digitata L.): A review of traditional uses, phytochemistry and pharmacology. *ACS Symposium Series*, **1021**, 51–84.

Calvin Rock Odhiambo., 2023. Kenyan baobab trees uprooted for export to Georgia; critics call it 'biopiracy'. Link; https://news.mongabay.com/2023/06/kenyan-baobab-trees-uprooted-for-export-to-georgia-critics-call-it-biopiracy/

Cen, H. & He, Y. (2007). Theory and application of near infrared reflectance spectrometer in determination of food quality. *Trends in Food Science & Technology*, **18**, 72–83.

Chadare, F.J. (2010). *Baobab (Adansonia digitata L.) foods from Benin: composition,*

processing and quality. Baobab (Adansonia digitata L.) foods from Benin: composition, processing and quality.

Chadare, F.J., Linnemann, A.R., Hounhouigan, J.D., Nout, M.J.R. & Boekel, M.A.J.S. Van. (2009). Baobab food products: A review on their composition and nutritional value. *Critical Reviews in Food Science and Nutrition*, **49**, 254–274.

Chen, L. & Opara, U.L. (2013). Texture measurement approaches in fresh and processed foods — A review. *Food Research International*, **51**, 823–835.

Chen, T., Zhang, J. & Luo, J. (2021). Differential game evolution of food quality safety based on market supply and demand. *Food Science and Nutrition*, **9**.

Chen, Y., Berkel, N. van, Luo, C., Sarsenbayeva, Z. & Kostakos, V. (2020). Application of miniaturized near-infrared spectrometer in pharmaceutical identification. *Smart Health*, **18**, 100126.

Chepngeno, J. (2018). The nutrient diversity of baobab Adansonia digitata L. across different geographic zones in Eastern Africa, **17**, 475–481.

Chepngeno, J., Imathiu, S., Owino, W.O. & Morlock, G.E. (2022a). Baobab pulp authenticity and quality control by multi-imaging high-performance thin-layer chromatography. *Food Chemistry*, **390**, 133108.

Chepngeno, J., Imathiu, S., Owino, W.O. & Morlock, G.E. (2022b). Baobab pulp authenticity and quality control by multi-imaging high-performance thin-layer chromatography. *Food Chemistry*, **390**, 133108.

Chia, K.S., Abdul Rahim, H. & Abdul Rahim, R. (2012). Prediction of soluble solids content of pineapple via non-invasive low cost visible and shortwave near infrared spectrometer and artificial neural network. *Biosystems Engineering*, **113**, 158–165.

Christine, B., Prehsler, S., Hartl, A. & Vogl, C.R. (2010). The importance of baobab (Adansonia digitata l.) in rural west african subsistence-suggestion of a cautionary approach to international market export of baobab fruits. *Ecology of Food and Nutrition*, **49**, 145–172.

Coe, S.A., Clegg, M., Armengol, M. & Ryan, L. (2013). The polyphenol-rich baobab fruit (Adansonia digitata L.) reduces starch digestion and glycemic response in humans. *Nutrition Research*, **33**, 888–896.

Cortés Rodríguez, M., Ciro Velásquez, H. & Hernández Sandoval, G. (2014). Effect of storage conditions on quality of a functional powder of cape gooseberry obtained by spray drying. *Cortés Rodríguez, Misael Ciro Velásquez, Héctor Hernández Sandoval, Gustavo*, **17**, 139–150.

Cortés, V., Ortiz, C., Aleixos, N., Blasco, J., Cubero, S. & Talens, P. (2016). A new internal quality index for mango and its prediction by external visible and near-infrared reflection spectrometer. *Postharvest Biology and Technology*, **118**, 148–158.

Coury, C. & Dillner, A.M. (2008). A method to quantify organic functional groups and inorganic compounds in ambient aerosols using attenuated total reflectance FTIR spectrometer and multivariate chemometric techniques. *Atmospheric Environment*, **42**.

Cristiano, M.C., Froiio, F., Costanzo, N., Poerio, A., Lugli, M., Fresta, M., Britti, D. & Paolino, D. (2019). Effects of flour mean particle size, size distribution and water content on rheological properties of wheat flour doughs. *European Food Research and Technology*, **245**.

Dandago, M.A. (2016). Proximate composition and effect of storage condition on Ascorbic acid content of Baobab fruits (Adonsonia digitate L .) pulp from Wudil , Kano State Article Information

Davey, M.W., Saeys, W., Hof, E., Ramon, H., Swennen, R.L. & Keulemans, J. (2009). Application of visible and near-infrared reflectance spectrometer (vis/NIRS) to determine carotenoid contents in banana (musa spp.) fruit pulp.

Denloye, A.A.B., Teslim, K.O., Fasasi, O.A., 2006. Insecticidal and repellency, EC, effects of smoke from plant pellets with or without D. 90 & against three medical insects. Journal of Entomology 3, 9–15. (n.d.). *entomology of baobab.pdf*.

Douie, C., Whitaker, J. & Grundy, I. (2015). Verifying the presence of the newly discovered African baobab, Adansonia kilima, in Zimbabwe through morphological analysis. *South African Journal of Botany*, **100**, 164–168.

Edogbanya, P.R.O. (2016). Comparative Study of the Proximate Composition of Edible Parts of Adansonia digitata L. obtained from Zaria, Kaduna State, Nigeria. *MAYFEB Journal of Biology*, **1**, 1–6.

Eldoom, E.A., Ali, A.E. & Abdel-razig, K.A. (2014). Baobab Fruits (with\without Shell) Affected by Wrapping and Type of Packaging Materials during Storage Period. *Asian Journal of Medical and Pharmaceutical Researches*, **4**, 46–52.

Everstine, K., Spink, J., & Kennedy, S. (2013). Economically motivated adulteration (EMA) of food: Common characteristics of EMA incidents. Journal of Food Protection, 76(4), 723-735.

FAO. (2021). Food fraud-Intention, detection and management. Food safety technical toolkit for Asia and the Pacific No. 5. Bangkok, 1–44.

Ferrara, G., Marcotuli, V., Didonna, A., Stellacci, A.M., Palasciano, M. & Mazzeo, A. (2022). Ripeness Prediction in Table Grape Cultivars by Using a Portable NIR Device. *Horticulturae*, **8**.

Ferreira, M.S.L., Santos, M.C.P., Moro, T.M.A., Basto, G.J., Andrade, R.M.S. &

Gonçalves, É.C.B.A. (2015). Formulation and characterization of functional foods based on fruit and vegetable residue flour. *Journal of Food Science and Technology*, **52**, 822–830.

Future Market Insights., 2021. Baobab Powder Market. https://www.futuremarketinsights.com/reports/baobab-powder-market

Galvin-King, P., Haughey, S.A. & Elliott, C.T. (2018). Herb and spice fraud; the drivers, challenges and detection. *Food Control*, **88**, 85–97.

Gebauer, J., El-Siddig, K. & Ebert, G. (2002). Baobab (Adansonia digitata L.): A Review on a multipurpose tree with promising future in the Sudan. *Gartenbauwissenschaft*, **67**, 155–160.

Hao, Y., Lu, Y. & Li, X. (2022). Study on robust model construction method of multi-batch fruit online sorting by near-infrared spectrometer. *Spectrochimica Acta Part A: Molecular and Biomolecular Spectrometer*, **280**, 121478.

Hasegawa, K. & Funatsu, K. (2012). Evolution of PLS for modeling SAR and omics data. *Molecular Informatics*, **31**.

Hemery, Y.M., Fontan, L., Laillou, A., Jallier, V., Moench-Pfanner, R., Avallone, S. & Berger, J. (2020). Influence of storage conditions and packaging of fortified wheat flour on microbial load and stability of folate and vitamin B12. *Food Chemistry: X*, **5**.

Huang, J., Wen, Q., Nie, Q., Chang, F., Zhou, Y. & Wen, Z. (2018). Miniaturized NIR spectrometer based on novel MOEMS scanning tilted grating. *Micromachines*, **9**.

Huang, L., Wen, Q., Huang, J., Yu, F., Lei, H. & Wen, Z. (2020). Miniature broadband NIR spectrometer based on FR4 electromagnetic scanning micro-grating. *Micromachines*, **11**.

Iacobucci, D., Schneider, M.J., Popovich, D.L. & Bakamitsos, G.A. (2016). Mean centering helps alleviate “micro” but not “macro” multicollinearity. *Behavior Research Methods*, **48**, 1308–1317.

Ibrahima, C., Didier, M., Max, R., Pascal, D., Benjamin, Y. & Renaud, B. (2013). Biochemical and nutritional properties of baobab pulp from endemic species of Madagascar and the African mainland. *African Journal of Agricultural Research*, **8**, 6046–6054.

Ismail, A.A., Cocciardi, R., Alvarez, P. & Sedman, J. (2005). Infrared and raman spectrometer in food science. In: *Handbook of Food Science, Technology, and Engineering - 4 Volume Set*.

Ismail, B.B., Pu, Y., Fan, L., Dandago, M.A., Guo, M. & Liu, D. (2019a). Characterizing the phenolic constituents of baobab (Adansonia digitata) fruit shell by LC-MS/QTOF and their in vitro biological activities. *Science of the Total Environment*, **694**, 133387.

Ismail, B.B., Pu, Y., Guo, M., Ma, X. & Liu, D. (2019b). LC-MS/QTOF identification of phytochemicals and the effects of solvents on phenolic constituents and antioxidant activity of baobab (Adansonia digitata) fruit pulp. *Food Chemistry*, **277**, 279–288.

Jafari, S.M., Jabari, S.S., Dehnad, D. & Shahidi, S.A. (2017). Effects of thermal processing by nanofluids on vitamin C, total phenolics and total soluble solids of tomato juice. *Journal of Food Science and Technology*, **54**.

Jakubíková, M., Sádecká, J., Kleinová, A. & Májek, P. (2016). Near-infrared spectrometer for rapid classification of fruit spirits. *Journal of Food Science and Technology*, **53**.

Jamal, S., Qazi, I.M. & Ahmed, I. (2016). Comparative studies on flour proximate compositions and functional properties of selected Pakistani rice varieties.

Proceedings of the Pakistan Academy of Sciences: Part B, **53**.

James, M., Owino, W., Imathiu, S. & Castillo, A. (2022). Microbial Contamination and Occurrence of Aflatoxins in Processed Baobab Products in Kenya. *International Journal of Food Science*, **2022**.

Jasinska, A., Wetli, E., & Schmid, O. (2006). Market development through certification in organic agriculture. Working paper. Research Institute of Organic Agriculture FiBL, CH-Frick.

Jay, J.M., Loessner, M.J. and Golden, D.A., 2005. Modern food microbiology 7th Edition. Springer Science, New York.

Jeon, H.J. & Kim, M.N. (2016). Isolation of mesophilic bacterium for biodegradation of polypropylene. *International Biodeterioration and Biodegradation*, **115**.

Jiang, Y., Li, C. & Takeda, F. (2016). Nondestructive Detection and Quantification of Blueberry Bruising using Near-infrared (NIR) Hyperspectral Reflectance Imaging. *Scientific Reports*, **6**.

Kabbashi, N.A., Mirghani, M.E.S., Alam, M.Z., Qudsieh, S.Y. & Bello, I.A. (2017). Characterization of the Baobab fruit shells as adsorption material. *International Food Research Journal*, **24**, 472–474.

Kamatou, G.P.P., Vermaak, I. & Viljoen, A.M. (2011). An updated review of Adansonia digitata: A commercially important African tree. *South African Journal of Botany*, **77**, 908–919.

Kouassi, K.S., Kouakou, A.T., Nanga, Y.Z., Kouakou, K.D. and Loukou, G.Y., 2021. Effect of Modified Atmosphere Packaging on the Physical, Chemical and Microbiological Properties of Baobab (Adansonia digitata L.) Fruit Pulp Powder. Food Processing & Technology, 12(1), pp.1-8.

Krishnan, A., Williams, L.J., McIntosh, A.R. & Abdi, H. (2011). Partial Least Squares (PLS) methods for neuroimaging: A tutorial and review. *NeuroImage*, **56**.

Lavine, B., Kaval, N., Westover, D. & Oxenford, L. (2006). New approaches to chemical sensing-sensors based on polymer swelling. *Analytical Letters*.

Lee, L.C., Liong, C.Y. & Jemain, A.A. (2018). Partial least squares-discriminant analysis (PLS-DA) for classification of high-dimensional (HD) data: A review of contemporary practice strategies and knowledge gaps. *Analyst*.

Li, J., Wang, Q., Xu, L., Tian, X., Xia, Y. & Fan, S. (2019). Comparison and Optimization of Models for Determination of Sugar Content in Pear by Portable Vis-NIR Spectrometer Coupled with Wavelength Selection Algorithm. *Food Analytical Methods*, **12**, 12–22.

Li, M., Ma, M., Zhu, K.X., Guo, X.N. & Zhou, H.M. (2017). Critical conditions accelerating the deterioration of fresh noodles: A study on temperature, pH, water content, and water activity. *Journal of Food Processing and Preservation*, **41**.

Lisao, K., Geldenhuys, C.J. & Chirwa, P.W. (2017). Traditional uses and local perspectives on baobab (Adansonia digitata) population structure by selected ethnic groups in northern Namibia. *South African Journal of Botany*, **113**, 449–456.

Liu, H., Xiang, B. & Qu, L. (2006). Structure analysis of ascorbic acid using near-infrared spectrometer and generalized two-dimensional correlation spectrometer. *Journal of Molecular Structure*, **794**, 12–17.

Liu, Y.-Y., Tu, Z.-H. & Chu, Q.-X. (2015). *A guide to near-infrared spectroscopic analysis of industrial manufacturing processes*. *2015 Asia-Pacific Microwave Conference (APMC)*.

Liu, Y., Sun, X. & Ouyang, A. (2010). Nondestructive measurement of soluble solid content of navel orange fruit by visible-NIR spectrometric technique with PLSR and PCA-BPNN. *LWT*, **43**.

Liu, Z., Zhang, R., Yang, C., Hu, B., Luo, X., Li, Y. & Dong, C. (2022). Research on moisture content detection method during green tea processing based on machine vision and near-infrared spectrometer technology. *Spectrochimica Acta Part A: Molecular and Biomolecular Spectrometer*, **271**, 120921.

Lorente, D., Aleixos, N., Gómez-Sanchis, J., Cubero, S., García-Navarrete, O.L. & Blasco, J. (2012). Recent Advances and Applications of Hyperspectral Imaging for Fruit and Vegetable Quality Assessment. *Food and Bioprocess Technology*.

Lu, Y.; Xia, Y.; Xu, J.; Chen, K. LED-Based NIR Spectrometer Sensor Development. Appl. Sci. 2019, 9 (11), 2358. https://doi.org/10.3390/app9112358. (3)

Maduro Dias, C.S.A.M., Nunes, H.P., Melo, T.M.M.V., Rosa, H.J.D., Silva, C.C.G. & Borba, A.E.S. (2021). Application of Near Infrared Reflectance (NIR) spectrometer to predict the moisture, protein, and fat content of beef for gourmet hamburger preparation. *Livestock Science*, **254**, 104772.

Magwaza, L.S. & Opara, U.L. (2015). Analytical methods for determination of sugars and sweetness of horticultural products-A review. *Scientia Horticulturae*.

Maleki, M.R., Mouazen, A.M., Ramon, H. & Baerdemaeker, J. De. (2007). Multiplicative Scatter Correction during On-line Measurement with Near Infrared Spectrometer. *Biosystems Engineering*, **96**.

Manjang, S., Issah, S., Thankappan, R., Fapetu, S., & Thomas, S. (2022). Baobab Seed Fibers as Potential Reinforcement for Polymer Composites. Polymers, 14(13), 2445.

Mart, M. V, Sharifzadeh, S., Wulfsohn, D., Clemmensen, H. & Toldam-andersen, T.B. (2013). A sampling approach for predicting the eating quality of apples using visible – near infrared spectrometer.

McGrath, T.F., Haughey, S.A., Patterson, J., Fauhl-Hassek, C., Donarski, J., Alewijn, M., Ruth, S. van & Elliott, C.T. (2018). What are the scientific challenges in moving from targeted to non-targeted methods for food fraud testing and how can they be addressed? – Spectrometer case study. *Trends in Food Science & Technology*, **76**, 38–55.

Meerza, S.I.A. & Gustafson, C.R. (2018). Consumer Response to Food Fraud, 1–20.

Mehmood, T., Martens, H., Sæbø, S., Warringer, J. & Snipen, L. (2011). A Partial Least Squares based algorithm for parsimonious variable selection. *Algorithms for Molecular Biology*, **6**.

Mgaya-Kilima, B., Remberg, S.F., Chove, B.E. & Wicklund, T. (2014). Influence of storage temperature and time on the physicochemical and bioactive properties of roselle-fruit juice blends in plastic bottle. *Food Science & Nutrition*, **2**.

Millington, D.S. & Stevens, R.D. (2011). Metabolic Profiling: Methods in Molecular Biology (Methods and Protocols). *Methods in Molecular Biology*, **708**.

Mishra, P. and Roger, J.M., 2022. Recent trends in near-infrared spectrometer and chemometrics. TrAC Trends in Analytical Chemistry, 146, p.116534.

Momanyi, D.K., Owino, W.O., Makokha, A., Evang, E. & Tsige, H. (2019). Gaps in food security , food consumption and malnutrition in households residing along the baobab belt in Kenya.

Mpofu, A., Linnemann, A.R., Sybesma, W., Kortbech-Olesen, R., Ndinteh, D.T., Sekwati-Monang, B., & Hagenimana, A. (2014). Baobab Dried Fruit Pulp: A Review of Key Processing Stages and Quality Attributes. Critical Reviews in Food Science and Nutrition, 54(11), 1365–1375.

Msalilwa, U.L., Makule, E.E., Munishi, L.K. & Ndakidemi, P.A. (2020). Physicochemical Properties, Fatty Acid Composition, and the Effect of Heating on the Reduction of Cyclopropenoid Fatty Acids on Baobab (Adansonia digitata L.) Crude Seed Oil. *Journal of Lipids*, **2020**.

Munawar, A.A., Hayati, R. & Fachruddin, F. (2021). Rapid determination of inner quality parameters of intact mango fruits using portable near infrared spectrometer. In: *IOP Conference Series: Earth and Environmental Science*.

Munissi, J.J.E., Thomsen, M.H., Jensen, J.S., Mazoko, G., Nyagava, S., & Eskildsen, C.E. (2022). Quality control of baobab (Adansonia digitata L.) fruit pulp towards development of a Tanzanian national standard. Food Control, 137, 108858.

Munyawiri, G., Chikamba, C., & Murungweni, C. (2022). Management of indigenous fruit tree resources for improved food security: The case of Adansonia digitata. In Rediscovering Indigenous Food Plants in Zimbabwe (pp. 137-159). Springer, Cham

Munyebvu, F., Mapaure, I. & Kwembeya, E.G. (2018). Abundance, structure and uses of Baobab (Adansonia digitata L.) populations in Omusati Region, Namibia. *South African Journal of Botany*, **119**, 112–118.

Masawat, P.; Harrabi, K.; Cole, M.; Georgiev, G.; Mandai, S.; Weiss, K.; Faul, C. LEDs as Visible and NIR Light Sources for Silicon Photomultipliers and Other Solid-State Photodetectors. Sensors 2020, 20 (3), 681. https://doi.org/10.3390/s20030681. (4)

Muthai, K.U., Karori, M.S., Muchugi, A., Indieka, A.S., Dembele, C., Mng'omba, S. &

Jamnadass, R. (2017). Nutritional variation in baobab (Adansonia digitata L.) fruit pulp and seeds based on Africa geographical regions. *Food Science and Nutrition*, **5**, 1116–1129.

Munissi, J.J.E., Thomsen, K.A., Soka, G.N., et al. (2022). A comparative study of nutrients, antinutrients, and toxic elements in baobab fruit pulp from Africa, Madagascar, and Australia. Food Chemistry, 387, 133059. https://doi.org/10.1016/j.foodchem.2022.133059

Mwale, M., Masamba, K.G., & Mtunzi, F. (2016). Utility of baobab (Adansonia digitata L.) pulp fibre as a feed resource for compounding rabbit pellets. Medwell Journals, 11(4), 300-305.

Ncama, K., Opara, U.L., Tesfay, S.Z., Fawole, O.A. & Magwaza, L.S. (2017). Application of Vis/NIR spectrometer for predicting sweetness and flavour parameters of 'Valencia' orange (Citrus sinensis) and 'Star Ruby' grapefruit (Citrus x paradisi Macfad). *Journal of Food Engineering*, **193**, 86–94.

Nguyen Do Trong, N., Tsuta, M., Nicolaï, B.M., De Baerdemaeker, J., & Saeys, W. (2014). Use of acoustic, X-ray, laser and hyperspectral imaging with multivariate data analysis to predict sweet cherry fruit characteristics. Postharvest Biology and Technology,

Nour, A., Magboul, B. & Kheiri, N. (1980). Chemical composition of baobab fruit (Adansonia digitata L.). *Tropical Science*.

Nyam, K.L., Tan, C.P., Lai, O.M., Long, K. & Che Man, Y.B. (2009). Physicochemical properties and bioactive compounds of selected seed oils. *LWT - Food Science and Technology*, **42**, 1396–1403.

Ocheme, O.B., Adedeji, O.E., Chinma, C.E., Yakubu, C.M. & Ajibo, U.H. (2018). Proximate composition, functional, and pasting properties of wheat and groundnut protein concentrate flour blends. *Food Science and Nutrition*.

Odriozola-Serrano, I., Hernández-Jover, T. and Martín-Belloso, O., 2009. Comparative evaluation of UV-HPLC methods and reducing agents to determine vitamin C in fruits. Food chemistry, 117(3), pp.391-396.

Oliveira, M.M., Cruz-Tirado, J.P. & Barbin, D.F. (2019). Nontargeted Analytical Methods as a Powerful Tool for the Authentication of Spices and Herbs: A Review. *Comprehensive Reviews in Food Science and Food Safety*, **18**, 670–689.

Oliveira, M.M., Cruz-Tirado, J.P., Roque, J. V., Teófilo, R.F. & Barbin, D.F. (2020a). Portable near-infrared spectrometer for rapid authentication of adulterated paprika powder. *Journal of Food Composition and Analysis*, **87**.

Oliveira, M.M., Cruz-Tirado, J.P., Roque, J. V., Teófilo, R.F. & Barbin, D.F. (2020b). Portable near-infrared spectrometer for rapid authentication of adulterated paprika powder. *Journal of Food Composition and Analysis*, **87**, 103403.

Oliveira, M.M., Cruz-Tirado, J.P., Roque, J.V., Teófilo, R.F. & Barbin, D.F. (2020c). Portable near-infrared spectrometer for rapid authentication of adulterated paprika powder. *Journal of Food Composition and Analysis*, **87**, 103403.

Olmos, V., Bedia, C., Tauler, R. & Juan, A. de. (2018). Preprocessing Tools Applied to Improve the Assessment of Aldrin Effects on Prostate Cancer Cells Using Raman Spectrometer. *Applied Spectrometer*, **72**.

Onyeaka, H., Agbugba, I., Ekwebelem, O.C., Anumudu, C., Anyogu, A., Odeyemi, O. & Agbagwa, S. (2021). Strategies to Mitigate the Impact of COVID-19 on Food Security and Malnutrition in Nigeria. *European Journal of Nutrition & Food Safety*.

Orequent, R., Haddi, Z., Mabrouk, S., Bouchra, B., Tarik, S., ... & Moulay, A. (2022). Honey adulteration screening by portable near infrared spectrometer and chemometrics. Food Control, 137, 108837.

Osman, M.A. (2004). Chemical and nutrient analysis of baobab (Adansonia digitata) fruit and seed protein solubility. *Plant Foods for Human Nutrition*, **59**, 29–33.

Ou, F., Klinken, A. van, Ševo, P., Petruzzella, M., Li, C., Elst, D.M.J. van, Hakkel, K.D., Pagliano, F., Veldhoven, R.P.J. van & Fiore, A. (2022). Handheld NIR Spectral Sensor Module Based on a Fully-Integrated Detector Array. *Sensors*, **22**.

Ozaki, Y., Mcclure, W.F. & Christy, A.A. (2006). *Near-Infrared Spectrometer in Food Science and Technology*. *Near-Infrared Spectrometer in Food Science and Technology*.

Pal, M. & Mahinder, M. (2020). Food adulteration: A global public health concern, **1**, 38–40.

Palermo, G., Piraino, P. & Zucht, H.D. (2009). Performance of PLS regression coefficients in selecting variables for each response of a multivariate PLS for omics-type data. *Advances and Applications in Bioinformatics and Chemistry*, **2**.

Pan, L., Lu, R., Zhu, Q., McGrath, J.M. & Tu, K. (2015). Measurement of moisture, soluble solids, sucrose content and mechanical properties in sugar beet using portable visible and near-infrared spectrometer. *Postharvest Biology and Technology*, **102**, 42–50.

Passos, M.L.C., Sarraguça, M.C. & Saraiva, M.L.M.F.S. (2019). Spectrophotometry | organic compounds. In: *Encyclopedia of Analytical Science*.

Pedro, A.M.K. & Ferreira, M.M.C. (2007). Simultaneously calibrating solids, sugars and acidity of tomato products using PLS2 and NIR spectrometer. *Analytica Chimica Acta*, **595**, 221–227.

Petriccione, M., Mastrobuoni, F., Pasquariello, M.S., Zampella, L., Nobis, E., Capriolo,

G. & Scortichini, M. (2015). Effect of chitosan coating on the postharvest quality and antioxidant enzyme system response of strawberry fruit during cold storage. *Foods*, **4**.

Pissard, A., Fernández Pierna, J.A., Baeten, V., Sinnaeve, G., Lognay, G., Mouteau, A., Dupont, P., Rondia, A. & Lateur, M. (2013). Non-destructive measurement of vitamin C, total polyphenol and sugar content in apples using near-infrared spectrometer. *Journal of the Science of Food and Agriculture*, **93**.

Qamar, S., Aslam, M., Huyop, F. & Javed, M.A. (2017). Comparative study for the determination of nutritional composition in commercial and noncommercial maize flours. *Pakistan Journal of Botany*, **49**.

Rahman, M.S. (2009). Food stability beyond water activity and glass transtion: Macro-micro region concept in the state diagram. *International Journal of Food Properties*, **12**.

Rahul, J., Jain, M.K., Singh, S.P., Kamal, R.K., Anuradha, Naz, A., Gupta, A.K. & Mrityunjay, S.K. (2015). Adansonia digitata L. (baobab): A review of traditional information and taxonomic description. *Asian Pacific Journal of Tropical Biomedicine*, **5**, 79–84.

Ramalho, F.M.G., Simetti, R., Arriel, T.G., Loureiro, B.A. & Hein, P.R.G. (2019). Influence of particles size on nir spectroscopic estimations of charcoal properties. *Floresta e Ambiente*, **26**.

Reeb, J. & Milota, M. (1999). MOISTURE CONTENT BY THE OVEN-DRY METHOD FOR INDUSTRIAL TESTING Weight of water Weight of wood MC -. *Wdka*.

Rinnan, Å., Berg, F. van den & Engelsen, S.B. (2009). Review of the most common pre-processing techniques for near-infrared spectra. *TrAC - Trends in Analytical Chemistry*, **28**, 1201–1222.

Rinnan, Å., 2021. Preprocessing in vibrational spectrometer – differences between NIR and MIR data analysed with chemometrics. Applied Spectrometer Reviews 56, 496–514.

Roger, J.M., Bellon-Maurel, V., 2020. Using NIR hyperspectral imaging for food quality analysis: A review. Applied Spectrometer Reviews 55, 167–201.

Roggo, Y., Chalus, P., Maurer, L., Lema-Martinez, C., Edmond, A. & Jent, N. (2007). A review of near infrared spectrometer and chemometrics in pharmaceutical technologies. *Journal of Pharmaceutical and Biomedical Analysis*.

Rongtong, B., Suwonsichon, T., Ritthiruangdej, P. & Kasemsumran, S. (2018). Determination of water activity, total soluble solids and moisture, sucrose, glucose and fructose contents in osmotically dehydrated papaya using near-infrared spectrometer. *Agriculture and Natural Resources*, **52**, 557–564.

Rop, O., Mlcek, J. and Jurikova, T., 2012. The role of antioxidant active substances in the total antioxidant activity of various non-traditional fruit species and their correlation between individual antioxidants. International journal of electrochemical science, 7(4), pp.3337-3350

Shewfelt, R.L. (2014). Measuring Quality and Maturity. In: *Postharvest Handling: A Systems Approach*.

Sandhya, 2010. Modified atmosphere packaging of fresh produce: Current status and future needs. LWT - Food Science and Technology, 43(3), pp.381-392

Shaw, R.A. and Mantsch, H.H., 2022. Infrared spectrometer in clinical and diagnostic analysis. Clinical Spectrometer, 1, p.100004.

Sidibe, M. & Williams, J.T. (2002). *Baobab. Adansonia digitata L. Adansonia*.

Silva, O. R. R. F., & Silva, M. R. (2021). Sustainable packaging for the commercialization of vegetable oils and fats. In Sustainable Vegetable Oils and Fats (pp. 105-137). AOCS Press

Sisouane, M., Cascant, M.M., Tahiri, S., Garrigues, S., Krati, M. EL, Boutchich, G.E.K., Cervera, M.L. & la Guardia, M. de. (2017). Prediction of organic carbon and total nitrogen contents in organic wastes and their composts by Infrared spectrometer and partial least square regression. *Talanta*, **167**.

Sorak, D.; Herberholz, L.; Iwascek, S.; Altinpinar, S.; Pfeifer, F.; Siesler, H. W. New Developments and Applications of Handheld Raman, Mid-Infrared, and Near-Infrared Spectrometers. Appl. Spectrosc. Rev. 2012, 47 (2), 83–115. https://doi.org/10.1080/05704928.2011.621067. (5)

Stadlmayr, B., Charrondière, U.R., Eisenwagen, S., Jamnadass, R. & Kehlenbeck, K. (2013). Nutrient composition of selected indigenous fruits from sub-Saharan Africa. *Journal of the Science of Food and Agriculture*, **93**, 2627–2636.

Stadlmayr, B., Wanangwe, J., Waruhiu, C.G., Jamnadass, R. & Kehlenbeck, K. (2020). Nutritional composition of baobab (Adansonia digitata L.) fruit pulp sampled at different geographical locations in Kenya. *Journal of Food Composition and Analysis*, **94**, 103617.

Tembo, D.T., Holmes, M.J. & Marshall, L.J. (2017). Effect of thermal treatment and storage on bioactive compounds, organic acids and antioxidant activity of baobab fruit (Adansonia digitata) pulp from Malawi. *Journal of Food Composition and Analysis*, **58**, 40–51.

Tewari, J.C. & Irudayaraj, J.M.K. (2005). Floral classification of honey using mid-infrared spectrometer and surface acoustic wave based z-Nose sensor. *Journal of Agricultural and Food Chemistry*, **53**.

Tugnolo, A., Giovenzana, V., Malegori, C., Oliveri, P., Casson, A., Curatitoli, M.,

Guidetti, R. & Beghi, R. (2021). A reliable tool based on near-infrared spectrometer for the monitoring of moisture content in roasted and ground coffee: A comparative study with thermogravimetric analysis. *Food Control*, **130**, 108312.

Vartiainen, J., Vähä-Nissi, M. & Harlin, A. (2014). Biopolymer Films and Coatings in Packaging Applications—A Review of Recent Developments. *Materials Sciences and Applications*, **05**.

Venter, S.M. & Witkowski, E.T.F. (2019). Phenology, flowering and fruit-set patterns of baobabs, Adansonia digitata, in southern Africa. *Forest Ecology and Management*, **453**, 117593.

Vikram, V.B., Ramesh, M.N. & Prapulla, S.G. (2005). Thermal degradation kinetics of nutrients in orange juice heated by electromagnetic and conventional methods. *Journal of Food Engineering*, **69**.

Vunain, E., Chirambo, F., Sajidu, S. & Mguntha, T.T. (n.d.). Proximate Composition , Mineral Composition and Phytic Acid in Three Common Malawian White Rice Grains, 87–108.

Wang, J., Wang, J., Chen, Z. & Han, D. (2017). Development of multi-cultivar models for predicting the soluble solid content and firmness of European pear (Pyrus communis L.) using portable vis–NIR spectrometer. *Postharvest Biology and Technology*, **129**, 143–151.

Wang, Y.J., Li, T.H., Li, L.Q., Ning, J.M. & Zhang, Z.Z. (2020). Micro-NIR spectrometer for quality assessment of tea: Comparison of local and global models. *Spectrochimica Acta Part A: Molecular and Biomolecular Spectrometer*, **237**, 118403.

Wickens, G.E. (2007). *The baobabs: Pachycauls of Africa, Madagascar and Australia*. *The Baobabs: Pachycauls of Africa, Madagascar and Australia*.

Wilcock, A.E. & Boys, K.A. (2014). Reduce product counterfeiting: An integrated approach. *Business Horizons*, **57**, 279–288.

Workman, J.. J. & Weyer, L. (2007). *Practical Guide to Interpretive Near-Infrared Spectrometer*. *Practical Guide to Interpretive Near-Infrared Spectrometer*.

Workman, J., 2020. A review of process near infrared spectrometer and chemometrics in pharmaceutical technologies. Applied Spectrometer Reviews 55, 391–428

Worley, B., Halouska, S. & Powers, R. (2013). Utilities for quantifying separation in PCA/PLS-DA scores plots. *Analytical Biochemistry*, **433**.

Wynberg, R., Laird, S., Niekerk, J. Van & Kozanayi, W. (2015). Formalization of the Natural Product Trade in Southern Africa: Unintended Consequences and Policy Blurring in Biotrade and Bioprospecting. *Society and Natural Resources*, **28**, 559–574.

Xie, L., Ye, X., Liu, D. & Ying, Y. (2011). Prediction of titratable acidity, malic acid, and citric acid in bayberry fruit by near-infrared spectrometer. *Food Research International*, **44**, 2198–2204.

Yan, M.R., Hsieh, S. & Ricacho, N. (2022). Innovative Food Packaging, Food Quality and Safety, and Consumer Perspectives. *Processes*.

Yao, H. & Lewis, D. (2010). Spectral Preprocessing and Calibration Techniques. In: *Hyperspectral Imaging for Food Quality Analysis and Control*.

Yegon, D., Ojijo, N.K., Tybussek, T. & Owino, W. (2023). Application of portable near-infrared spectrometer for rapid detection and quantification of adulterants in baobab fruit pulp. *International Journal of Food Science & Technology*, 1–9.

Zhou, Y., Wen, Q., Wen, Z. & Yang, T. (2016). Modeling of MOEMS electromagnetic scanning grating mirror for NIR micro-spectrometer. *AIP Advances*, **6**.

Zhu, D., Development, N., Ji, B. & Wang, C. (2010). The Detection of Quality Deterioration of Apple Juice by Near Infrared and The Detection of Quality Deterioration of Apple Juice by Near Infrared and Fluorescence Spectrometer.

Ziegel, E.R. (2004). A User-Friendly Guide to Multivariate Calibration and Classification.

APPENDICES

Appendix I: Set-up for the storage experiment.

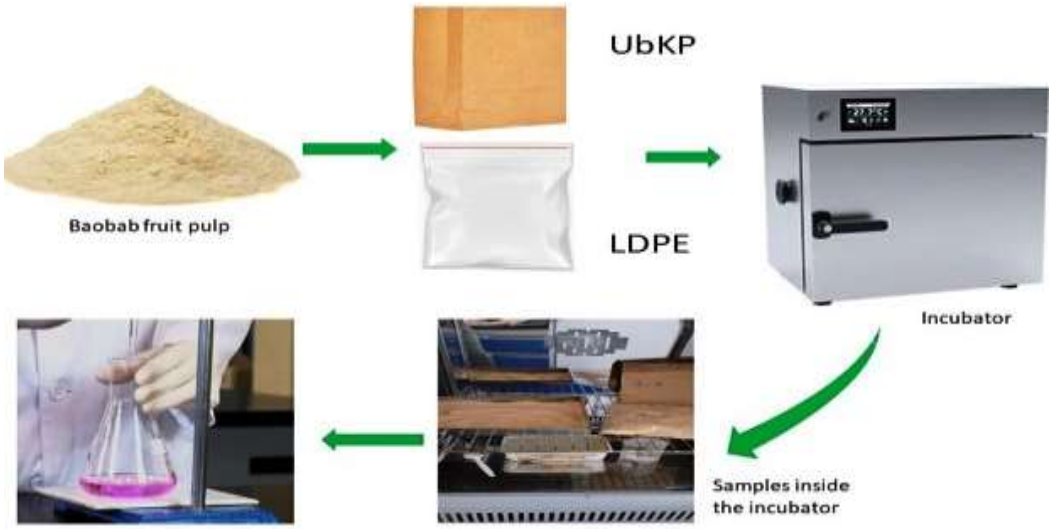

Appendix II: NIR spectra pre-processed with (A) Raw (Unprocessed), (B) Smoothed with SG, (C) Multiplicative scatter correction and mean-centered (MSC+MC), (D)Standard Normal Variate (SNV).

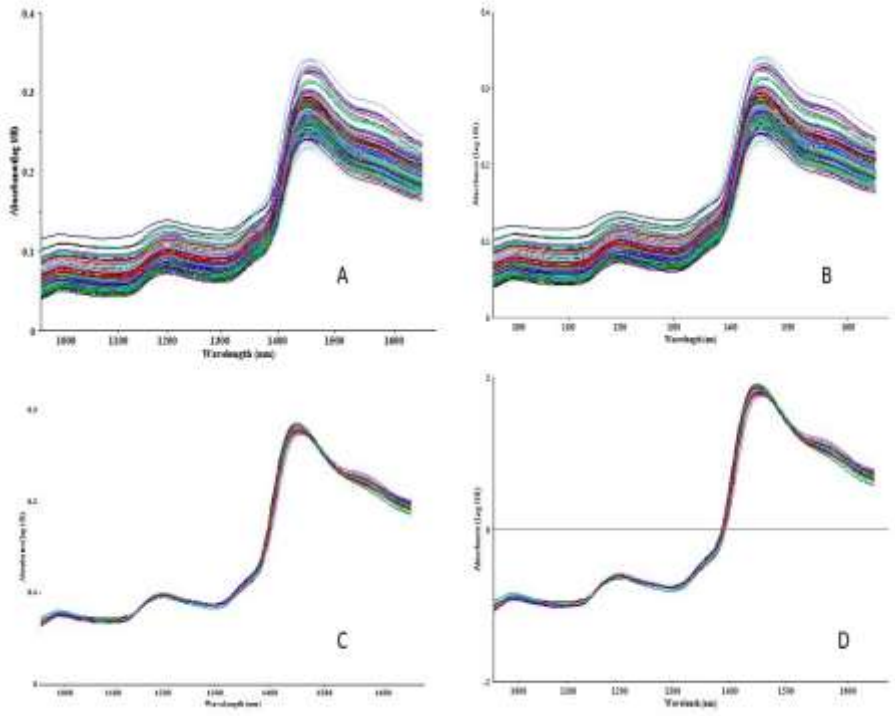

Appendix III: Summary of statistical results for models predicting baobab quality attributes developed using different pre-processing methods.

	Calibration Set				Prediction Set		
Parameter/Model	**Pre-processing**	**Factors**	**R^2**	**RMSE**	**R^2**	**RMSE**	**Bias**
TTA	Raw	5	0.34	1.53	N/A	1.80	-1.11
	Smoothing+BO	10	0.42	1.43	0.38	1.80	-1.11
	Smoothing+AN	10	0.42	1.43	0.07	1.38	-0.80
	SNV	**7**	**0.81**	**0.77**	**0.82**	**0.70**	**0.09**
	SNV+MC	7	0.79	0.89	0.77	0.88	0.10
	SNV+AS	6	0.83	0.81	N/A	0.98	0.03
	MSC	4	0.45	0.98	0.51	0.87	-0.65
	FD+MC	7	0.53	1.28	0.52	1.28	-0.87
	MSC	7	0.39	1.47	N/A	1.57	-0.85
	FD+BO	7	0.54	1.27	0.46	10.76	-10.66
TSS	Raw	1	0.30	0.25	0.14	0.21	-0.01
	MSC+AS	3	0.08	0.21	0.14	0.21	-0.01
	MSC+MC	3	0.09	0.21	0.13	0.19	-0.01
	MSC+BO	3	0.08	0.25	0.14	0.21	-0.01
	MSC+FD	1	0.25	0.27	0.34	0.22	-0.02
	Smoothing	**4**	**0.62**	**0.15**	**0.63**	**0.16**	**0.09**
	AN	4	0.54	0.17	0.40	0.22	0.10
	Detrend	6	0.48	0.27	0.49	0.20	-0.02
	SNV	5	0.46	0.17	N/A	0.22	-0.09
	SNV+MS	5	0.47	0.17	N/A	0.22	-0.08
	OSC	4	0.56	0.17	O.57	0.17	0.10
Vitamin C	Raw	5	0.49	12.16	0.48	12.02	3.34
	MSC	6	0.54	13.45	0.56	14.56	2.68
	MSC+MC	**6**	**0.72**	**9.29**	**0.74**	**9.67**	**2.115**
	SNV	4	0.54	11.45	0.47	14.68	3.67
	SNV+AS	3	0.55	11.01	0.51	18.99	4.46
	SNV+MC	4	0.53	12.98	0.50	16.77	4.44
	AN	4	0.34	21.34	N/A	17.86	1.86
	Detrend	6	0.64	15.33	N/A	14.23	3.01
	OSC	7	0.55	16.77	0.50	17.98	-1.14
	SGS+BO	7	0.67	34.55	N/A	37.68	2.78
Moisture	Raw	4	0.94	1.38	0.94	1.88	0.53
	MSC	4	0.94	1.40	0.93	2.73	0.38
	MSC+MC	**4**	**0.94**	**1.40**	**0.95**	**1.31**	**0.38**
	MSC+AS	3	0.87	1.56	0.90	1.56	0.40

	Detrend	2	0.67	1.89	0.65	1.95	-1.34
	OSC	5	0.88	1.37	N/A	1.37	-1.62
	SNV	4	0.94	1.40	0.79	6.08	-1.48
	SNV+AS	4	0.94	1.41	0.04	6.08	-1.48
	AN	3	0.90	1.76	0.81	2.67	-0.11
	SGS+BO	3	0.92	1.55	0.91	1.87	0.55

R^2-R-squared/Correlation coefficient

RMSE-Root means square error

TTA-Total titratable acidity

TSS-Total soluble solids

Raw- (Unprocessed spectra)

MSC-Multiplicative scatter correction

MC- Mean Centering

SNV- Standard normal variate

AS- Autoscalling

AN-Area normalization

SGS-Savitzky Golay smoothing

BO-Baseline offset

Appendix IV: Summary of statistical results for models predicting the amounts of adulterants trained after pre-processing raw spectra using different methods.

	Calibration Set				Prediction Set		
Parameter/ Model	**Pre-processing**	**Factors**	**R^2**	**RMSE**	**R^2**	**RMSE**	**Bias**
RF	Raw	7	0.86	7.34	0.80	8.57	-3.95
	Smoothing + BO	4	0.84	7.68	0.84	7.26	-2.39
	Smoothing + AN	2	0.83	7.87	0.84	7.53	-1.16
	SNV	4	0.86	7.19	0.81	8.20	-4.43
	SNV+MC	2	0.84	7.83	0.86	7.16	0.00
	SNV+AS	2	0.84	7.66	0.84	7.57	-1.98
	MSC	4	0.86	7.27	0.81	8.20	-4.44
	MSC+MC	4	0.86	7.26	0.81	8.21	-4.44
	FD+BO	5	0.86	7.35	N/A	24.09	9.56
	FD+MC	**4**	**0.94**	**4.57**	**0.98**	**2.74**	**1.11**
	FD+AS	5	0.94	3.85	0.94	4.63	-2.52
MF	Raw	7	0.65	11.61	0.70	10.36	0.41
	MSC	7	0.74	9.91	0.70	10.44	1.19
	MSC+MC	7	0.75	9.84	0.70	10.45	1.19
	SNV	7	074	9.93	0.70	10.45	1.20
	SNV+MC	7	0.74	10.00	0.74	9.53	1.32
	SNV+AS	7	0.75	9.78	0.75	9.53	1.32
	AN	4	0.14	18.12	N/A	20.18	2.01
	Smoothing + BO	3	0.61	12.33	0.57	12.41	3.17
	FD+MC	**5**	**0.85**	**6.95**	**0.88**	**6.20**	**2.41**
	FD+AS	5	0.83	7.34	0.80	7.35	2.40
	SD	3	0.65	11.55	N/A	60.01	56.27
	Detrend	6	0.81	8.24	0.73	9.73	0.26
WF	Raw	6	0.91	5.81	0.91	5.78	0.51
	MSC	2	0.91	5.86	0.91	5.60	0.33
	MSC+MC	6	0.91	5.93	0.92	5.00	1.34
	MSC+AS	6	0.91	5.93	0.91	5.65	0.81
	SNV	2	0.91	5.83	0.91	5.60	0.33
	SNV+MC	2	0.91	5.88	0.91	5.60	0.33
	SNV+AS	2	0.90	6.14	0.90	5.98	-0.17
	FD+MC	3	0.89	6.76	0.87	6.74	0.42
	FD+AS	**3**	**0.93**	**5.07**	**0.94**	**4.86**	**0.30**

R^2-R-squared/Correlation coefficient

RMSE-Root means square error

MF-Maize flour

RF-Rice flour

WF-Wheat flour

Raw- (Unprocessed spectra)

MSC-Multiplicative scatter correction

MC- Mean centering

SNV- Standard normal variate

AS- Autoscalling

AN-Area normalization

BO-Baseline offset

Appendix V: X-loading weight plots of the optimal models for (a) TTA prediction, (b) TSS prediction, (c) Vitamin C prediction, and (d) moisture content prediction

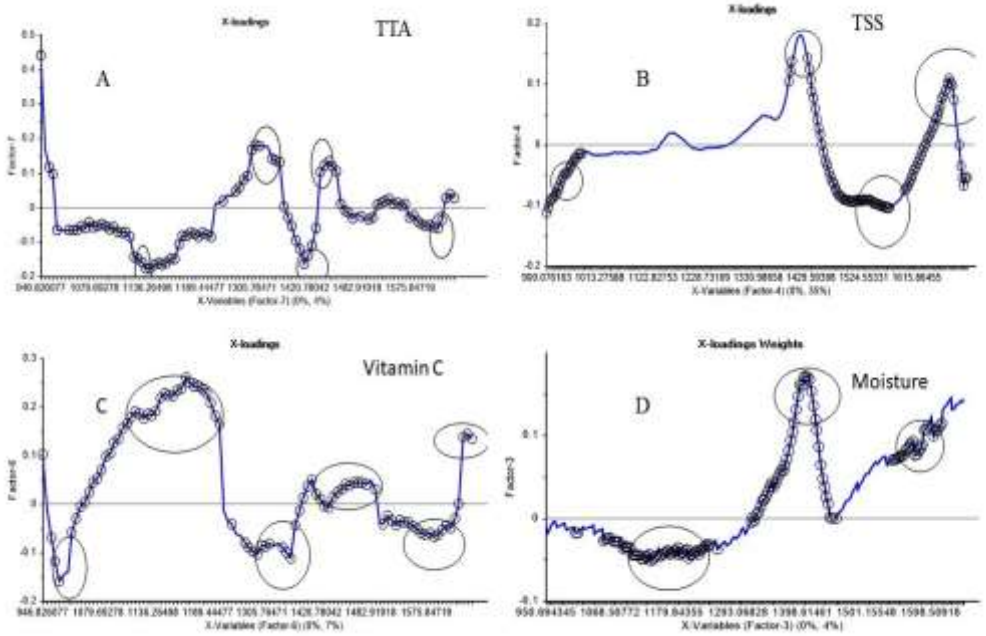

Appendix VI: RMSECV against LVs plot for baobab fruit pulp adulterated with; (A) rice flour, (B) wheat flour, (C) maize flour, and (D) all adulterants.